Examination of the asymmetric inheritance of mitochondria in yeast cells

Dissertation

zur Erlangung des akademischen Grades einer Doktorin der Naturwissenschaften

in der Bayreuther Graduiertenschule für Mathematik und Naturwissenschaften (BayNAT)

der Universität Bayreuth

vorgelegt von

Veronika Johanna Bartosch geb. Link

aus Eichstätt

Bayreuth, 2025

Die vorliegende Arbeit wurde in der Zeit von 10/2017 bis 02/2025 in Bayreuth am Institut für Zellbiologie unter Betreuung von Herrn Prof. Dr. Benedikt Westermann angefertigt.

Vollständiger Abdruck der von der Bayreuther Graduiertenschule für Mathematik und Naturwissenschaften (BayNAT) der Universität Bayreuth genehmigten Dissertation zur Erlangung des akademischen Grades einer Doktorin der Naturwissenschaften (Dr. rer. nat.).

Form der Dissertation: Monographie

Dissertation eingereicht am: 11.03.2025

Zulassung durch die Leitungsgremium: 12.03.2025

Wissenschaftliches Kolloquium: 30.06.2025

Amtierender Direktor: Prof. Dr. Jürgen Köhler

Prüfungsausschuss:

Prof. Dr. Benedikt Westermann (Gutachter)

Prof. Dr. Olaf Stemmann (Gutachter)

Prof. Dr. Angelika Mustroph (Vorsitz)

Prof. Dr. Matthias Weiss

Die vorliegende Arbeit ist als Monographie verfasst.

Teile der Arbeit sind bereits in den folgenden Publikationen erschienen:

Chelius, X., Bartosch, V., Rausch, N., Haubner, M., Schramm, J., Braun, R. J., Klecker, T. and Westermann, B. (2023). Selective retention of dysfunctional mitochondria during asymmetric cell division in yeast. *PLoS biology*. **21**, e3002310. doi:10.1371/journal.pbio.3002310.

Chelius, X., Rausch, N., Bartosch, V., Klecker, M., Klecker, T. and Westermann, B. (2025). A protein interaction map of the myosin Myo2 reveals a role of Alo1 in mitochondrial inheritance in yeast. *Journal of cell science*; **138 (3)**, JCS263678. doi:10.1242/jcs.263678

Diese Publikationen sind in der vorliegenden Arbeit zitiert.

Table of Contents

List of Abbreviations

Abbreviation	Full text
5-FOA	5-fluoroorotic acid
AID	auxin-inducible degron
APS	ammonium persulfate
ARE	aggregate retention efficiency
BF	bright-field microscopy
CT	C-terminal
D	Dextrose (in this work always glucose)
D-Ala	D-alanine
DAO	D-amino acid oxidase 1 from *Rhodotorula gracilis*
DHFR	dihydrofolate reductase
DIC	differential interference contrast
ER	endoplasmic reticulum
ERCs	extrachromosomal rDNA circles
ERMES	ER-mitochondria encounter structure
G	glycerol
Gal	galactose
gDNA	genomic DNA
GSH	monomeric glutathione
IAA	indole-3-acetic acid
IMiQ	intramitochondrial quality control compartment
IMM	inner mitochondrial membrane
IMS	inter membrane space
INQ	Intranuclear quality control site
IPOD	insoluble protein deposit
JUNQ	juxtanuclear quality control site
L-Ala	L-alanine
MAGIC	mitochondria as guardian in cytosol
MOM	mitochondrial outer membrane
MSG	monosodium glutamate
mt-	mitochondrially targeted
mtDNA	mitochondrial DNA
NAA	1-naphthaleneacetic acid
OD	optical density
OMM	outer mitochondrial membrane
ORF	open reading frames
Raf	raffinose
ROS	reactive oxygen species
SC	synthetic complete medium
SD	standard deviation
TEMED	tetramethylethylenediamine
TM	transmembrane
TORC1	Target of rapamycin complex 1
ts	temperature-sensitive
yEGFP	yeast enhanced GFP
YNB	yeast nitrogen base
YP	yeast peptone complete medium

Summary

The budding yeast *Saccharomyces cerevisiae* performs asymmetric cell division resulting in two cells differing in replicative age. This is achieved by the asymmetric inheritance of cellular factors, including damaging aging factors that are selectively retained in the mother cell during budding, thus allowing the daughter cell to have full replicative capability. One supposedly asymmetrically inherited cellular structure is the mitochondrial network. A dual role for the involvement of mitochondria in achieving the daughter's rejuvenation has been proposed with both a direct part through a quality-based selection during inheritance of mitochondria, leading to preferential inheritance of high-functioning mitochondria to the daughter, as well as an indirect role through the tethering of misfolded cytosolic protein aggregates to the mitochondrial surface. This supposedly aids the limitation of their movement, thereby contributing to their retention and consequently contributing to their detoxification, sequestration and degradation.

The first part of this thesis aims to characterize the relationship between protein aggregates and mitochondria and to investigate potentially unknown factors involved in the establishment of a proposed attachment. While no mutants displaying an increased inheritance of protein aggregates could be detected, the blocking of the mitochondrial import by clogging the import pores reduced the proportion of observable aggregates associated with mitochondria. Similarly, some genes could be identified whose deletion results in a disruption of the fusion of small aggregates into larger structures. This is a process that usually occurs quickly after the formation of aggregates and has been described to facilitate their asymmetric inheritance. The mutants found here however, displayed reduced aggregate fusion without an impact on aggregate retention or cellular survival.

The second part focused on identifying unknown cellular factors involved in mitochondrial inheritance. In *S. cerevisiae* mitochondrial inheritance is mediated by the motor protein Myo2 along actin cables. The recruiting of Myo2 to mitochondria requires at least one of the adaptor proteins Mmr1 and Ypt11. In a microscopy-based screen for aberrant mitochondrial morphology and inheritance in deletion mutants of 30 candidate genes chosen through an educated guess approach, no unknown candidates could be uncovered. Moreover, a multicopy suppressor screen in the mitochondrial transport incompetent Δ*mmr1 Δypt11* double mutant sought to find genes whose overexpression could rescue mitochondrial inheritance. Of over 10,000 transformants covering the yeast genome several times, 54 candidates stably rescued the double mutant strain. All the candidates that could be confirmed manually were rescued by either *MMR1* or *YPT11*, suggesting that there are no further factors involved in mitochondrial inheritance that act independently of these two proteins. Another aspect of this part aimed to characterize the relationship between mitochondrial inheritance, oxidative stress and the

mechanism behind selective inheritance of mitochondria during budding. To induce reactive oxygen species (ROS) production resulting in oxidative stress inside mitochondria, a matrix-targeted D-amino acid oxidase 1 enzyme was expressed and induced by the addition of D-Ala to the culture. The induction caused a strong inheritance defect of mitochondria which was not caused by actin depolymerization or disruption of the functionality of the Myo2 motor protein. Mmr1 on the other hand was frequently observed redistributed from mitochondrial foci to a broad cytosolic localization upon oxidative stress. Furthermore, mitochondrial inheritance could be rescued to wildtypical levels by enforcing mitochondrial transport to the bud through permanently anchoring Myo2 to the mitochondrial surface as well as overexpression of its mitochondrial adaptor Mmr1. Finally, cells lacking Mmr1 did not display a mitochondrial inheritance defect upon oxidative stress, indicating a key role of Mmr1 in the recognition of damaged mitochondria and the prevention of their inheritance.

Zusammenfassung

Die Bäckerhefe *Saccharomyces cerevisiae* führt eine asymmetrische Zellteilung durch, bei der zwei Zellen entstehen, die sich im replikativen Alter unterscheiden. Erreicht wird dies durch die asymmetrische Vererbung zellulärer Faktoren, einschließlich schädlicher Alterungsfaktoren, die während der Knospung selektiv in der Mutterzelle zurückgehalten werden, so dass die Tochterzelle volles replikatives Potential besitzt. Eine potentiell asymmetrisch vererbte zelluläre Struktur ist das mitochondriale Netzwerk. Es wurde eine doppelte Rolle für die Beteiligung von Mitochondrien an der Verjüngung der Tochter vermutet, und zwar sowohl eine direkte Rolle durch eine qualitätsbasierte Selektion bei Vererbung von Mitochondrien, die eine bevorzugte Vererbung hochfunktionaler Mitochondrien an die Tochter bewirkt, als auch eine indirekte Rolle durch die Bindung fehlgefalteter cytosolischer Proteinaggregate an die mitochondriale Oberfläche. Dies trägt vermutlich dazu bei, ihre Bewegung einzuschränken, wodurch sie in der Mutter zurückgehalten werden und folglich zu ihrer Detoxifizierung, Sequestrierung und ihrem Abbau.

Der erste Teil dieser Arbeit zielt darauf ab, die Beziehung zwischen Proteinaggregaten und Mitochondrien zu charakterisieren und potenziell unbekannte Faktoren zu ermitteln, die an der Herstellung der vorgeschlagenen Bindung beteiligt sind. Während keine Mutanten gefunden werden konnten, die eine erhöhte Vererbung von Proteinaggregaten aufweisen, reduzierte die Blockierung des mitochondrialen Imports durch Verstopfung der Importporen den Anteil der beobachteten Aggregate in Assoziation mit Mitochondrien. In diesem Zusammenhang konnten auch einige Gene identifiziert werden, deren Deletion eine Störung der Fusion kleiner Aggregate zu größeren Strukturen zur Folge haben. Dies ist einProzess, der in der Regel schnell nach der Bildung von Aggregaten stattfindet und deren asymmetrische Vererbung fördert. Die hier gefundenen Mutanten zeigten jedoch eine reduzierte Aggregatfusion, ohne dass dies Auswirkungen auf die Aggregatretention oder das Überleben der Zellen hatte.

Der zweite Teil konzentrierte sich auf die Identifizierung unbekannter zellulärer Faktoren, die an der mitochondrialen Vererbung beteiligt sind. In *S. cerevisiae* findet die mitochondriale Vererbung durch das Motorprotein Myo2 entlang von Aktinkabeln statt. Die Rekrutierung von Myo2 an Mitochondrien erfordert mindestens eines der Adaptorproteine Mmr und Ypt11. In einem mikroskopiebasierten Screening nach abweichender mitochondrialer Morphologie und Vererbung in Deletionsmutanten von 30 Kandidatengenen, die mit Hilfe eines "educated guess"-Ansatzes ausgewählt wurden, konnten keine unbekannten Kandidaten identifiziert werden. Darüber hinaus wurde in einem Multicopy-Suppressor-Screening in der Doppelmutante Δ*mmr1* Δ*ypt11*, die nicht zum mitochondrialen Transport fähig ist, nach Genen gesucht, deren Überexpression die mitochondriale Vererbung retten kann. Von

über 10.000 Transformanten, die das Hefegenom mehrfach abdeckten, retteten 54 Kandidaten den Doppelmutantenstamm stabil. Alle Kandidaten, die sich manuell bestätigen ließen, wurden entweder durch *MMR1* oder *YPT11* gerettet, was darauf hindeutet, dass es keine weiteren Faktoren gibt, die an der mitochondrialen Vererbung beteiligt sind, die unabhängig von diesen beiden Proteinen agieren. Ein weiterer Aspekt dieses Projekts war die Charakterisierung der Beziehung zwischen mitochondrialer Vererbung, oxidativem Stress und dem Mechanismus hinter der selektiven Vererbung von Mitochondrien während der Knospung. Um die gezielte ROS-Produktion in Mitochondrien zu ermöglichen, welche zu oxidativem Stress führt, wurde das Enzym D-Aminosäure-Oxidase 1 mit einer Matrix-Importsequenz exprimiert und durch die Zugabe von D-Ala zur Kultur induziert. Die Induktion führte zu einem starken Vererbungsdefekt der Mitochondrien, der nicht durch eine Aktin-Depolymerisation oder eine Beeinträchtigung der Funktionalität des Motorproteins Myo2 verursacht wurde. Demgegenüber wurde jedoch beobachtet, dass Mmr1 bei oxidativem Stress häufig von mitochondrialen Foci zu einer allgemeinen cytosolischen Lokalisierung wechselte. Darüber hinaus konnte die mitochondriale Vererbung auf ein wildtypisches Niveau gerettet werden, indem der Transport der Mitochondrien in die Knospe durch eine dauerhafte Verankerung von Myo2 an der mitochondrialen Oberfläche, sowie durch eine Überexpression seines mitochondrialen Adapters Mmr1 verstärkt wurde. Außerdem zeigten Zellen, denen Mmr1 fehlte, bei oxidativem Stress keinen Defekt bei der Mitochondrienvererbung, was auf eine zentrale Rolle von Mmr1 bei der Identifizierung von geschädigten Mitochondrien und der Vermeidung ihrer Vererbung hinweist.

Introduction

1.1 Yeast as a model organism

The baker's yeast *Saccharomyces cerevisiae* is a unicellular, eukaryotic fungus that is used extensively for molecular and cellular biology. In 1996 it became the first eukaryotic species with a fully sequenced genome (Goffeau et al., 1996). Due to the high sequence homology with higher eukaryotes and especially the human genome (Bassett et al., 1996) along with its easy cultivation and fast replication time, baker's yeast is a well-established model organism for higher eukaryotes which allows basic research like the discovery of fundamental cellular processes as well as a goal-oriented investigation of human diseases (Lasserre et al., 2015). Its fast generation time, cultivation requirements and high potential for chromosomal manipulation through homologous recombination have further fostered *S. cerevisiae*'s popularity with researchers (Botstein and Fink, 2011; Gietz and Schiestl, 2007; Sherman, 2002). The commercial availability of various yeast libraries containing, for example, deletion mutants (Giaever et al., 2002), conditional alleles (Ben-Aroya et al., 2008; Mnaimneh et al., 2004) and fusion alleles covering the whole genome (Huh et al., 2003) allow both the quick and easy examination of specific genes and proteins as well as large-scale genome-wide screens (Tong and Boone, 2006). Interestingly, yeast cells have the ability for sexual and asexual reproduction via budding and can stably live in both a haploid state, where they occur in two different mating types (*MAT*a and *MAT*α), and a diploid state (*MAT*a/α) (Haber, 2012). Two cells of opposing mating types can mate to form a zygote that produces diploid daughters, and during deteriorating environmental conditions diploids can undergo sporulation and form four haploid spores called a tetrad. This process is often used in yeast genetics to examine the genetic interactions of certain mutations by tetrad analysis after tetrad dissection with a micromanipulator.

S. cerevisiae is a suitable model to investigate the subjects of this thesis like the inheritance of mitochondria and protein aggregates due to several reasons. One major factor in this is that baker's yeast divides asymmetrically by budding, resulting in two non-identical yeast cells. Cells form a bud on one cell pole and many cellular components like the mitochondria or mRNAs must be actively transported there as the bud grows as a prerequisite for its survival. On the other hand, many harmful damages that a yeast cell has accumulated over its lifespan, like protein aggregates or lower-functioning organelles, are purposefully retained and not transported into the newly forming cell, allowing this daughter cell to achieve rejuvenation with full replicative potential (Jazwinski, 2004). The two cells resulting after cell division are termed and will further be referred to as 'mother' and 'daughter' who differ from one another based on their replicative potential. The mechanisms behind

asymmetric cell division are also relevant in higher eukaryotes, for example to maintain stemness in stem cells (Katajisto et al., 2015), and can be investigated very efficiently in yeast due to its unicellularity. Another factor qualifying *S. cerevisiae* for the investigations in this work is its ability to produce energy through glycolysis as well as respiration. This allows the partial loss of mitochondrial function, including oxidative phosphorylation and the complete loss of mitochondrial DNA (Tzagoloff and Dieckmann, 1990).

1.2 Mitochondria

1.2.1 Mitochondrial function, origin and structure

Mitochondria are semi-autonomous organelles that are essential in almost all eukaryotic cells due to their role in cellular metabolism (Malina et al., 2018). The endosymbiotic hypothesis explains the origin of mitochondria as alpha-proteobacteria that were taken up by another cell through phagocytosis where they were able to escape degradation and instead formed a codependent relationship with the host cell (Cavalier-Smith, 1987; Zimorski et al., 2014). Mitochondria are surrounded by two membranes, the inner mitochondrial membrane (IMM) and the outer mitochondrial membrane (MOM), thus creating two separate compartments: one between the two membranes and one enclosed by the inner membrane. The compartment between the two bilayer membranes is termed the intermembrane space (IMS). The mitochondrial matrix is the compartment enclosed by the IMM. The inner mitochondrial membrane forms characteristic invaginations known as cristae where ATP is generated by the electron transport chain and ATP synthase (Frey and Mannella, 2000; Wurm and Jakobs, 2006). This special structure of the organelles is fundamentally required for the process of mitochondrial energy production but also introduces unique obstacles to the cells regarding, for example, protein import or signal transduction across two membranes.

Due to their origin from an independent organism, mitochondria possess their own mitochondrial genome (mtDNA) using an alternative genetic code and displaying some prokaryotic features. Over the course of the incorporation into the host cell the majority of genes were, however, transferred to the nucleus. The size of the mitochondrial genome and the number of genes differs greatly between organisms. In *S. cerevisiae*, the mtDNA contains eight genes coding for components of the respiratory chain and oxidative phosphorylation as well as a ribosomal subunit and t- and rRNAs (Foury et al., 1998). Every cell contains many copies of the mitochondrial genome which are organized in 10-15 nucleoids per cell that are dispersed throughout the mitochondrial network (Chen and Butow, 2005).

Mitochondria cannot be formed *de novo* but are necessary for cellular survival, thus their inheritance must be tightly regulated. They perform a large variety of specialized biological functions including the Krebs cycle and oxidative phosphorylation and the resulting proton gradient across the IMM is the driving force behind ATP production by the ATP synthase (Malina et al., 2018). Additionally, mitochondria are also key in the metabolism of amino acids and lipids. Furthermore, mitochondria are necessary for the production of important co-factors like hemes and the assembly of iron sulfur clusters (Lill and Mühlenhoff, 2005). In line with their multiple functions in the metabolism of eukaryotic cells, mitochondrial dysfunction has been linked to cellular decline, cellular aging and over 150 diseases (Lasserre et al., 2015; Wallace, 2010).

1.2.2 Mitochondrial dynamics and morphology

Contrary to the way mitochondria are commonly displayed in textbooks, the mitochondria in a cell are not a collection of immobile individual organelles but rather form a highly dynamic and interactive network (Westermann, 2008). Studying mitochondria in *S. cerevisiae* has played a major role in understanding mitochondrial dynamics. The mitochondrial network undergoes constant restructuring by fusion and fission events while simultaneously being transported along the cytoskeleton, as there are about 2.5 fusion and fission events occurring in a cell at any given minute (Jakobs et al., 2003). More than 20 yeast genes are necessary for normal mitochondrial morphology, although that number is most likely underestimated, which indicates that mitochondrial dynamics and morphology are complex processes (Berman et al., 2008). The overall mitochondrial morphology in budding yeast cells is dependent on a large variety of factors. This is especially important to remember when designing experiments involving the evaluation of mitochondrial morphology in different strains or treatment conditions as was often the case in this thesis. One of these factors is the growth phase. Cells in the logarithmic growth phase usually display a mostly interconnected network of tubular mitochondria while cells in the stationary phase or older cells tend to display fragmented mitochondria with many individual, separated fragments (Scheckhuber et al., 2007). Another important factor to keep in mind is that the mitochondrial morphology changes depending on carbon metabolism due to the availability of different carbon sources in the growth medium. Cells growing in medium containing non-fermentable carbon sources like glycerol or ethanol display an overall larger and more connected mitochondrial network compared to cells growing on fermentable carbon sources like glucose, where the mitochondria form a simpler structure with less branches (Egner et al., 2002).

There are three proteins well known to mediate mitochondrial fusion in yeast: Fzo1, Ugo1 and Mgm1. Fzo1 (Hermann et al., 1998) and Ugo1, respectively, are responsible for the separate fusion of the outer

mitochondrial membranes (Sesaki and Jensen, 2004). Fusion of the inner membrane additionally requires the protein Mgm1 which is involved in two different isoforms (Herlan et al., 2003; Wong et al., 2003). Deletion of the genes encoding for these three proteins leads to mitochondrial fragmentation as the continuous fission events are no longer compensated for by fusion events, resulting in the cells having many small mitochondrial units that are separated from one another. This phenotype has been found to coincide with increased levels of mtDNA loss finally leads to the loss of respiratory function (Hermann et al., 1998; Rapaport et al., 1998). Additionally, fragmented mitochondria are transported less efficiently, leading to inheritance defects in the respective mutants (Böckler et al., 2017; Higuchi-Sanabria et al., 2016).

Similarly, mitochondrial fission in *S. cerevisiae* is mostly dependent on four proteins: Dnm1, Fis1, Mdv1 and Caf4 (Griffin et al., 2005; Mozdy et al., 2000; Otsuga et al., 1998; Tieu and Nunnari, 2000). Dnm1 is a small dynamin-related GTPase which oligomerizes to assemble into a contractile ring that constricts to separate two mitochondria from one another (Ingerman et al., 2005). Interestingly, division mostly occurs at ER-mitochondria encounter structure (ERMES) organelle-organelle contact sites with the ER, where the ER tubules wrap around mitochondria, constricting them to allow the formation of the Dnm1 ring (Friedman et al., 2011). Actively replicating mtDNA nucleoids also reside at these sites, which allows the distribution of genetic material into both of the resulting mitochondria (Murley et al., 2013). The Dnm1 receptor on the mitochondrial outer membrane is the transmembrane protein Fis1, which is required for proper Dnm1 ring assembly (Mozdy et al., 2000). Mdv1 and Caf4 serve as redundant adaptors between Fis1 and Dnm1 (Fekkes et al., 2000; Griffin et al., 2005). Most recently two studies have described the involvement of a previously undescribed protein – Mdi1 or Atg44 - in the division of the mitochondrial membranes (Connor et al., 2023; Fukuda et al., 2023). Atg44 has been shown to be required for the completion of mitochondrial fission by Dnm1 as well as mitochondrial fission during mitophagy (Furukawa et al., 2024). The mitochondria in mutants displaying defective mitochondrial fission form a highly connected network.

1.2.3 The actin and septin cytoskeleton

Eukaryotic and prokaryotic cells have a cytoskeleton that consists of different filaments that form the structural basis of cellular organization. It serves mechanical functions as well as playing a role in signaling pathways and as scaffolding during transport processes (Fletcher and Mullins, 2010). The eukaryotic cytoskeleton consists of three main filament types: the actin cytoskeleton (or microfilaments), microtubules and intermediate filaments. Intermediate filaments are involved in maintaining the shape of the cell, anchoring organelles in the cytoplasm and for cell-cell contact sites. In many eukaryotic cells and cell types, including human neurons, mitochondria are transported along microtubules by dynein and kinesin motor proteins, depending on the direction of transport (Melkov and Abdu, 2018). However, in baker's yeast organelles, vesicles, mRNAs and a large variety of other cargos are transported along the actin cytoskeleton while microtubules only play a comparably small role in *S. cerevisiae*, where they are only involved in mitosis and meiosis (Mishra et al., 2014; Pruyne et al., 2004b).

Actin is highly conserved throughout eukaryotes and occurs in cells in two different forms: the monomeric G-actin and the filamentous F-actin (Pollard, 2016). In budding yeast actin is encoded by the *ACT1* gene (Ng and Abelson, 1980). F-actin consists of highly dynamic, polymeric filaments made up of G-actin. The two ends of a filament differ from one another, thus creating an orientation. Polymerization occurs faster at the barbed end than at the pointed end. In yeast, there are three different structures formed by actin: actin patches, the actomyosin ring and actin filaments (Adams and Pringle, 1984; Mishra et al., 2014). The localization and organization of these different structures varies strongly throughout the cell cycle. Actin patches occur at places of polarized growth and are essential for clathrin-based endocytosis and vesicle formation (Galletta and Cooper, 2009). Their formation is driven by the Arp2/3 complex which consists of the two actin-related-proteins Arp2 and Arp3 that start polymerization of branches of actin filaments by acting as a nucleation core for polymerization in an ATP-dependent manner (Pollard, 2007). Additionally, the complex includes five other proteins: Arc15, Arc18, Arc19, Arc35, and Arc40. The interaction between the complex and nucleation-promoting factors, which in *S. cerevisiae* include Abp1, Las17 and Myo5, is required for its activation (Kaksonen et al., 2003; Kaksonen et al., 2005). In small- to medium-budded cells, these patches are usually concentrated at the daughter cell tip and later at the mother-bud neck. The actomyosin ring is a contractile ring at the mother-bud neck, generating the mechanical force necessary for cell division during cytokinesis (Wloka and Bi, 2012). Lastly, actin filaments are linear cables throughout the cell that are present at all points of the cell cycle (Adams and Pringle, 1984). Their formation is nucleated by formins using the polarisome as a starting point and their assembly and disassembly is highly dynamic, displaying a half-life of less than one minute (Drake et al., 2012;

Pruyne et al., 2004a). Since the formins Bnr1 and Bni1 localize to the bud neck and bud tip, a retrograde actin cable flow towards the mother cell is created as actin is polymerizing at the formins' location (Kikyo et al., 1999; Ozaki-Kuroda et al., 2001). Thus, actin filaments are inherently involved in creating cell polarity. In yeast they act as tracks for the directed transport of a large variety of cargos into the daughter cell including organelles like peroxisomes, the vacuole late Golgi elements as well as secretory vesicles and RNAs and are even involved in the orientation of the nucleus (Pruyne et al., 2004b). *S. cerevisiae* has two motor proteins transporting these cargos: Myo2 and Myo4 are both class V myosins using energy from ATP hydrolysis to move their cargos toward the barbed end of the actin filaments where polarized growth takes place (Hammer and Sellers, 2012). Myo4's cargos include mRNAs and the cortical endoplasmic reticulum (ER) (Estrada et al., 2003) while Myo2 carries the majority of organelles and will be discussed further below (Shepard et al., 2003).

Another cytoskeletal component that is present mostly in animal and fungal cells are the septins (Douglas et al., 2005; Marquardt et al., 2019). Septins are a family of GTP-binding proteins that oligomerize into non-polar filaments and can form rings and other higher-order structures (Bertin et al., 2011; Byers and Goetsch, 1976). *S. cerevisiae* expresses a total of seven septin proteins: Cdc3, Cdc10, Cdc11, Cdc12, Shs1, Spr3 and Spr28. Spr3 and Spr28 are only expressed during sporulation while the others are mainly expressed during mitotic growth. Among these Cdc3, Cdc11 and Cdc12 are essential while deletion mutants of the other four septins are viable but still typically display abnormal cell morphology with elongated buds and defective cytokinesis (Longtine et al., 1996). These mutants additionally often display pseudohyphal growth which is growth where the yeast cells do not perform correct cell division but instead form long continuous structures and are prone to develop multiple buds at the same time. In contrast to proper hyphal growth these cells do not have shared cytoplasm. All septins share a characteristic conserved domain and all of them with the exception of Cdc10 possess a coiled-coil domain (Casamayor and Snyder, 2003). Posttranslational modifications, especially phosphorylation of a large number of proteins including most notably actin and Cdc42, were found to be regulators of septin polymerization often in a cell cycle-dependent fashion (Caviston et al., 2003; Dobbelaere et al., 2003; Versele and Thorner, 2004). The core structure is formed by Cdc11, Cdc12 and Cdc3 but the place of Cdc11 can also be taken by Shs1 depending on GTP availability (Weems and McMurray, 2017). These core trimers are then connected by a homodimer of Cdc10 binding to Cdc3. Septins serve as scaffolding for other proteins for example during cytokinesis and mating and are involved in bud-site selection and cell cycle regulation. They perform many of these functions through their direct interaction with actin filaments and the promotion of actin polymerization with the help of the formin Bnr1 (Buttery et al., 2012). During cell division a septin ring forms at the mother-bud neck, expands over time into an hourglass structure and later splits into two rings which can be found on the mother and daughter cell wall respectively after division. While septins are not required for

constricting of the actomyosin ring in budding yeast, as was assumed previously, they are necessary to recruit Myo1 to initiate the formation of the actomyosin ring (Feng et al., 2015; Tamborrini et al., 2018). Additionally, septins have been found to form diffusion barriers at the mother-bud neck, thus promoting the asymmetry between mother and daughter. The barrier has been found to restrict the movement of lipids (Manford et al., 2012), cytosolic aggregated Sup35 [PSI+] (Tartakoff et al., 2013) , misfolded ER proteins (Clay et al., 2014) and damaged nuclear pore complexes (Shcheprova et al., 2008).

1.2.4 Mitochondrial transport and inheritance

In most eukaryotes directed mitochondrial transport occurs along microtubules using kinesin and dynein motor proteins. Mitochondrial movement in *S. cerevisiae* however has long been found insensitive to β-tubulin (*TUB2*) mutation and the inhibition of microtubule polymerization (Huffaker et al., 1988; Jacobs et al., 1988). Instead, long-distance transport of mitochondria uses actin cables as tracks and consequently mitochondrial movement can be stopped and their morphology altered by disrupting the actin cytoskeleton both genetically or chemically (Boldogh et al., 1998; Drubin et al., 1993; Simon et al., 1997). Furthermore, a reversible interaction between mitochondria and actin can be reproduced *in vitro* in an ATP-dependent manner (Lazzarino et al., 1994). The polarity of the actin cable network allows the distinction of two different directions of mitochondrial movement: anterograde transport towards the daughter cell pole and retrograde transport towards the mother cell pole. Due to the mechanics of actin polymerization by formins at the bud tip a retrograde cable flow towards the mother is intrinsically generated. The mechanism behind retrograde mitochondrial transport remains unknown and no proteins have been linked to it yet. Nonetheless, the mitochondrial movement in the retrograde direction has been suggested to be driven by attachment to the moving cables and thus retrograde cable flow itself (Fehrenbacher et al., 2004).

As mitochondria cannot be formed *de novo*, anterograde transport towards the daughter cell to allow the inheritance of mitochondria is essential for survival of the offspring while the mother cell at the same time also has to ensure the retention of a critical mass of mitochondria. Mitochondria are usually transported to the daughter already about 10 to 20 minutes after bud emergence during the early stages of bud growth (Li et al., 2021). Regarding the mechanism of anterograde transport along actin cables two conflicting models have been proposed. Many observations point toward a model assigning the class V myosin motor protein Myo2 as the motor for mitochondrial transport (Altmann et al., 2008; Chernyakov et al., 2013; Förtsch et al., 2011; Itoh et al., 2002; Itoh et al., 2004). This model is supported by the observation that the binding of mitochondria to actin filaments *in vitro* is dependent on Myo2

and the detection of Myo2 on isolated mitochondria using immuno-EM (Altmann et al., 2008). While deletion mutants lacking Myo2 are not viable, conditional mutants as well as viable Myo2 mutants display disturbed anterograde movement and mitochondrial morphology (Eves et al., 2012; Itoh et al., 2002). Accordingly, its permanent anchoring to the mitochondrial surface led to an elevated amount of bud-directed mitochondrial transport, resulting in the accumulation of mitochondria inside the bud (Förtsch et al., 2011). As mentioned above, this motor protein has already been found responsible for the bud-directed transport of most other organelles (Beach et al., 2000; Fagarasanu et al., 2006; Govindan et al., 1995; Hill et al., 1996; Rossanese et al., 2001). In order to achieve efficient transport of the variety of cargos a large number of organelle-specific adaptor and receptor proteins, which are often Rab GTPases, are involved (Wong and Weisman, 2021). The binding regions of these proteins on the Myo2 cargo binding domain have been mapped into two distinct subdomains, each containing the binding sites for more than one organelle (Catlett and Weisman, 1998; Eves et al., 2012; Schott et al., 1999). These binding sites were identified through the introduction of point mutations and the observation of Myo2's ability to bind and transport specific organelles. Subdomain I consists of the binding sites for secretory vesicles, late-Golgi elements and peroxisomes, while Subdomain II comprises the binding sites of vacuoles and mitochondria.

For mitochondrial transport two proteins involved in the recruitment of Myo2 to the mitochondrial surface and anterograde movement have been identified: Mmr1 and Ypt11 (Eves et al., 2012; Itoh et al., 2002; Itoh et al., 2004; Lewandowska et al., 2013). Mmr1 (mitochondrial Myo2 receptor-related) is a protein that is peripherally associated with the mitochondrial outer membrane and was identified to be a high-dose suppressor of mitochondrial inheritance defects (Chernyakov et al., 2013; Itoh et al., 2004). Its interactions with phospholipids in membranes, Myo2, as well as itself are necessary for functional mitochondrial inheritance (Chen et al., 2018). The cellular localization of Mmr1 has been either reported as polarized at the bud tip along with Myo2 or alternatively on the leading tip of mitochondria moving towards the bud combined with a diffuse cytosolic signal (Eves et al., 2012; Xu and Bretscher, 2014). Under starving conditions Mmr1 relocalizes to the whole mitochondrial network. In addition to its colocalization with mitochondria in fluorescence microscopy (Swayne et al., 2011), Mmr1 can be co-immunoprecipitated (Itoh et al., 2004) as well as co-crystallized with Myo2 (Tang et al., 2019). Interestingly, Δ*mmr1* cells display only a relatively small defect with a delay in mitochondrial inheritance by 30 to 40% in small-budded cells. Larger-budded Δ*mmr1* cells even display a wild type-like level of mitochondria present in the daughter cell. Additionally, Mmr1 has been implicated to be involved in anchoring mitochondria at the bud tip during inheritance and a potential quality control during mitochondrial inheritance. This will be discussed at a later point.

The cytosolic small Rab-like GTPase Ypt11 (Yeast Protein Two 11), which was linked to the Myo2-mediated transport of the cortical ER and late Golgi (Arai et al., 2008) by some publications, is also involved in mitochondrial inheritance (Frederick et al., 2008). Since the endogenous *YPT11* promoter expresses the protein at very low levels, studies investigating the protein's location have employed the use of stronger promoters to locate the protein's GFP-fusion in fluorescence microscopy, mostly colocalizing with the ER. Later it was shown that the observed localization at the ER is overrepresented due to the unphysiologically high protein levels (Lewandowska et al., 2013). Similar to Mmr1, it has been co-immunoprecipitated with Myo2, Ypt11 overexpression can rescue mitochondrial inheritance mutants and Δ*ypt11* mutants display a delay of inheritance (Itoh et al., 2002). This delay albeit is even less prominent than in Δ*mmr1* cells with only 10 to 20% less mitochondria in small-budded cells compared to the wild type. The deletion of both *MMR1* and *YPT11* simultaneously, on the other hand, lowers mitochondrial inheritance to a lethal level (Itoh et al., 2004) or depending on yeast strain background leads to a severe growth defect (Frederick et al., 2008). The comparatively small effect of the single deletions on mitochondrial inheritance indicates that the two proteins act in parallel to each other in the same pathway. If only one of the proteins is missing the other one can compensate for that loss indicating at least some extent of redundancy between the two proteins. Additionally, the relatively small inheritance defects caused by the single deletions could indicate the involvement of another, currently unknown protein functioning as the mitochondrial Myo2-receptor. For this role an integral mitochondrial outer membrane protein seems most likely.

Alternatively to Myo2-mediated transport along actin cables, it has been proposed that anterograde and retrograde mitochondrial transport is driven by rapid actin polymerization on the mitochondrial surface mediated by the Arp2/3 complex (Boldogh et al., 2001). Many major cellular functions in eukaryotic cells are driven by the Arp2/3 complex including membrane trafficking, cell movement and endo- and exocytosis (Goley and Welch, 2006). Furthermore, the complex is probably best-known for driving the intracellular movement of pathogens like *Listeria monocytogenes* or *Rickettsia conorii* inside host cells (Gouin et al., 1999; Moreau et al., 2017; Teysseire et al., 1992; Welch et al., 1997). According to this theory of mitochondrial transport via the Arp2/3 complex, the binding between mitochondria and actin cables is facilitated by a complex of Mmm1, Mdm10 and Mdm12 that was termed mitochore (Boldogh et al., 2003). The mitochore complex was described to consist of integral membrane proteins of both mitochondrial membranes and thus would be able to stably attach mitochondria directly to actin filaments for both anterograde and retrograde mitochondrial movement. For anterograde movement the Arp2/3 complex would drive polymerization while retrograde transport is achieved passively through the actin cable flow (Boldogh et al., 2003). The recruitment of the Arp2/3 complex to mitochondria and the mitochore complex is facilitated through the proteins Jsn1 and Puf3 (Fehrenbacher et al., 2005; García-Rodríguez et al., 2007). In this model

Myo2 is only indirectly involved in mitochondrial inheritance by functioning as a transporter for a retention factor – Ypt11 was suggested – in the bud (Boldogh et al., 2004). This proposed model is based on immunofluorescence observations of Arp2 at mitochondria, the detection of two members of the Arp2/3 complex in protein extracts of isolated mitochondria and the observation of a weak and diffuse actin signal colocalizing with mitochondria after disturbing the actin cytoskeleton with sodium azide treatment which was interpreted as actin clouds (Boldogh et al., 2001). These little-convincing findings along with the later correction of the localization of Mmm1 in the ER and its role in mediating mitochondria-ER contact sites in the ERMES (Kornmann et al., 2009) complex make this mechanism for mitochondrial transport appear very unlikely. The Myo2-based model (Förtsch et al., 2011) which is mostly considered consensus by now due to the evidence supporting it.

To allow both mother and daughter cells to obtain sufficient amounts of mitochondrial mass during cell division to allow cellular survival, cortical anchors at the mother and bud poles have been suggested based on microscopical observation of mitochondrial localization during cell division (Simon et al., 1997; Yang et al., 1999). The localization of mitochondria in the bud throughout the cell cycle is reminiscent of observed localization of Myo2: an accumulation at the bud tip in small buds and a later shift towards a concentration of Myo2 at the mother-bud neck closer to cytokinesis. At the mother cell pole the cortical protein Num1 has been shown to be the cortex anchor for mitochondria (Klecker et al., 2013; Lackner et al., 2013). This protein has previously been known for its involvement in nuclear migration and inheritance through interacting with dynein and microtubules (Farkasovsky and Küntzel, 2001) and had been implicated to be involved in mitochondrial distribution and fission (Cerveny et al., 2007; Dimmer et al., 2002) prior to its identification as a cortex anchor. With its pleckstrin homology domain Num1 is able to bind phosphatidylinositol 4,5-bisphosphate in the plasma membrane while simultaneously attaching to mitochondrial outer membrane lipids through its coiled-coil domain (Ping et al., 2016). Another protein involved in anchoring in the mother is Mdm36 which seems to mediate the formation of Num1 clusters thus promoting its binding to mitochondria. Additionally, Num1s other function in the binding of dynein and orienting the mitotic spindle is performed independently from Mdm36 by another population of Num1 foci as Mdm36 and dynein likely bind to the same regions of Num1 (Omer et al., 2020). The role that Mdm36 plays and its relationship with Num1 is not completely understood yet but mutants of both proteins display a similar phenotype (Hammermeister et al., 2010; Klecker et al., 2013). Furthermore, Mfb1 is also involved in mitochondrial retention (Pernice et al., 2016). It acts independently in parallel from the Num1-mediated anchor and Δ*mfb1* and Δ*num1* double mutants display a complete loss of mitochondrial retention in the mother.

Regarding the retention of transported mitochondria inside the daughter cell Mmr1, additionally to its role in Myo2-mediated transport, has been implicated in serving as a cortex anchor at mitochondria-

ER contact sites at the bud tip (Swayne et al., 2011). This idea is supported by the finding that *MMR1* mRNA is asymmetrically located in the bud (Shepard et al., 2003) and by the observation that simultaneous Δ*num1* and Δ*mmr1* or Δ*mfb1* and Δ*mmr1* deletion being able to rescue the mitochondrial inheritance defects observable in the single mutants (Klecker et al., 2013; Pernice et al., 2016). Additionally, as described above Myo2 accumulates at the bud tip in small to medium sized buds (Lillie and Brown, 1994), a similar accumulation of its mitochondrial adaptor at the bud tip with simultaneous presence of mitochondria can be expected. Upon glucose starvation Mmr1 relocalizes to the entire mitochondrial network while Myo2 also loses its polarized localization at the bud tip (Xu and Bretscher, 2014). While the proposed role as an anchor could provide an alternative explanation for the reduced level of mitochondrial inheritance in Δ*mmr1* mutants this is unlikely as the majority of observations support a role in Myo2-mediated mitochondrial transport.

1.2.5 Oxidative stress and ROS

ROS are oxygen containing oxidants that possess extremely high potential for non-specific reactions with other molecules (Sies et al., 2022). Whilst there are several sources of ROS production, mitochondria are widely considered to be the main source as the creation of ROS is a regular though harmful byproduct of the ATP production through oxidative phosphorylation (Murphy, 2009). As electrons are transferred to allow the creation of the proton-motive force across the inner mitochondrial membrane, superoxide (O_2^-) and hydrogen peroxide (H_2O_2) are constantly produced by several different steps. Due to their high reactivity ROS cause the damaging of proteins, DNAs, RNAs and lipids by oxidizing them (Juan et al., 2021). This toxicity links ROS with pathologies such as diabetes and neurological disorders, and cellular aging and ROS levels are higher in old yeast cells (Laun et al., 2001). One easily trackable consequence of ROS is the carbonylation of proteins. With progressing age carbonylated proteins accumulate in the cell and are inherited asymmetrically (Aguilaniu et al., 2003; Erjavec et al., 2007). Damaged proteins and their inheritance will be discussed in more detail later. Regardless of ROS production taking place in the mitochondrial matrix and intermembrane space, they possess the ability to cross membranes to escape into the cytosol.

Along with the negative effects, ROS are also valuable players in redox signaling and as second messengers in prokaryotes as well as eukaryotes ranging from yeasts to plants and mammals. ROS signaling has for example been shown to induce autophagy and apoptosis (Chen et al., 2007; Redza-Dutordoir and Averill-Bates, 2016). In signaling their high reactivity is often used to alter target protein activity through the oxidation of for example cysteines at the catalytically active site of phosphatases (Rhee et al., 2000). ROS direct role in signaling allows immediate transfer of information between

mitochondria and the remainder of the cell. Hydrogen peroxide for example has been shown to alter the expression of transcription factors to better adapt to stress situations and thus allow the cell to respond accordingly by altering mitochondrial metabolism (Collins et al., 2012). It is important to note that changes of the base level of ROS production in both directions can cause physiological changes.

Cells have evolved many antioxidant systems to detoxify ROS production that exceeds the steady-state level. Those defenses include enzyme families like superoxide dismutases, peroxiredoxins and catalase. The ROS detoxifying enzyme catalase Ctt1 is displaying higher activity in buds and active, undamaged Ctt1 proteins are preferentially inherited by the daughter cells (Erjavec and Nyström, 2007). One of the most important antioxidant systems across species is the glutathione system. Monomeric glutathione (GSH) becomes oxidized by ROS and transforms to its dimeric form GSSG via the disulfide bond crosslinking of cysteines. The enzyme glutathione reductase then recovers the reduced GSH using NADPH. Many of the enzymes involved in ROS detoxifications have mitochondrial isoforms to directly interfere at the place of ROS production as well as cytosolic isoforms. Naturally, this means that the regulation of the amount of ROS scavenging influences the amount of ROS signaling possible. According to the 'free radical theory of aging', the accumulation of damage caused by ROS over a lifetime is the reason for cellular aging, although the validity of this theory remains a topic of debate (Gladyshev, 2014; Harman, 1956). Contrastingly, the lifespan extension observable in *S. cerevisiae* cells grown under caloric restriction has been traced back to an increase in mitochondrial ROS production (Mesquita et al., 2010). It has however long been agreed upon that mitochondrial dysfunction is promoted by ROS production (Kowaltowski and Vercesi, 1999).

As the point of origin for most ROS molecules in the cells, the influence of ROS on mitochondria is of special interest. A frequent target of ROS damage is mtDNA due to its location in the mitochondrial matrix by ROS reacting with the nucleobases or introducing single or double strand breaks (Richter et al., 1988; Wallace, 2002). Damaged mitochondria can be selectively degraded through mitophagy (Bhatia-Kissova and Camougrand, 2021). In yeast mitochondrial units are engulfed by an autophagosome and consequently degraded if they present Atg32 on their surface. This allows to reduce the ROS production by low-quality mitochondria through their removal from the cell. Accordingly, cells where mitophagy is blocked display increased ROS production resulting in mtDNA damage and loss (Kurihara et al., 2012). The addition of external H_2O_2 to cell cultures induces a reversible fragmentation of mitochondria into many small units (Cooper et al., 2014; Vowinckel et al., 2015). This morphological consequence can be explained as a functional membrane potential is required for fusion of the mitochondrial inner membrane and extreme oxidative stress eliminates the membrane potential, thus leaving the mitochondria fusion incompetent (Meeusen et al., 2004). Furthermore, oxidative stress has been shown to target the actin cytoskeleton as treatment with low

levels of oxidizing agents leads to a reversible actin depolarization (Vilella et al., 2005). In mammalian cells a direct connection between reduced mitochondrial movement and high ROS levels could be shown although mitochondrial transport cannot easily be compared to yeast in these experiments since the mitochondrial motor as well as the cytoskeletal track differ (Debattisti et al., 2017).

1.2.6 Asymmetric inheritance of mitochondria

As mentioned above *S. cerevisiae* has been shown to perform asymmetrical cell division resulting in two non-identical cells. Since the decline of mitochondrial fitness and loss of mtDNA are considered to contribute to cellular aging, the selective inheritance of high-functioning mitochondria is supposedly contributing to the rejuvenation of the daughter cell. Asymmetric division including specifically the differential distribution of differently aged mitochondria has been proven to be required to maintain stemness in mammalian cells (Katajisto et al., 2015). Since in budding yeast, mothers produce virgin daughters up to the end of their replicative life span after 20 to 30 divisions, it was proposed that amongst the asymmetrically divided factors like protein aggregates and extrachromosomal rDNA circles (ERCs) – these will be described further in chapter 1.3 – are also higher quality mitochondria. In this model the high functioning mitochondria are preferentially transported to the buds, and this results in a higher replicative lifespan compared to the mother which retains the mitochondria that are lower functioning (Denoth Lippuner et al., 2014). There are several observations supporting the unequal distribution of mitochondria including the asymmetrical inheritance of the protein aconitase inside mitochondria after oxidative stress (Klinger et al., 2010), aged cells displaying lower membrane potential also producing daughters with lower membrane potential (Lai et al., 2002) as well as the mitochondria inside the bud displaying lower ROS levels than mitochondria in the mother (McFaline-Figueroa et al., 2011). Fluorescent redox sensors show that there is also a portion of reduced mitochondria anchored to the mother cortex, most likely to ensure that mother cells keep at least a small portion of high-functioning mitochondria themselves to maintain functionality (Pernice et al., 2016). Furthermore, the mitochondrial mass that is inherited is kept constant in relation to the cell size, but this ability continuously declines with the mothers replicative age (Rafelski et al., 2012).

However, the mechanism behind a putative quality control during mitochondrial inheritance in dividing yeast cells is completely unknown and there are many questions open regarding this process. Investigations described mitochondrial fragmentation with increasing replicative age that goes along with a decreased membrane potential (Hughes and Gottschling, 2012). Mitochondrial fragmentation is known to decrease mitochondrial transport and inheritance so aged mitochondria might be separated from the fitter mitochondria through fragmentation and thus more likely be retained in the

mother (Böckler et al., 2017). How are mitochondrial fitness levels signaled and recognized? Which components of the transport machinery are affected? Another possible mechanism could be increased retrograde transport of damaged mitochondria back into the mother while anterograde transport is unaffected by mitochondrial fitness. Again, Mmr1 has been connected to this process of mitochondrial quality control during inheritance although many of these findings could support its proposed role as a cortex anchor as well. Importantly, the deletion of *YPT11* or *MMR1* influences the replicative lifespan of daughters. The deletion of *YPT11* was shown to lead to a delayed ratio of mitochondrial inheritance in the bud which disappears by the time of separation likely through reduced velocity of bud growth (Rafelski et al., 2012). Furthermore, Δ*ypt11* mutants separate into two groups with either longer or shorter replicative lifespans than the wildtype. Similarly, the deletion of *MMR1* results in two different populations of daughter cells regarding their replicative potential: One long- and one short-lived (McFaline-Figueroa et al., 2011). The population with high replicative potential displays accelerated generation times and altered age asymmetry. Furthermore, the long lived Δ*mmr1* cells were described to display lower superoxide levels than their short-lived counterparts and WT cells. Remarkably, the offspring of short-lived cells are always short-lived themselves while long-lived cells can produce both long- and short-lived daughters. Overall, these findings indicate a link between *MMR1*, mitochondrial inheritance and mitochondrial fitness or ROS. The overexpression of *MMR1*, interestingly, also decreases replicative life span (Higuchi-Sanabria et al., 2016). Similarly, the *myo2(LQ)* mutant also produces a subpopulation of daughters with very low replicative potential (Böckler et al., 2017). A recent study described the necessity for Mmr1 degradation in the daughter in order to release mitochondria from the actin cytoskeleton and its impairment led to disturbed mitochondrial morphology and increased ROS levels (Obara et al., 2022). Furthermore, it has been hypothesized that retrograde actin cable flow itself may pose as a barrier that mitochondria have to overcome and fitter mitochondria with a more reduced redox state are more likely to make their way into the bud (Vevea et al., 2014). In favor of this idea, it was observed that the enhancement of actin flow rate results in extended replicative lifespan and increased fitness of inherited mitochondria depending on intact mtDNA (Higuchi et al., 2013). In conclusion, the mitochondrial dynamics, anchoring and transport machineries all seem to be involved in the asymmetrical inheritance of mitochondria, but little is currently understood about this process.

1.3 Protein aggregates and their asymmetric inheritance

The accumulation of damage acquired throughout a lifetime causing age-associated changes over time is believed to drive, or at least contribute to cellular aging (Gladyshev, 2014). In order to maintain

viability on a population level, *S. cerevisiae* cells have to achieve rejuvenation of daughter cells during cell division and throughout their lifespan. This rejuvenation capability is known to decline as the mother cell approaches the end of its replicative life (Johnston, 1966; Kennedy et al., 1994). The observation of the failure of daughter cell rejuvenation by old mothers suggests that the accumulation of senescence factors does indeed play a role in aging and that their asymmetric inheritance can no longer be maintained once their quantity has surpassed a critical amount. For a factor to be defined as an aging factor, four criteria must be met:: accumulation during aging, increase of the factor in young cells must cause a reduction of lifespan, reduction of the factor must increase lifespan, and asymmetric segregation to the older cell (Henderson and Gottschling, 2008). Among the most discussed aging factors are misfolded proteins and protein aggregates. Cells spend a significant portion of their available energy on proteostasis yet the effectivity of this process declines with maturing age and as external and internal stresses increase (Hipp et al., 2019). Notably, protein aggregates form in a variety of neurodegenerative pathologies such as Alzheimer's or Parkinson's. Protein aggregates are harmful for cells through their interference with surrounding structures and processes as well as the loss of functionality of the misfolded proteins themselves and requiring resources for detoxification. Cells employ three general pathways to detoxify protein aggregates and misfolded proteins: sequestration, refolding by chaperones and removal by autophagy or degradation by the ubiquitin-proteasome system.

A clear link exists between increased inheritance of protein aggregates (and other aging factors) and reduced replicative lifespan, as observed in Δ*sir2* deletion mutants. Sir2 is a histone deacetylase involved in the modulation of gene expression and has been found to be crucial for the retention of damaged proteins along with a decreased replicative lifespan (Aguilaniu et al., 2003). This loss of mother-daughter asymmetry was linked to Sir2s involvement in the expression of – amongst others – the actin cytoskeleton and the Myo2 motor protein (Song et al., 2014).

As the distribution of aggregates was observed to be asymmetrical with the mother cell retaining nearly all aggregates, a number of studies has tried to investigate whether this unequal distribution is achieved by an active mechanism actively transporting aggregates back from the daughter to the mother or blocking inheritance in the first place by for example a diffusion barrier for aggregates on the mother-bud neck. Inside the ER, a diffusion barrier dependent on septins and sphingolipids has been shown to confine misfolded proteins to the mother cell (Clay et al., 2014). Similar barriers govern the age-dependent asymmetric inheritance of nuclear pore complexes (Colombi et al., 2013; Shcheprova et al., 2008). Whether cytosolic protein aggregates are also affected by the diffusion barrier remains unknown. Alternatively, simulations were used to determine whether this phenomenon is based on stochastic effects making inheritance unlikely due to the geometric

constraints (Zhou et al., 2011) created by the mother-bud neck while others argue for various active mechanisms (Liu et al., 2010; Song et al., 2014; Spokoini et al., 2012). Generally, it remains unclear whether aggregates move through the cell by diffusion or through some other, more directed mode.

The molecular chaperone Hsp104 has been used as a marker to allow the observation of protein aggregates through fluorescence microscopy (Huh et al., 2003; Zhou et al., 2011). While *hsp104* mutants are viable and usually display a mostly wild type-like phenotype, the deletion mutant inherits protein aggregates symmetrically and produces offspring with reduced replicative lifespan (Erjavec et al., 2007; Spokoini et al., 2012).At least one observable Hsp104 focus is observable in most cells with numbers increasing with age, however it is necessary to note that aggregate formation is often induced by the application of external stressors in the form of chemicals or heat in these studies (Erjavec et al., 2007; Zhou et al., 2011). Consequently, the conclusions drawn from these studies only apply to the respective type of aggregates. Experiments observing heat-induced aggregates can, for example, only provide limited insights into natural aging processes. Through the use of time-lapse microscopy aggregates have been tracked over longer time periods and appeared to be transported back into the mother cell in a polarisome- and Sir2-dependent manner (Liu et al., 2010). The retention of protein aggregates and low-functioning mitochondria as well as the role of this retention in cellular aging have been linked to the differential inheritance of the microtubule-organizing centers (Manzano-Lopez et al., 2019).

Overall, asymmetric inheritance appears to rely on on at least three principles: sequestration in large deposit sites (Miller et al., 2015b), retrograde actin cable flow to transport aggregates in the bud towards the mother cell (Liu et al., 2010), and anchoring of aggregates at the mitochondrial and ER surfaces to limit their mobility (Spokoini et al., 2012; Zhou et al., 2014). However, little is understood especially about the last two models. It has been shown that heat stress causes the formation of a large number of cytosolic foci of aggegrated proteins termed CytoQ which over time coalesce into larger aggregates which are then stored in larger protein sequestration sites (Grousl et al., 2018; Kaganovich et al., 2008; Miller et al., 2015a). These sequestration sites are thought to differ in their ability to dissolve aggregates or retain them indefinitely although there have been contradictory findings regarding this. These sequestration sites are often directly linked to a specific organelle, thus linking the control of aggregate inheritance to the already controlled process of organellar inheritance (Spokoini et al., 2012). One of these sites sequestering insoluble proteins without the ability to dissolve them is the Insoluble Protein Deposit (IPOD) associated with the vacuole. It is typically associated with immobile aggregates and amyloid proteins that are commonly introduced into yeast cells for researching the corresponding diseases. In association with the nucleus the juxtanuclear quality control site (JUNQ) and the intranuclear quality control site (INQ) have been proposed. Whether INQ

and JUNQ represent two distinct sites or are actually the same structure remains a topic of discussion. Their close localization and overlap in substrates suggest they might only be one site while other studies describe differences in stress response and the requirement for substrate ubiquitination (Gallina et al., 2015; Mathew et al., 2017; Miller et al., 2015a). A recent paper suggested them to be for cytosolic and nuclear protein substrates respectively and describes them as two separate compartments in close proximity only separated by the nuclear envelope (Sontag et al., 2023). In contrast to IPOD, JUNQ and INQ are thought to harbor proteins for disaggregation, refolding and degradation. Cells that are unable to efficiently transport aggregates to the sequestration sites are unable to maintain their asymmetric inheritance.

There have been several processes described concerning the relationship between protein aggregates and mitochondria. One of these is the attachment of aggregates to the mitochondrial surface after being captured on the ER surface and transferred at ER-mitochondria organelle-organelle contact sites (Zhou et al., 2014). The proportion of protein aggregates colocalizing with mitochondria and the ER gradually declines with progressing replicative age of the mother cell. Anchoring of protein aggregates to mitochondria could be an elegant mechanism linking aggregate retention with the proposed theory of selective inheritance of specific mitochondria. Supporting this idea, mitochondria in the bud have been found to usually not be associated with aggregates. In this model aggregates would preferentially be bound to mitochondria displaying lower fitness levels and thus be retained in the mother cell along with them. How aggregates are attached to the mitochondrial surface, which proteins are involved in this interaction or how they are transferred from the ER is unknown. The only currently known mutant displaying reduced aggregate-mitochondria colocalization is Δ*fis1*. Increasing mitochondrial transport towards the bud through the expression of the mitochondrially-anchored Myo2-Fis1 also enhances the amount of protein aggregates inherited by the daughter cell (Böckler et al., 2017). Interestingly, impaired mitochondrial transport caused by the *myo2(LQ)* mutant also results in an increased level of aggregate inheritance. Likely, the decreased mitochondrial mobility in these cells interferes with the binding of aggregates in order to limit their movement as the number of free aggregates is increased in this mutant.

Furthermore, aggregates formed inside of mitochondria have been found to be sequestered in a deposit site termed ‘intramitochondrial protein quality control compartment’ (IMiQ) which interestingly is dependent on active mitochondrial fission (Bruderek et al., 2018). This compartment appears to function solely as a deposit, not as a site for disaggregation or degradation. Accordingly, the IMiQ is retained by the mother cell during division. Additionally, it has even been shown that cytosolic proteins prone to aggregation are imported into mitochondria to be degraded by mitochondrial proteases (Ruan et al., 2017). It was also recently discovered that aggregation of

incorrectly processed mitochondrial proteins containing a N-terminal mitochondrial targeting sequence in the mitochondrial matrix triggers a mitochondrial unfolded protein response-like pathway (Poveda-Huertes et al., 2020). This immediate reaction ensures the maintenance of mitochondrial import and translation as well as mtDNA maintenance. Aggregates colocalizing with mitochondria have been shown to dissolve more quickly depending on mitochondrial function (Babazadeh et al., 2019). It also linked the relationship of aggregates and mitochondria to the ER, to Golgi anterograde trafficking, and vCLAMP vacuole-mitochondria contact sites, thus linking aggregate clearance to spatial protein quality control as well as revealing the involvement of a large variety of cellular components and processes with mitochondria-aggregate relations. Overall, a number of connections between protein aggregates and mitochondria have been discovered but much about their interaction remains unresolved.

1.4 Aim of the thesis

The asymmetric inheritance of both cytosolic protein aggregates and mitochondria have been observed in *S. cerevisiae* although the mechanism and regulation of both remain largely unknown. The goal of this thesis was to gain insights into pathways or identify factors involved in these two processes.

To investigate the retention of aggregates in the mother cell and their proposed attachment to the ER and the mitochondrial outer membrane the behavior of aggregates in different mutated yeast cells was examined. The aim for this project was the identification of mitochondrial proteins influencing the retention and behavior of protein aggregates. Furthermore, the project wanted to contribute to the understanding of cellular processes and non-protein factors involved in the asymmetric inheritance of protein aggregates. For these experiments protein aggregation was induced by heat shock and aggregates were traced in fluorescence microscopy using the inactive *hsp104*^{Y662A}*-GFP* allele. Based on recent publications, cells displaying blocked mitochondrial import or deletions of a set of candidate genes were examined (Boos et al., 2019; Hansen et al., 2018). Furthermore, the septin cytoskeleton has previously been shown to act as a diffusion barrier for aging factors between mother and daughter cells during inheritance and was thus a further candidate structure for closer examination (Clay et al., 2014).

A second objective was the examination of mitochondrial inheritance and the search for potentially unknown proteins involved in the recruitment of Myo2 to mitochondria or mitochondrial transport and inheritance. As described in chapter 1.2.4. the current state of knowledge about the recruitment of Myo2 to mitochondria and the observed effects of the deletion of *MMR1* and *YPT11* both separately and simultaneously could point towards another protein's involvement in this process. To investigate this the mitochondrial inheritance was scored using fluorescence microscopy in a set of deletion mutants that were chosen based on an educated guess approach. Additionally, a genome-wide multicopy suppressor screen in Δ*mmr1* Δ*ypt11* cells that are unable to transport mitochondria was performed to identify genes whose overexpression can rescue mitochondrial inheritance.

Furthermore, another goal was to gain insights into the existence of a quality control mechanism of mitochondria during mitochondrial inheritance and consequently the identification of factors involved in this mechanism. For this, it was necessary to first establish a tool for the specific induction of oxidative stress inside mitochondria and confirm and characterize the functionality and effectivity of this tool. In order to observe the effect of oxidative stress on mitochondrial inheritance it was a goal to establish Su9-DAO as a tool to produce intramitochondrial ROS and to optimize assays that allowed its use in microscopy experiments. In this system the Su9-DAO enzyme is directed to the mitochondrial matrix by the Su9 mitochondrial targeting sequence where then it deaminates D-amino acids and

produces hydrogen peroxide as a byproduct (Pollegioni et al., 2002). The effects of Su9-DAO-caused oxidative stress originating inside of mitochondria on known factors in mitochondrial inheritance like Myo2-localization and the actin cytoskeleton were observed and compared to the effects of external hydrogen peroxide treatment for the validation of the new tool. Subsequently, the Su9-DAO system was used to further understand the molecular mechanism behind selective mitochondrial inheritance in *S. cerevisiae* through attempts to overcome this selective mitochondrial inheritance using several, different methods to enforce mitochondrial transport towards the daughter and by examining the effects of the removal of factors with known functions in inheritance. These experiments allowed the identification of an important protein involved in mitochondrial quality control during mitochondrial inheritance.

2 Materials and methods

2.1 Yeast cell biology and genetics

2.1.1 Yeast strains

All strains used in this study are listed in Table 1. Strains marked with BYx resulted from tetrad dissection so their markers, especially *LYS2* and *MET15* in relation to the mating type may not be corresponding to BY4741 and BY4742.

Table 1: List of yeast strains used in this study

Isogenic	Name	Genotype	Source
BY4741	BY4741 WT	*MAT*a *his3Δ1 leu2Δ0 met15Δ0 ura3Δ0*	Brachmann et al., 1998
BY4742	BY4742 WT	*MAT*alpha *his3Δ1 leu2Δ0 lys2Δ0 ura3Δ0*	Brachmann et al., 1998
BYx	*CDC10-AID*-6FLAG*	*MAT*a *his3Δ leu2Δ met15Δ ura3Δ CDC10-AID*-6FLAG::hphB*	this study
BYx	*CDC10-AID*-6FLAG OsTIR1*	*MAT*a *his3Δ leu2Δ ura3Δ CDC10-AID*-6FLAG::hphB ho::ADH1p-OsTIR1-KanMX4*	this study
BY4743	*CDC11-AID* OsTIR1*	*MAT*a/alpha *leu2Δ0/leu2Δ0 met15Δ0/MET15 lys2Δ0/LYS2 his3Δ1/his3Δ1 ura3Δ0/ura3Δ0 CDC11-AID*::hphB/CDC11 ho::ADH1p-OsTIR1-KanMX4/HO*	this study
BYx	*CDC11-AID*-6FLAG OsTIR1* hsp104^{Y662A}-GFP	*MATalpha leu2Δ0 lys2Δ0 his3Δ1 ura3Δ0 CDC11-AID*-6FLAG::hphB ho::ADH1p-OsTIR1-KanMX4 hsp104Y662A-GFP::HIS3*	this study
BYx	*CDC11-AID**	*MAT*alpha *leu2Δ0 lys2Δ0 his3Δ1 ura3Δ0 CDC11-AID*::hphB*	this study
BY4743	*CDC11-AID*-6FLAG*	*MAT*a/alpha *leu2Δ0/leu2Δ0 met15Δ0/MET15 lys2Δ0/LYS2 his3Δ1/his3Δ1 ura3Δ0/ura3Δ0 CDC11-AID*-6FLAG::hphB/CDC11*	this study
BY4743	*CDC11-AID*-6FLAG OsTIR1*	*MAT*a/alpha *leu2Δ0/leu2Δ0 met15Δ0/MET15 lys2Δ0/LYS2 his3Δ1/his3Δ1 ura3Δ0/ura3Δ0 CDC11-AID*-6FLAG::hphB/CDC11 ho::ADH1p-OsTIR1-KanMX4/HO*	this study
BYx	*CDC11-AID*-6FLAG OsTIR1*	*MAT*a *leu2Δ0 met15Δ0 his3Δ1 ura3Δ0 CDC11-AID*-6FLAG::hphB ho::ADH1p-OsTIR1-KanMX4*	this study
BYx	*CDC11-AID*-6FLAG OsTIR1* hsp104^{Y662A}-GFP	*MAT*a *leu2Δ0 met15Δ0 his3Δ1 ura3Δ0 CDC11-AID*-6FLAG::hphB ho::ADH1p-OsTIR1-KanMX4 hsp104Y662A-GFP::HIS3*	this study
S288C	*cdc12-1* YYB440	*MAT*a, *his3-Δ200 leu2 ura3-52 lys2-801 ade2-101 trp1-Δ63 cdc12-1*	Barral et al., 2000
S288C	*cdc12-1* YYB440 hsp104^{Y662A}-GFP	*MAT*a, *his3-Δ200 leu2 ura3-52 lys2-801 ade2-101 trp1-Δ63 cdc12-1 hsp104Y662A-GFP::HIS3*	this study
S288C	*cdc12-6* YYB440 hsp104^{Y662A}-GFP	*MAT*a, *his3-Δ200 leu2 ura3-52 lys2-801 ade2-101 trp1-Δ63 cdc12-6 hsp104Y662A-GFP::HIS3*	this study

Isogenic	Name	Genotype	Source
S288C	*cdc12-6* YYB970	*MAT*a, *his3-Δ200 leu2 ura3-52 lys2-801 ade2-101 trp1-Δ63 cdc12-6*	Barral et al., 2000
BY4743	*CDC12-AID*-6FLAG*	*MAT*a/alpha *leu2Δ0/leu2Δ0 met15Δ0/MET15 lys2Δ0/LYS2 his3Δ1/his3Δ1 ura3Δ0/ura3Δ0 CDC12-AID*-6FLAG::hphB/CDC11*	this study
BY4743	*CDC12-AID*-6FLAG OsTIR1*	*MAT*a/alpha *leu2Δ0/leu2Δ0 met15Δ0/MET15 lys2Δ0/LYS2 his3Δ1/his3Δ1 ura3Δ0/ura3Δ0 CDC12-AID*-6FLAG::hphB/CDC11 ho::ADH1p-OsTIR1-KanMX4/HO*	this study
BY4741	hsp104^{Y662A}-GFP	*MAT*a *his3Δ1 leu2Δ0 met15Δ0 ura3Δ0 hsp104Y662A-GFP::HIS3*	Zhou et al., 2011
BY4742	hsp104^{Y662A}-GFP *OsTIR1*	*MAT*alpha *his3Δ1 leu2Δ0 lys2Δ0 ura3Δ0 hsp104Y662A-GFP::HIS3 ho::ADH1p-OsTIR1-KanMX4/HO*	this study
BY4741	hsp104^{Y662A}-mCherry	*MAT*a *his3Δ1 leu2Δ0 met15Δ0 ura3Δ0 hsp104 Y662A-mCherry::hphMX4*	Liu et al., 2011
BY4741	MMR1-yEGFP	*MAT*a *his3Δ1 leu2Δ0 met15Δ0 ura3Δ0 MMR1-yeGFP::CaURA3*	this study
BY4741	MMR1-yEGFP Su9-DAO	*MAT*a *his3Δ1 leu2Δ0 met15Δ0 ura3Δ0 ho::Su9-DAO::natMX mmr1-yeGFP::CaURA3*	this study
BY4741	MYO2-yEGFP	*MAT*a *his3Δ1 leu2Δ0 met15Δ0 ura3Δ0 myo2-yeGFP::CaURA3*	this study
BY4741	MYO2-yEGFP Su9-DAO	*MAT*a *his3Δ1 leu2Δ0 met15Δ0 ura3Δ0 ho::Su9-DAO::natMX myo2-yeGFP::CaURA3*	Chelius et al., 2023
BY4743	WT	*MAT*a/alpha *leu2Δ0/leu2Δ0 met15Δ0/MET15 lys2Δ0/LYS2 his3Δ1/his3Δ1 ura3Δ0/ura3Δ0*	N. Hock, Zellbiologie, Bayreuth
BY4741	WT Su9-DAO	*MAT*a *his3Δ1 leu2Δ0 met15Δ0 ura3Δ0 ho::Su9-DAO::natMX*	Chelius et al., 2023
S288C	WT YYB384	*MAT*a, *his3-Δ200 leu2 ura3-52 lys2-801 ade2-101 trp1-Δ63*	Barral et al., 2000
S288C	WT YYB384 hsp104^{Y662A}-GFP	*MAT*a, *his3-Δ200 leu2 ura3-52 lys2-801 ade2-101 trp1-Δ63 hsp104Y662A-GFP::HIS3*	this study
BY4741	Δ*age2* hsp104^{Y662A}-GFP	*MAT*a *his3Δ leu2Δ met15Δ ura3Δ Δage2::kanMX4 hsp104Y662A-GFP::HIS3*	this study
BY4741	Δ*aim32* hsp104^{Y662A}-GFP	*MAT*a *his3Δ leu2Δ met15Δ ura3Δ Δaim32::kanMX4 hsp104Y662A-GFP::HIS3*	this study
BY4741	Δ*arl1* hsp104^{Y662A}-GFP	*MAT*a *his3Δ leu2Δ met15Δ ura3Δ Δarl1::kanMX4 hsp104Y662A-GFP::HIS3*	this study
BY4741	Δ*bar1*	*MAT*a *his3Δ1 leu2Δ0 met15Δ0 ura3Δ0 Δbar1::kanMX4*	Giaever et al., 2002
BY4741	*Δbar1* Su9-DAO	*MAT*a *his3Δ1 leu2Δ0 met15Δ0 ura3Δ0 ho::Su9-DAO::natMX Δbar1::hphNT1*	this study
BY4741	Δ*caf4*	*MAT*a *his3Δ1 leu2Δ0 met15Δ0 ura3Δ0 Δcaf4::kanMX4*	Giaever et al., 2002
BY4741	Δ*djp1* hsp104^{Y662A}-GFP	*MAT*a *his3Δ leu2Δ met15Δ ura3Δ Δdjp1::kanMX4 hsp104Y662A-GFP::HIS3*	this study
BY4741	Δ*dpi8*	*MAT*a *his3Δ1 leu2Δ0 met15Δ0 ura3Δ0 Δdpi8::kanMX4*	this study
BY4741	Δ*ema17* hsp104^{Y662A}-GFP	*MAT*a *his3Δ leu2Δ met15Δ ura3Δ Δema17::kanMX4 hsp104Y662A-GFP::HIS3*	this study
BY4741	Δ*ema19* hsp104^{Y662A}-GFP	*MAT*a *his3Δ leu2Δ met15Δ ura3Δ* Δema*19::kanMX4 hsp104Y662A-GFP::HIS3*	this study

Isogenic	Name	Genotype	Source
BY4741	Δ*ema35* hsp104^{Y662A}-GFP	*MAT*a *his3Δ leu2Δ met15Δ ura3Δ Δema35::kanMX4 hsp104Y662A-GFP::HIS3*	this study
BY4741	Δ*fis1*	*MAT*a *his3Δ1 leu2Δ0 met15Δ0 ura3Δ0 Δfis1::kanMX4*	Giaever et al., 2002
BY4741	Δ*fis1* hsp104^{Y662A}-GFP	*MAT*a *his3Δ1 leu2Δ0 met15Δ0 ura3Δ0 Δfis1::kanMX4 hsp104Y662A-GFP::HIS3*	This study
BY4741	Δ*fmp52*	*MAT*a *his3Δ1 leu2Δ0 met15Δ0 ura3Δ0 Δfmp52::kanMX4*	Giaever et al., 2002
BY4741	Δ*fun14*	*MAT*a *his3Δ1 leu2Δ0 met15Δ0 ura3Δ0 Δfun14::kanMX4*	B. Westermann, Zellbiologie, Bayreuth
BY4741	Δ*fzo1* Δ*dnm1* hsp104^{Y662A}-GFP	*MAT*a *his3Δ1 leu2Δ0 met15Δ0 ura3Δ0 Δfzo1::kanMX4 Δdnm1::kanMX4 hsp104Y662A-GFP::HIS3*	X. Chelius, Zellbiologe, Bayreuth
BY4741	Δ*gem1*	*MATalpha his3Δ1 leu2Δ0 lys2Δ0 MET15 ura3Δ0 Δgem1::kanMX4*	J. König, Zellbiologie, Bayreuth
BY4741	Δ*idp2* hsp104^{Y662A}-GFP	*MAT*a *his3Δ leu2Δ met15Δ ura3Δ Δidp2::kanMX4 hsp104Y662A-GFP::HIS3*	this study
BY4741	Δ*iml2*	*MAT*a *his3Δ1 leu2Δ0 met15Δ0 ura3Δ0 Δiml2::kanMX4*	Giaever et al., 2002
BY4741	Δ*mco1*	*MAT*a *his3Δ1 leu2Δ0 met15Δ0 ura3Δ0 Δmco13::kanMX4*	this study
BY4741	Δ*mcp1*	*MAT*a *his3Δ1 leu2Δ0 met15Δ0 ura3Δ0 Δmcp1::kanMX4*	Giaever et al., 2002
BY4741	Δ*mcy1*	*MAT*a *his3Δ1 leu2Δ0 met15Δ0 ura3Δ0 Δmcy1::kanMX4*	Giaever et al., 2002
BY4741	Δ*mmr1*	*MAT*a *his3Δ1 leu2Δ0 met15Δ0 ura3Δ0*	Giaever et al., 2002
BYx	Δ*mmr1 Su9-DAO*	*MAT*a *his3Δ1 leu2Δ0 LYS2 MET15 ura3Δ0 Δmmr1::kanMX4 ho::Su9-DAO::NatMX*	Chelius et al., 2023
BY4743	Δ*mmr1* Δ*ypt11*	*MAT*a/alpha *his3Δ1/his3Δ1 leu2Δ0/leu2Δ0 ura3Δ0/ura3Δ0 LYS2/lys2Δ MET15/met15Δ Δypt11::HISMX6/YPT11 Δmmr1::kanMX4/MMR1*	this study
BY4743	Δ*mmr1* Δ*ypt11* *	*MAT*a/alpha *leu2Δ0/leu2Δ0 met15Δ0/MET15 lys2Δ0/LYS2 his3Δ1/his3Δ1 ura3Δ0/ura3Δ0 Δypt11::HIS3MX6/Δypt11::HIS3MX6 Δmmr1::kanMX4/Δmmr1::kanMX4*	this study
BYx	Δ*mmr1* Δ*ypt11* *	*MAT*a *leu2Δ0 lys2Δ0 his3Δ1 ura3Δ0 Δypt11::HIS3MX6 Δmmr1::kanMX4*	this study
BYx	Δ*mmr1* Δ*ypt11* *	*MAT*alpha *leu2Δ0 met15Δ0 his3Δ1 ura3Δ0 Δypt11::HIS3MX6 Δmmr1::kanMX4*	this study
BY4741	Δ*mmr1* Δ*ypt11* †	*MAT*a *his3Δ1 leu2Δ0 LYS2 met15Δ0 ura3Δ0 Δmmr1::kanMX4 Δypt11::HISMX6*	this study
BY4741	Δ*mmr1* Δ*ypt11 Su9-DAO* †	*MAT*a *his3Δ1 leu2Δ0 LYS2 met15Δ0 ura3Δ0 Δmmr1::kanMX4 Δypt11::HISMX6 ho::Su9-DAO::NatMX*	this study
BY4741	Δ*msc7*	*MAT*a *his3Δ1 leu2Δ0 met15Δ0 ura3Δ0 Δmsc7::kanMX4*	Giaever et al., 2002
BY4741	Δ*om14*	*MAT*a *his3Δ1 leu2Δ0 met15Δ0 ura3Δ0 Δom14::kanMX4*	Giaever et al., 2002
BY4741	Δ*om45*	*MATa his3Δ1 leu2Δ0 met15Δ0 ura3Δ0 Δom45::kanMX4*	Giaever et al., 2002
BY4741	Δ*pet10*	*MATa his3Δ1 leu2Δ0 met15Δ0 ura3Δ0 Δpet10::kanMX4*	Giaever et al., 2002

Isogenic	Name	Genotype	Source
BY4741	Δ*pex21* hsp104^{Y662A}-GFP	*MAT*a *his3Δ leu2Δ met15Δ ura3Δ Δpex21::kanMX4 hsp104Y662A-GFP::HIS3*	this study
BY4741	Δ*por2*	*MAT*a *his3Δ1 leu2Δ0 met15Δ0 ura3Δ0 Δpor2::kanMX4*	Giaever et al., 2002
BY4741	Δ*ppa2*	*MAT*a *his3Δ1 leu2Δ0 met15Δ0 ura3Δ0 Δppa2::kanMX4*	Giaever et al., 2002
BY4741	Δ*ptc1*	*MAT*a *his3Δ1 leu2Δ0 met15Δ0 ura3Δ0 Δptc1::kanMX4*	Giaever et al., 2002
BY4741	Δ*ptc1 Su9-DAO*	*MAT*a *his3Δ1 leu2Δ0 met15Δ0 ura3Δ0 Δptc1::kanMX4 ho::Su9-DAO::natMX*	this study
BY4741	Δ*puf3*	*MAT*a *his3Δ1 leu2Δ0 met15Δ0 ura3Δ0 Δpuf3::kanMX4*	Giaever et al., 2002
BY4741	Δ*scm4*	*MAT*a *his3Δ1 leu2Δ0 met15Δ0 ura3Δ0 Δscm4::kanMX4*	Giaever et al., 2002
BY4741	Δ*set2* hsp104^{Y662A}-GFP	*MAT*a *his3Δ leu2Δ met15Δ ura3Δ Δset2::kanMX4 hsp104Y662A-GFP::HIS3*	this study
BY4741	Δ*tmh11*	*MAT*a *his3Δ1 leu2Δ0 met15Δ0 ura3Δ0 Δtmh11::kanMX4*	Giaever et al., 2002
BY4741	Δ*tmh18*	*MAT*a *his3Δ1 leu2Δ0 met15Δ0 ura3Δ0 Δtmh18::kanMX4*	Giaever et al., 2002
BY4741	Δ*ubp16*	*MAT*a *his3Δ1 leu2Δ0 met15Δ0 ura3Δ0 Δubp16::kanMX4*	Giaever et al., 2002
BY4741	Δ*ubx2*	*MAT*a *his3Δ1 leu2Δ0 met15Δ0 ura3Δ0 Δpor2::kanMX4*	Giaever et al., 2002
BY4741	Δ*whi2* hsp104^{Y662A}-GFP	*MAT*a *his3Δ1 leu2Δ0 met15Δ0 ura3Δ0 Δwhi2::kanMX4 hsp104Y662A-GFP::HIS3*	This study
BY4741	Δ*ygr266w*	*MAT*a *his3Δ1 leu2Δ0 met15Δ0 ura3Δ0 Δygr266w::kanMX4*	Giaever et al., 2002
BY4741	Δ*yim1*	*MAT*a *his3Δ1 leu2Δ0 met15Δ0 ura3Δ0 Δyim1::kanMX4*	Giaever et al., 2002
BY4741	Δ*ynr021w*	*MAT*a *his3Δ1 leu2Δ0 met15Δ0 ura3Δ0 Δynr021::kanMX4*	Giaever et al., 2002
BY4741	Δ*ypt11*	*MAT*alpha *his3Δ1 leu2Δ0 lys2Δ0 ura3Δ0 Δypt11::HISMX6*	this study
BY4741	Δ*ypt11*	*MAT*a *his3Δ1 leu2Δ0 met15Δ0 ura3Δ0 Δypt11::kanMX4*	Giaever et al., 2002
BY4741	Δ*ypt11 Su9-DAO*	*MAT*a *his3Δ1 leu2Δ0 met15Δ0 ura3Δ0 Δypt11::kanMX4 ho::Su9-DAO::natMX*	Chelius et al., 2023
BY4741	Δ*ypt31*	*MAT*a *his3Δ1 leu2Δ0 met15Δ0 ura3Δ0 Δypt31::kanMX4*	Giaever et al., 2002
BY4741	Δ*ypt32*	*MAT*a *his3Δ1 leu2Δ0 met15Δ0 ura3Δ0 Δypt32::kanMX4*	Giaever et al., 2002
BY4741	Δ*ypt7*	*MAT*a *his3Δ1 leu2Δ0 met15Δ0 ura3Δ0 Δypt11::kanMX4*	Giaever et al., 2002
BY4741	Δ*ysc83*	*MAT*a *his3Δ1 leu2Δ0 met15Δ0 ura3Δ0 Δysc83::kanMX4*	Giaever et al., 2002

* These strains were complemented with pRS416-*MMR1*.

† These strains were complemented with pRS416-Tom20-Inp2-GFP.

2.1.2 Media and cultivation of yeast

Yeast cells were cultivated on complete medium (YP) or synthetic complete medium (SC) as described in Sherman (2002) using 0.67% yeast nitrogen base (YNB) with ammonium sulfate and without amino acids and with 2% glucose (D), 2% galactose (Gal) or 3% glycerol and 2% EtOH (GE). Alternatively, SC medium was supplemented with a synthetic complete mix which was modified to achieve optimal growth in the BY strain background (see Table 2, composition modified from Hanscho et al., 2012). Optional supplements were omitted as described in Table 2 for marker selection. Media for agar plates additionally contained 2% agar. For SC plates with antibiotics and all experiments involving Su9-DAO instead of YNB, 0.1% monosodium glutamate (MSG) and 0.17% YNB without ammonium sulfate and amino acids were used.

Table 2: Composition of BY-optimized synthetic complete mix

Constituent	**Final concentration [mg/l]**
Adenine Sulfate	40
L-Arginine-HCl	20
L-Aspartic acid	100
L-Glutamic acid	100
Myo-Inositol	4
L-Tyrosine	30
L-Phenylalanine	50
L-Serine	375
L-Threonine	200
L-Valine	150
Optional supplements	
Constituent	**Final concentration [mg/l]**
L-Histidine	40
L-Leucine	110
L-Lysine	120
L-Methionine	40
L-Tryptophane	60
Uracil	40

The standard incubation temperature for liquid culture and cultivation on agar plates was 30°C unless otherwise indicated. Liquid cultures were grown in glass tubes or flasks and agitated at 150 rpm in an orbital motion. For yeast stocks cell material was resuspended in 15% glycerol and frozen at -80°C for permanent storage.

2.1.3 Transformation of yeast

Homologous recombination for genomic tagging or knockout of genes was performed using plasmids and primer design described in Longtine et al. (1998), Janke et al. (2004), Sheff and Thorne (2004) or

by amplification of large DNA fragments from genomic DNA (gDNA) including large flanking homologous sequences. For transformation, cells were grown to stationary phase in liquid culture overnight, diluted and incubated further until harvest during the logarithmic growth phase. Cells were resuspended in a transformation mix consisting of 33% PEG4000 (w/v), 0.1 M lithium acetate (pH 7.5), 0.27 mg/ml denatured single-stranded salmon sperm carrier DNA and ≥ 1 µg transformation DNA. Cells were incubated in the transformation mix at room temperature without shaking for at least 90 min and subsequently a 42°C heat shock was performed for 30 min. Cells were then pelleted, resuspended in sterile ddH_20 and plated on appropriate selection medium if the transformed DNA complemented an auxotrophy marker. For selection markers conferring antibiotic resistance the cells were plated on YPD complete medium and transferred to the appropriate selection plate after incubation overnight on the following morning using sterile velvet. Temperature sensitive strains and otherwise difficult to transform strains were incubated in the transformation mix overnight and plated on an appropriate medium plate. For the transformation of plasmids, the incubation in transformation mix was omitted and cells were directly subjected to heat shock for 1 h. After incubation for several days single colonies were picked and streaked onto a second selection plate to make sure the selection marker was permanently integrated.

The correct insertion of DNA after homologous recombination was checked via colony PCR using a cassette specific primer paired with primer(s) binding to genomic sequences.

2.1.4 Mating, sporulation and tetrad dissection

For mating of haploid cells of different mating types, roughly equal volumes of cell mass from both mating partners from agar plates were resuspended in liquid YPD medium and incubated at standard conditions for at least 6 h to allow mating. Afterwards 150 µl culture volume was plated on appropriate selection medium selecting diploid cells and incubated for 2 days. From there single colonies were picked and streaked onto a second diploid selection plate and incubated overnight to ensure cells were diploid.

To increase sporulation efficiency cells were always taken from complete medium (YPD/YPG) agar plates. Sporulation media plates contained 1% (w/v) potassium acetate and 2% (w/v) agar. The cells were streaked onto sporulation media in patches and were allowed to sporulate for 7 to 14 days at 22°C. During this time sporulation efficiency was checked microscopically until a sufficient sporulation rate for tetrad dissection was reached.

Tetrad dissection was done using a micromanipulator (Singer MSM Series 300 with an Acer n30 pocket PC, Singer Instruments). For this a small amount of cell material was resuspended in sterile ddH_2O and asci were digested by incubation with zymolyase (final concentration 2 mg/ml) for 10 min at room temperature. Afterwards a small volume of cell suspension was pipetted on the side of a YPD or YPG agar plate and allowed to dry. Per plate 16 tetrads were dissected and placed in a grid to keep track of which colonies belonged to the same tetrad. The plates were incubated for several days and then photographed before the colonies were transferred to selection media using sterile velvet for genotyping. Only complete tetrads with correct segregation of marker alleles were used for further experiments. Genotypes and mating types were verified by colony PCR.

2.1.5 Aggregate retention efficiency (ARE) Assay

Stationary overnight cultures were diluted 1:10 in 2 ml fresh selection medium and incubated for ~3 h. To distinguish buds and cells formed after heat shock a calcofluor staining was performed (see 2.2.2). For the heat shock cells were incubated at 42°C for 5 min while shaking and subsequently cooled shortly on ice. The cultures were transferred to tubes and incubated for at least 3 h at 30°C to allow recovery from the heat shock, fusion of aggregates and the formation of new buds. Afterwards the cells were fixed with formaldehyde (see 2.2.1) and stored at 4°C until microscopy.

The aggregate retention efficiency was defined as the percentage of cells with small to medium sized buds not stained with calcofluor (so formed after heat shock) which did not contain aggregates. Colocalization of aggregates with mitochondria was evaluated manually in z-stacks (not-projected).

2.1.6 Clogger assay with ARE

The ‘Clogger’ plasmids were kindly provided by the Johannes Herrmann lab, University of Kaiserslautern, Germany.

Cultures were grown to stationary phase overnight in SC-LU medium with 2% raffinose (Raf) + 0.1% dextrose (D). Then the cultures were diluted 1:10 in SCRaf-LU and incubation was continued for 3 h. Expression was induced by the addition of Gal (2% final concentration) followed by incubation for 1 h. If necessary for the experiment, a calcofluor staining war performed at this point (see 2.2.2). For the heat shock 500 µl culture were harvested and resuspended in 200 µl YPGal. Heat shock and the following steps were performed as described in 2.1.5.

2.1.7 Auxin-inducible degron (AID) assay (with ARE Assay)

The cell cultures were grown to stationary phase overnight in 10 or 20 ml YPD for blotting or SCGal-L + 2% Raff or SCD-L for microscopy. All cultures were then diluted to an OD_{600} of 0.1 in YPD/SCGal-L/SCD-L and incubation was continued for at least 3 h. The degron was induced by addition of 0.5 mM 1-naphthaleneacetic acid (NAA) or indole-3-acetic acid (IAA) to the culture medium. For microscopy in combination with ARE, cells in the logarithmic growth phase were submitted to 5 min heat shock at 42°C and afterwards immediately treated with 0.5 mM auxin. Samples were fixed with formaldehyde after 150 min recovery from the heat shock (see also 2.1.5).

2.1.8 Multicopy suppressor screen

The multicopy suppressor screen in this work aimed to identify unknown components involved in mitochondrial inheritance. For this the inviable double mutant Δ*mmr1* Δ*ypt11* was employed. A homozygous diploid Δ*mmr1* Δ*ypt11* strain was constructed by mating haploid double mutants containing the rescuing pRS416-MMR1 plasmid. A homozygous diploid strain was used for the screen to decrease the probability of rescue by suppressor mutations.

The 'minimal' set of the 'Yeast Genomic Tiling Collection' plasmid library which overexpresses 3 to 5 genes per plasmid was transformed using the lithium acetate/PEG-transformation described in 2.1.3 (Jones et al., 2008). This transformation was optimized in regards of used cell and DNA amounts to obtain at least 10,000 transformants to statistically cover the entire library several times. pAG415GPD-YPT11 was used as a positive control and the empty library vector (pGP564) as a negative control. Cells were plated on SCD-L media plates which selects for the library and control plasmids but allows the cells to lose the pRS416-MMR1 rescue plasmid. After incubation at 30°C for 3 days cells were replica plated onto SCD-L plates using sterile velvet and again incubated for 1 day. Next the cells were replica plated onto SCD-L and SCD-L plates + 0.1% (w/v) 5-fluoroorotic acid (5-FOA). 5-FOA allows selection against cells expressing the *URA3* gene, in this case cells that have not lost the original rescue plasmid. After incubation for 3 and 4 days single colonies that were able to grow on 5-FOA were picked from the corresponding SCD-L plate, streaked onto SCD-L and SCD-L + 5-FOA plates and incubated for 1 day. All candidates that showed reproducible growth on 5-FOA were picked again from the corresponding SCD-L plate and stocked in 15% glycerol in a 96-well plate. This stock plate was frozen at -80°C.

For further testing of the candidates, a ROTOR HDA robot (Singer Instruments) for automated replica plating of the stock plate and transfer to selection media in the 96-well format was used. From the

thawed and mixed stock 96-well plate, the cells were plated on SCD-L (selection for library plasmid) and incubated for 3 days. Next, the cells were replica plated to SCD-L again to achieve uniform colony size for the next step and incubated for 1 day. Then the colonies were replica plated onto SCD-L, SCD-U and SCD-L + 5-FOA plates. The SCD-U plates select for colonies that carry the pRS416-MMR1 rescue plasmid. After 1 and 2 days of incubation pictures of all plates were taken, and growth was analyzed and compared to controls.

Plasmids from all reproducible candidates were isolated by minipreps. Due to slow growth in liquid medium yeast cultures were grown in 2 ml precultures in SCD-L for 10 hours. The whole preculture was used to inoculate 10 ml overnight cultures in SCD-L. The following morning the whole cultures were harvested by centrifugation and the cell pellets were frozen at -20°C. Miniprep was performed using the QiaPrep Spin Miniprep Kit (Qiagen) with the manufacturer's recommended adjustments for isolation of plasmids ≥ 10 kb (larger buffer volumes: P1 = 500 µl, P2 = 500 µl, N3 = 700 µl; heat EB to 70°C before elution). Then the isolated plasmids were transformed into XL1Blue *E. coli* (Stratagene) or in difficult cases commercial 'OneShot TOP10F' Chemically Competent *E. coli*' (Thermo Fisher Scientific) using heat shock according to standard methods. The plasmids were isolated from *E. coli* using the QiaPrep Spin Miniprep Kit (Qiagen) as instructed and sequenced using the oligonucleotides 'pGP564 seq fw' and 'pGP564 seq rev' (see Table 3 to identify the identity of the rescuing plasmids by comparison with the library.

2.1.9 DAO assay

Cells were grown to stationary phase overnight in appropriate selection medium with MSG and YNB without ammonium sulfate. The cultures were then diluted to an OD_{600} = 0.05 and incubation was continued for about 10 h. During this time the doubling time of each culture was determined, and two overnight cultures were inoculated in a way that the cultures were still in the logarithmic growth phase on the following morning. The cells were thus kept in the logarithmic growing phase for ≥ 24 h which was found to be optimal for tubular mitochondrial morphology. For DAO induction 0.1 M D-alanine (D-Ala) or as a control L-alanine (L-Ala) were added to the cultures and incubation was continued for 3 h. Depending on the experiment the yeasts were either directly fixed using formaldehyde or microscopy was performed on live cells.

2.1.10 Culture synchronization with mating factor alpha

The following protocol was developed based on Futcher (1999) and Zhuk et al. (2017). Stationary overnight cultures grown in YPD were adjusted to the same optical density (OD_{600} = 0.1) and incubated for 3 h. 500 µl of the cultures were transferred to a new glass tube and 140 µM Alpha-Factor Mating Pheromone (Zymo Research) were added. If Δ*bar1* cells were used, only 5 µM alpha factor were used. After about 3 h incubation the cell cycle arrest was confirmed microscopically, and the cells were released by washing 3 times with sterile YPD. The cells were resuspended in fresh medium and incubated for up to 3 h. During this time samples were taken regularly to check cell cycle progression and bud sizes using a microscope until the desired bud size was reached and the cells were fixed using formaldehyde.

If synchronization was done concurrently with the DAO assay, alpha factor was added 1 h before DAO induction with D-Ala. After 3 h of cell cycle arrest, the cultures were released but incubation with D-Ala continued after washing. Bud sizes were regularly checked, and cells were fixed using formaldehyde when the newly formed buds had the desired size (about 120 min post release).

2.1.11 Drop dilution assay

Yeast cultures were incubated overnight in appropriate liquid media. On the following day the cultures were diluted to the same OD_{600} in sterile ddH_2O in the wells of a sterile 96-well plate and diluted 1:10 five times in sterile ddH_2O. The different serial dilutions were transferred to appropriate agar plates using a metal pin and incubated at appropriate temperatures. The agar plates were evaluated and photographed after several days of incubation.

2.2 Fluorescence microscopy

2.2.1 Microscopes and conditions

Fluorescence microscopy of living and fixed cells was performed using a Leica Dmi8 microscope (Leica Microsystems GmbH) with a HC PL APO 100x/1.40 oil objective, a Lumencor Spectra X light source and the following fluorescence filter sets: FITC: ex. 460-500 nm; em. 512-542 nm; TXR: ex. 540-580 nm; em. 592-668 nm; QUAD-P-T ex. 397-413 nm, 484-496 nm, 557-567 nm, 629-645 nm, em. external filter wheel 425-475 nm. The used camera was a DFC9000GT-VSC07400 with sCMOS sensor. For microscopy and image acquisition the Leica LAS X software was used (version 3.4.2.18368). Z-stacks were acquired

using the system optimized step size except for time-lapse microscopy where z-stacks were acquired with double the optimized step size. If multiple fluorescences were examined the order was ‘z then Lambda’.

Microscopy was performed either in live or fixed cells taken from logarithmic growing cultures unless indicated otherwise. For fixing cells, 3.7% formaldehyde was added to the cultures followed by 10 min incubation in darkness at room temperature while shaking. The samples were then washed twice with 1x PBS (137 mM NaCl, 2.7 mM KCl, 19 mM Na_2HPO_4, 1.7 mM $KH_2 PO_4$; pH 7.4). The fixed samples were stored at 4°C until microscopy for up to one week.

Image processing (cropping of images, cropping of z-stacks and z-projection) was performed using the Leica LAS X software (version 3.7.1.21655). For deconvolution of z-stacks in the Huygens Deconvolution Software (version 18.10, Scientific Volume Imaging) the ‘Express Wizard’ with standard settings was utilized on non-projected z-stacks. Further image processing (adjustment of contrast, cropping, overlaying channels, z-projection) was done using Adobe Photoshop CS5 (Adobe Systems) and Fiji (Schindelin et al., 2012).

2.2.2 Staining of cellular structures

Mitochondria were stained with mitochondrial targeted mtGFP, mtyEGFP or mtERFP expressed from plasmids. The ER was stained by expressing ymScarlet from p416GPD-CPY-ymScarlet-HDEL.

The actin cytoskeleton was stained with rhodamine phalloidine. For this, cells were first fixed with formaldehyde and washed as described in 2.2.1. Next, the cell pellets were resuspended in 20 µl 1x PBS and 2 µl rhodamine phalloidine (200 U/ml in methanol; Invitrogen) was added. This was incubated for 1 h in darkness while shaking. Afterwards the cells were washed four times in 1x PBS and subsequently resuspended in PBS and analyzed using fluorescence microscopy.

Staining of cell walls was conducted using the fluorescent dye calcofluor (Fluorescent Brightener 28, Sigma Aldrich). Cells were resuspended in 10 mM HEPES (pH 7.2) with 2% D with 25 µM calcofluor and incubated for 30 min while shaking. Afterwards the cells were washed with buffer once before being resuspended in appropriate selection medium and treated as required.

2.2.3 Time-lapse live-cell microscopy

For time-lapse microscopy in live cells logarithmic cultures were used. The cells were immobilized and analyzed using an 8-well µ-slide (uncoated; ibidi) coated with concanavalin A. For coating the wells were covered with 250 µl/ml concanavalin A in ddH_2O so that the bottom of the well was well covered by the liquid. The slide was left to dry overnight with open lid under a fume hood. Before use the coated well was washed three times with sterile ddH_20. Next, 300 µl culture were added to the well and cells were allowed to settle to the bottom for 15 min. The supernatant was carefully removed, and the well was washed with appropriate medium three times to remove unbound cells. Finally, the cells were covered with 300 µl medium. If cells were treated with H_2O_2, this medium included 0.5 mM H_2O_2. For continuous heat shock the incubation chamber of the microscope was set to 35.5°C 30 to 60 min before starting microscopy.

2.3 Cloning, plasmids and oligonucleotides

A full list of plasmids and oligonucleotides used in this study can be found in Table 3 and Table 4. Additionally, the 'minimal' plasmid set of the 'Yeast Genomic Tiling Collection' which overexpresses genomic fragments containing 3 to 5 genes per plasmid, was used in the multi-copy suppressor screen (Jones et al., 2008).

Table 3: Plasmids used and cloned in this study

Name	Characteristics (yeast ORI, yeast selection marker, promoter)	Expressed protein (yeast)	Reference
p416GPD	ARS/CEN, *URA3*, *GPD* prom	-	Mumberg et al., 1995
p416GPD-CPY-ymScarlet-HDEL	ARS/CEN, *URA3*, *GPD* prom	CPY-ymScarlet-HDEL	This study
p426ADH	2µ, *URA3*, *ADH1* prom.	-	Mumberg et al., 1995
p426GAL	2µ, *URA3*, *GAL1*	-	Mumberg et al., 1995
p426GAL-b2-DHFR	2µ, *URA3*, *GAL1*	b2(167)-DHFR	J. Herrmann, Kaiserslautern
p426GAL-b2Δ-DHFR	2µ, *URA3*, *GAL1*	b2(167)Δ-DHFR	J. Herrmann, Kaiserslautern
p426GAL-DHFR	2µ, *URA3*, *GAL1*	DHFR	J. Herrmann, Kaiserslautern
pAG415GPD-ccdB	ARS/CEN, *LEU2*, *GPD* prom.	-	Alberti et al., 2007
pAG415GPD-MMR1	ARS/CEN, *LEU2*, *GPD* prom.	Mmr1	Chelius et al., 2023
pAG415GPD-YPT11	ARS/CEN, *LEU2*, *GPD* prom.	Ypt11	Böckler et al., 2017
pGEM-T-Hsp104-Y662A-GFP	-	Hsp104-Y662A-GFP	Xenia Chelius, Zellbiologie, Bayreuth
pGP564	2µ, *LEU2*, -	-	Jones et al., 2008

Name	Characteristics (yeast ORI, yeast selection marker, promoter)	Expressed protein (yeast)	Reference
pHyg-AID*	-, HygR, -	AID*	Addgene #99515, Morawska and Ulrich, 2013
pHyg-AID*-6FLAG	-, HygR, -	AID*-6FLAG	Addgene #99519, Morawska and Ulrich, 2013
pKT0209	-, Ca*URA3*, -	yEGFP-CaUra3 (for C-terminal tagging of proteins)	Sheff and Thorn, 2004
pOsTIR1w/oGFP	-, kanMX4, *ADH1* prom	OsTIR1	Addgene #102883, Papagiannakis et al., 2017
pRS416	ARS/CEN, *URA3*, -	-	Sikorski and Hieter, 1989
pRS416-MMR1	ARS/CEN, *URA3*, *MMR1* prom.	Mmr1	This study
pRS416-myo2-fis1	ARS/CEN, *URA3*, *MYO2* prom.	Myo2-Fis1	Förtsch et al., 2011
pRS416-TOM20-INP2-GFP	ARS/CEN, *URA3*, *TOM20* prom.	Tom20-Inp2-GFP	Chelius et al., 2023
pRS425	2µ, *LEU2*, -	-	Sikorski and Hieter, 1989
pRS426-myo2-GFP-fis1	2µ, *URA3*, *MYO2* prom.	Myo2-GFP-Fis1	Förtsch et al., 2011
pXRNX-Su9-DAO	ARS/CEN, NatMX6, *TEF* prom.	Su9-DAO	Chelius et al., 2023
pYX122-mtGFP	ARS/CEN, *HIS3*, *TPI* prom	mtGFP	Westermann and Neupert, 2000
pYX142-mtERFP	ARS/CEN, *LEU2*, *TPI* prom.	mtERFP	Scholz et al., 2013
pYX142-mtGFP	ARS/CEN, *LEU2*, *TPI* prom.	mtGFP	Westermann und Neupert 2000
pYX142-yEGFP	ARS/CEN, *LEU2*, *TPI* prom.	yEGFP	Chelius et al 2023
ymScarlet	ARS/CEN, *LEU2*, *GPD* prom.	ymScarlet	Albakri et al., 2018

Cloning and amplification of plasmids was done using standard methods. PCR for cloning was performed using Phusion High-Fidelity DNA Polymerase (Thermo Fisher Scientific) or Allin HiFi DNA Polymerase (highQU) according to manufacturer's instructions. Minipreps were performed using the QiaPrep Spin Miniprep Kit (Qiagen). gDNA extractions from *S. cerevisiae* were performed using the cell material from 1 ml stationary overnight culture with the MasterPure Yeast DNA Purification Kit (Lucigen). To generate the ER marker p416GPD-CPY-ymScarlet-HDEL, the DNA sequence encoding the fluorophore was amplified from ymScarlet (Addgene #111917, Albakri et al., 2018). The DNA sequence encoding the signal sequence of CPY, the HDEL ER retention sequence and *Bam*HI/*Xho*I restriction site were added by using the primers 'CPY-mScarlet-HDEL fw1', 'CPY-mScarlet-HDEL fw2' and 'CPY-mScarlet-HDEL rev' in two subsequent PCRs. The amplicon was cloned into p416GPD using the *Bam*HI and *Xho*I sites (Mumberg et al., 1995). For pRS416-MMR1 *MMR1* was amplified from BY4741 WT gDNA including its endogenous promoter and terminator using 'MMR1-XhoI fw' and 'MMR1-SacI rev' and ligated into the *Xho*I and *Sac*I restriction sites of pRS416 (Sikorski and Hieter, 1989).

The DNA sequence encoding Su9-DAO was introduced to cells via the linearized integrative plasmid pXRNX-Su9-DAO (restriction digest with *Asc*I). Su9-DAO integration into the *HO* locus and unwanted tandem integration of the insert was tested for using the sequences recommended in the paper (primers 'DAO integr fw', 'DAO integr rev' and 'DAO tandem rev') describing the integrative plasmids (Chou et al., 2015).

For tagging of *CDC10*, *CDC11* and *CDC12* with AID*-6FLAG or AID*, the respective S2 and S3 tagging primers were used to amplify DNA from the template plasmids pHyg-AID*-6FLAG or pHyg-AID*. The DNA encoding the tag was introduced to the yeast genome via homologous recombination and the insertion was confirmed with suitable primers. OsTIR1 was introduced into the *HO* locus after amplifying the insert from pOsTIR1-w/oGFP using the primers 'OsTIR1 fw' and 'OsTIR1 rev' and insertion was confirmed with 'Kan fw' and 'HO rev'.

Tagging of *MYO2* and *MMR1* with yEGFP was achieved by amplifying the *yEGFP-CaURA3* cassette from pKT0209 with the primers 'MYO2 F5' and 'MYO2 R3' or 'MMR1 F5' and 'MMR1 R3' respectively and transforming the resulting DNA into yeast cells using heat shock. The genomic insertion was confirmed with 'TEF-Term fw' and 'MYO2 rev' or 'CaURA3 fw' and 'MMR1 rev'.

Table 4: Oligonucleotides used in this study

Name	Sequence 5'-3'
CaURA3 fw	TGGGTGGCCAAGAAGAAG
CDC10 fw	CCTCACATTTGATTGATTCTGC
CDC10 rev	CCAAACGAGAAGGTGATAGC
CDC10 S2	AATTCTTAATAACATAAGATATATAATCACCACCATTCTTATGAGATTCAATCGATGAATT CGAGCTCG
CDC10 S3	ATGCGAATAGTCGTTCCTCAGCTCATATGTCTAGCAACGCCATTCAACGTCGTACGCTGC AGGTCGAC
CDC11 fw	CATTATCAGGTGAATCTGTCG
CDC11 rev	AAATACTCCAAAGGTGGAGC
CDC11 S2	TATATATATAGAGAAAGAAGAAATAAGTGAGGAAGCCAAAAGCGGACTCAATCGATGA ATTCGAGCTCG
CDC11 S3	GAGAAATTGAAGCCAGGTTGGAAAAAGAGGCGAAAATCAAACAGGAAGAACGTACGCT GCAGGTCGAC
CDC12 fw	CAAGGAAATTGTCACACAATCC
CDC12 rev	CAGAACGGTACCTAAGTGC
CDC12 S2	GAGATAGGCGTTGAAATTGACGAGACAAAGAGGAAGACATTAATTAATCAATCGATGA ATTCGAGCTCG
CDC12 S3	AACTAGAAGAGCAGGTCAAAAGCTTGCAAGTAAAAAAATCCCATTTAAAACGTACGCTG CAGGTCGAC
CPY-mScarlet-HDEL fw1	ACTAGGCCTGTCCACTACACTCGCTAAGGCCATCTCAGTTTCTAAAGGTGAAGCAGT
CPY-mScarlet-HDEL fw2	TATAGGATCCATGAAAGCATTCACCAGTTTACTATGTGGACTAGGCCTGTCCACTACAC
CPY-mScarlet-HDEL rev	TAATCTCGAGTTACAATTCATCATGTTTGTATAATTCATCCATACCAC
DAO integr fw	GTTCATGTGTACAATGTTCATTATCTC
DAO integr rev	AGACAAGCTGTGACCGTCT
DAO tandem rev	ATTAGGTGATATCAGATCCACTAGC
HO rev	GCGTATTTCTACTCCAGCATTC
hphNT fw	TCGGGCGTACACAAATCG

Name	Sequence 5'-3'
Hsp104^{Y662A}GFP fw	AAACCTTCTGCACCATTTTTA
Hsp104^{Y662A}GFP rev	CCCGTATTCTAATAATGGACCA
Kan fw	CCGGATTCAGTCGTCACTCATGG
MMR1 F5	CCAACTTAACCTTCCTGTCCAAGTGGAGAAGAAGGAAAAAGGTGACGGTGCTGGTTTA
MMR1 fw	ACGGATGCTAATACTAGCGAAG
MMR1 R3	GTTTGTGTAAAATAAGTTAATTTAATTTGAAGTTGACGCTTCGATGAATTCGAGCTCG
MMR1 rev	GGTTTAGGTCGTGGTACTGCTG
MMR1-SacI rev	TTAATCGAGCTCACAAGCCCTTTGAAGTTCAG
MMR1-XhoI fw	ATATACTCGAGATACGGATTTTCACCAAAGC
MYO2 F5	AGTTGACCTTGTTGCCCAACAAGTCGTTCAAGACGGCCACGGTGACGGTGCTGGTTTA
myo2 fw	GATTAGAGGAATGGTGCAAGAC
MYO2 R3	TTAGCATTCATGTACAATTTTGTTTCTCGCGCCATCAGTTTCGATGAATTCGAGCTCG
myo2 rev	GATGACACGGTGGGAATAATGAGAG
osTIR1 fw	AATTATCCTGGGCACGAG
osTIR1 rev	ACTGTAAGATTCCGCCAC
osTIR1 seq fw	GATGCTTCTCCTGTTTGCC
pGP564 seq fw	GCGCGCAATTAACCCTCA
pGP564 seq rev	GCGAATTGGGTACCGGGC
TEF-Term fw	TTTCGCCTCGACATCATCTG

2.4 SDS-PAGE, western blotting and immunodetection

Cell extracts were prepared similarly as described in Kushnirov (2000). To prepare cell extracts, the equivalent of 2.5 OD_{600} values of cells in logarithmic growth phase were harvested from liquid cultures by centrifugation and washed with ddH_2O. The cells were next resuspended and incubated in 200 µl 0.2 M NaOH at room temperature for 10 min. Subsequently the cells were pelleted, the supernatant was discarded, and the pellet was resuspended in 1x SDS sample buffer (75 mM Tris-HCl pH 6.8, 10% glycerol, 4% β-mercaptoethanol, 2% SDS, 0.0025% bromophenol blue). The samples were either frozen at -80°C or loaded onto a SDS polyacrylamide gel immediately. Before gel loading, cell extracts were boiled at 95°C for 5 min while shaking and the cell debris was pelleted by centrifugation.

The cell extracts were loaded onto SDS polyacrylamide gels and proteins were separated by SDS-PAGE. The gels were discontinuous with 5% acrylamide-bisacrylamide (Roth) stacking gels (60 mM Tris-HCl pH 6.8; 0.1% SDS, 0.05% ammonium persulfate (APS) and 0.035% tetramethylethylenediamine (TEMED)) and 8% acrylamide-bisacrylamide resolving gels (385 mM Tris-HCl pH 8.8, 0.1% SDS, 0.05% APS and 0.035% TEMED). Gel electrophoresis was performed using the Mini-PROTEAN Tetra Electrophoresis System (BioRad) with SDS running buffer (0.1% SDS, 192 mM glycine, 25 mM Tris) at a current of 10 to 25 mA per gel.

Subsequently, the proteins were transferred to PVDF (BioRad) or nitrocellulose (Amersham Biosciences) membranes by semi-dry blotting using the same BioRad chambers for 1 h with

1.5 mA/cm^2. Transfer buffer (0.72% glycine; 0.152% Tris; 1% methanol) was used to wet all components and to fill the blotting chamber.

Table 5: List of antibodies used in this study. All antibodies were diluted in TBST with 2% milk powder.

Antibody	Organism	Use	Dilution	Source
anti-Hxk	rabbit	primary	1:15,000	100-4159, Biotrend Biochemikalien
anti-FLAG	mouse	primary	1:5,000	F3165, Sigma Aldrich
anti-rabbit HRP	goat	secondary	1:10,000	W4011, Promega
anti-mouse HRP	goat	secondary	1:10,000	#31440, Thermo Scientific

To confirm the transfer of protein, the membranes were stained with Ponceau solution (0.5% Ponceau S; 1% acetic acid) for 5 min and then destained using ddH_2O and TBST (6% Tris; 8.8% NaCl, 0.5% Tween20; pH 7.5). For blocking the membrane was incubated in TBST buffer with 2% milk powder for 1 to 2 h at room temperature on an orbital shaker. The membrane was then incubated with primary antibody (see Table 5) at 4°C overnight. The blot was washed 3 to 4 times in TBST and afterwards incubated with the secondary antibody for 1 to 2 h at room temperature. After again washing 3 to 4 times with TBST, the proteins were detected by adding developing solution consisting of 2 ml solution 1 (1.12% Tris, 0.025% luminol), 800 µl solution 2 (0.11% coumaric acid in DMSO), 2.4 µl 30% HCl and 2.2 ml ddH_2O to the membrane. Luminescence was detected with an ImageQuant LAS-4000 gel documentation unit (GE Healthcare).

3 Results

3.1 Investigations of the asymmetric inheritance of protein aggregates

Aging factors like protein aggregates are asymmetrically divided between cells during budding, leading to a mother cell with limited replicative lifespan and a rejuvenated daughter (Aguilaniu et al., 2003; Hill et al., 2016; Saarikangas et al., 2017; Spokoini et al., 2012; Zhou et al., 2011; Zhou et al., 2014). To achieve this one principle employed by cells is attaching protein aggregates to organellar surfaces or importing misfolded proteins into these organelles (Ruan et al., 2017; Zhou et al., 2014). This work focuses on the relationship between protein aggregates and mitochondria and investigating whether the proposed association of protein aggregates with the mitochondrial surface is mediated directly, for example via a specific binding protein.

To examine the connection between mitochondria and mitochondrial inheritance and the retention and sequestration of cytosolic protein aggregates, the catalytically inactive *Y662A* mutant of the molecular chaperone Hsp104 fused to GFP was used as an aggregate tracker (Zhou et al., 2011). This mutated enzyme binds protein aggregates but has no catalytic activity to dissolve them (Lum et al., 2004).

3.1.1 Investigating the relationship between mitochondria and protein aggregates

Zhou et al. (2014) performed a microscopy-based screen searching for mitochondrial outer membrane proteins that are involved in aggregate-mitochondria association by looking at the association between aggregates and mitochondria in deletion mutants of non-essential proteins located in the outer mitochondrial membrane. They found that deletion of the mitochondrial fission protein Fis1 results in reduction of the association of around 30%. They described this reduced association to also be accompanied by an increased leakage of aggregates into the daughter and a higher mobility of aggregates in general.

It was possible to reproduce the observation that the amount of Hsp104 foci colocalizing with mitochondria is strongly reduced in Δ*fis1* cells in this study (Figure 1A). As Δ*fis1* cells are known to frequently develop secondary mutations in the *WHI2* gene (Cheng et al., 2008), the mitochondria-aggregates association was also evaluated in the Δ*whi2* mutant but found to be comparable to WT. This confirms that the reduction of association is in fact caused by the lack of the Fis1 protein as opposed to the secondary mutation. Additionally, Δ*fzo1* Δ*dnm1* cells were included since a link

between mitochondrial dynamics and aggregate association has been described previously (Böckler et al., 2017). In the double knock-out mutant both the mitochondrial fission and fusion machineries are impaired which leads to morphologically wildtypical but static mitochondria. The double mutant cells displayed a reduced level of association compared to wild type cells. However, neither Δ*fzo1* Δ*dnm1*, Δ*whi2* nor the Δ*fis1* mutants displayed a decreased rate of aggregate retention in the mother cell (Figure 1B). Overall, even though the association of protein aggregates to mitochondria was lowered in Δ*fis1*, the aggregate retention efficiency was not affected. This could indicate that the interaction between aggregates and mitochondria is not crucial for the maintenance of the mother-daughter asymmetry. Most likely other redundant modes of retention are able to compensate for the loss of this system.

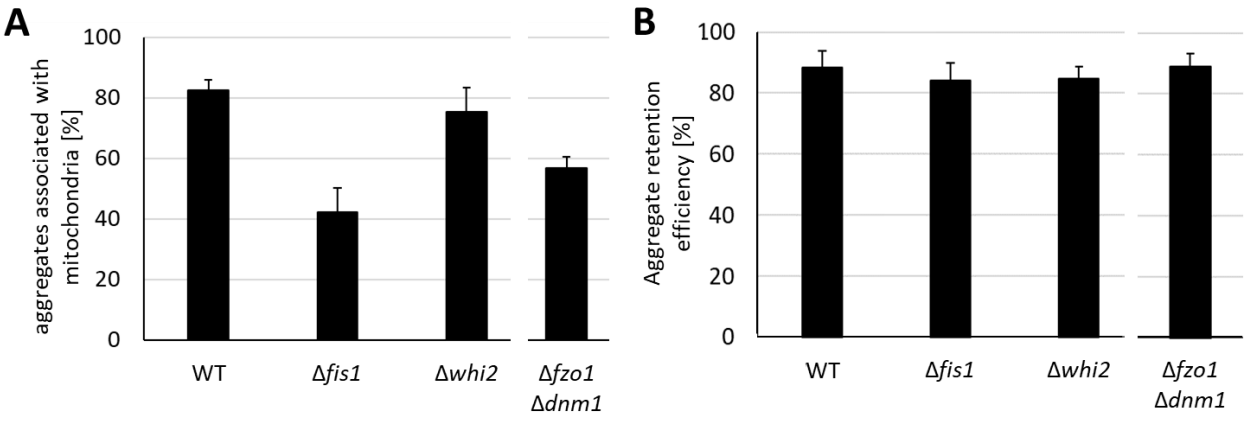

Figure 1: Investigating the relationship between mitochondria and protein aggregates (A) Analysis of the colocalization of protein aggregates and mitochondria. Cells of the indicated genotypes expressing Hsp104^{Y662A}-GFP and a mitochondrial marker were grown to logarithmic phase in selective medium. After calcofluor staining, heat shock was performed at 42°C for 5 min to induce aggregate formation. After 3 h incubation at 30°C, the cells were fixed in formaldehyde and analyzed by fluorescence microscopy. Aggregate-mitochondria association was quantified by checking the planes of z-stacks manually. At least 100 Hsp104-foci were analyzed per strain. Bars represent the mean percentages of three technical replicates and their standard deviation (SD). The data from the Δ*fzo1* Δ*dnm1* double mutant were performed in separate experiment that was performed identically. **(B)** Quantification of aggregate retention efficiency in cells treated as in (A). Cells were scored for aggregate retention (small to medium sized buds without calcofluor staining not containing aggregate foci). At least 100 cells were analyzed per strain. Bars represent the mean percentages of three technical replicates with three clones and their SD over all values.

3.1.2 Impaired mitochondrial import leads to lower aggregate-mitochondria association

It was described that in the fission yeast *Schizosaccharomyces pombe* there is a direct link between mitochondrial fission and fusion activity and the mitochondrial fitness (Dong et al., 2022). In this study the impairment of mitochondrial dynamics was connected to cell cycle progression, the maintenance of mitochondrial membrane potential and respiration. Interestingly, ageing yeast cells are known to

display mitochondrial fragmentation (Hughes and Gottschling, 2012) and the reduction of fission leads to an increased lifespan and cellular fitness (Scheckhuber et al., 2007). Since protein import into mitochondria requires a membrane potential it is directly impacted by mitochondrial fitness. With the MAGIC (mitochondria as guardian in cytosol) pathway, a mechanism for the detoxification of misfolded proteins in the cytosol by import into mitochondria has been described (Ruan et al., 2017). It is thus conceivable that active protein import into mitochondria through the TOM and TIM import complexes may be a relevant factor in the relationship between cytosolic aggregates and mitochondria. It was previously found that Δ*fis1* cells have lower capacity to retain protein aggregates (Zhou et al., 2014) and the non-dynamic mitochondria in cells expressing Myo2-Fis1 and especially *myo2(LQ)* displayed lower aggregate retention efficiency (Böckler et al., 2017). On the other hand, it was proposed that smaller mitochondrial units, like in fusion defective mutants, are less likely to be inherited by daughter cells as they are generally transported less efficiently. Furthermore, as age related mitochondrial fragmentation increases at the same time as the rate of aggregate retention decreases in *S. cerevisiae* this could hint at a connection between mitochondrial fitness, mitochondrial morphology and aggregate retention.

To investigate this model we utilized the 'clogger' constructs recently developed and characterized by Johannes Herrmann's lab (Boos et al., 2019). These constructs consist of mitochondrial targeting sequences fused to mouse dihydrofolate reductase (DHFR) under a strong and inducible promotor. DHFR is a protein that is folded very tightly which causes its import into mitochondria to be very inefficient. DHFR thus clogs the pores of the import machinery which additionally leads to increased proteostatic stress and reduced cell growth among other cell-wide effects. To better understand the resulting effects of clogger expression, DHFR was targeted to three different compartments resulting in different levels of stress: cytosolic DHFR without targeting sequence, b_2Δ-DHFR (matrix-targeted) and b_2-DHFR (intermembrane space-targeted) with the complete or modified targeting sequence of cytochrome b_2.

A drop dilution assay showed that the constructs do not affect the growth of yeast cells on agar plates without expression (SCD) (Figure 2A). On expression medium (SCGal) the strains displayed a growth defect of varying severity depending on the used clogger construct. While cells expressing cytosolic DHFR displayed no growth defect, the matrix (b_2Δ) and especially the intermembrane space targeted (b_2) constructs drastically reduced cell growth. The colony size in these two strains was also reduced compared to the controls. For analysis of the effects of expression of the clogger constructs on the behavior of heat-induced aggregates, Hsp104^{Y662A}GFP cells were cultured in selection medium with raffinose as carbon source (no induction of the clogger constructs). Clogger expression was induced by the addition of 2% galactose and protein aggregate formation was triggered by a 5 min heat shock at

42°C. In this experiment, only buds formed after the heat shock were evaluated which was made visible by calcofluor staining performed prior to the heat shock. As previously described in Zhou et al (2011) although they first described this phenomenon using enzymatically active Hsp104-GFP, a high rate of asymmetry in aggregate inheritance was observed (Figure 2B and C). Almost 90% of observed aggregates were located in the mother cell. As the level of aggregate retention is the same in strains expressing the cytosolic and mitochondrial targeted DHFR constructs as in the WT control, this indicates that the reduction of mitochondrial import due to the clogger constructs does not appear to have a negative influence on the successful retention of protein aggregates during cell division.

Additionally, the association of protein aggregates with mitochondria was analyzed (Figure 2B and D). Association was defined as colocalization of at least part of both fluorescent signals. For this evaluation, the planes of the z-stack were checked manually since the assessment in projections overestimated the association rate. In the empty vector and cytosolic DHFR controls the rate of colocalization of Hsp104 foci and mitochondria was found to be around 70%. In strains expressing the matrix and intermembrane space targeted clogger constructs this number was found to be reduced to about 50%. This could implicate that while the impairment of protein import does not alter the rate of aggregate retention, it could still play a role in the capturing of protein aggregates on the mitochondrial surface. It can, however, not be clearly distinguished whether this is a direct effect of the reduced mitochondrial import or a secondary effect due to another unknown factor. For example, a mitochondrial outer membrane protein involved in the process might not be imported correctly or the change in mitochondrial morphology and dynamics due to the import stress leads to less effective capturing of cytosolic aggregates. During the evaluation of these experiments, it was noteworthy that the cells expressing $b_2\Delta$-DHFR and b_2-DHFR harbored a larger number of aggregates per cell which additionally appeared to be smaller on average than foci in the control stains. This would be in line with the proposed model according to which the binding of misfolded aggregates to the ER and mitochondrial surfaces allows their fusion into larger aggregates due to the spatial restriction. Reduced aggregate fusion does not lead to increased aggregate inheritance

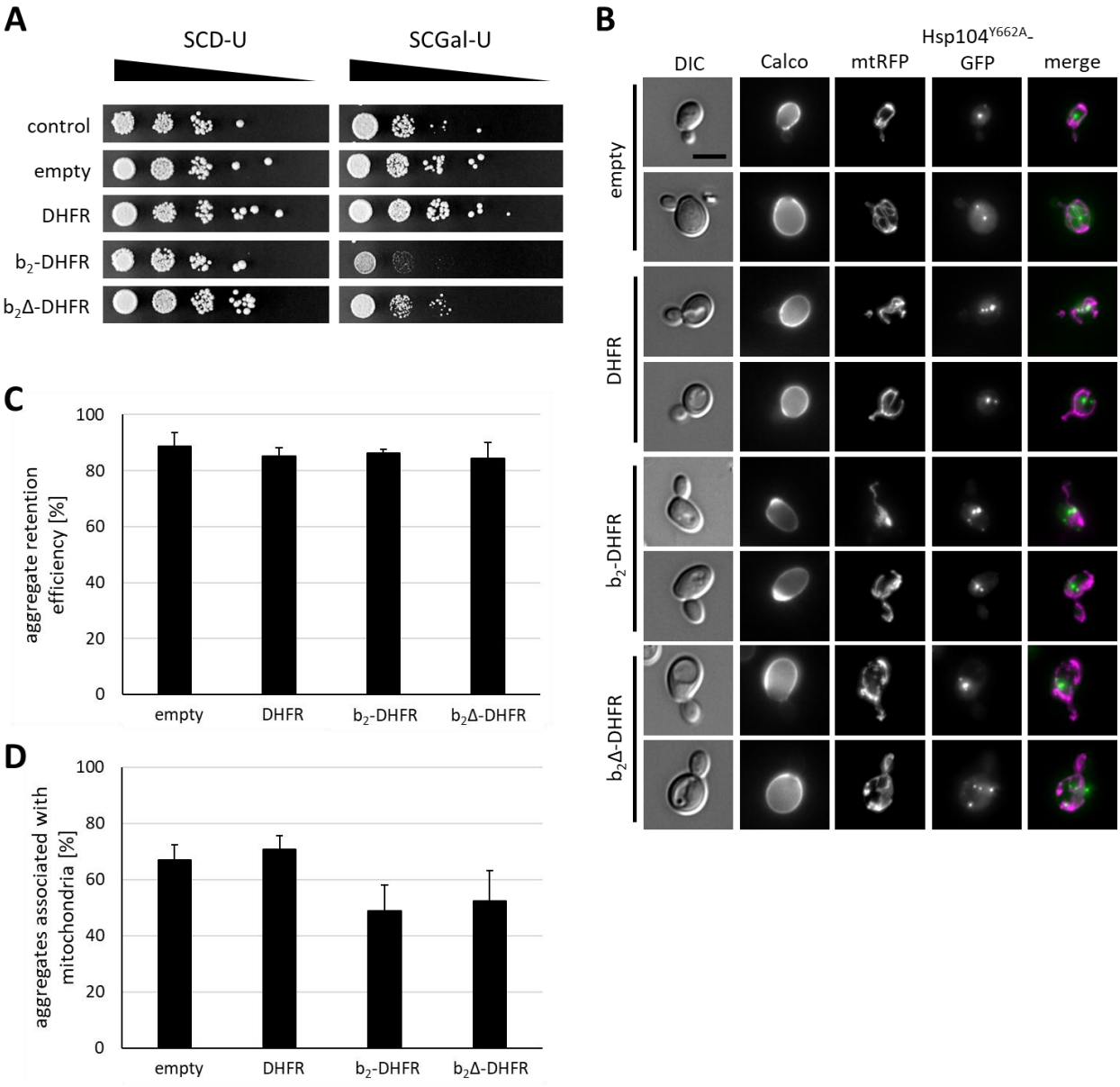

Figure 2: Analysis of the effects of 'clogger' expression on protein aggregates. (A) Hsp104^{Y662A}GFP cells expressing the indicated constructs from a galactose-inducible promotor were adjusted to the same optical density and diluted in 1:10 serial steps. The dilutions were plated on SCD-U and SCGal-U to select for cells containing the clogger plasmids. Plates were incubated at 30°C for 3 days. **(B)** Fluorescence microscopy of Hsp104^{Y662A}GFP cells expressing the clogger constructs. Mitochondria were stained with mitochondria-targeted RFP (mtRFP). Cultures were grown to logarithmic growth phase in SCRaf-LU to select for the mitochondrial marker and the clogger plasmids, then expression was induced by addition of 2% Gal. After 1 h expression calcofluor staining was performed followed by heat shock to induce aggregate formation. After 3 h the cells were fixed in formaldehyde and analyzed by fluorescence microscopy. All images except DIC and calcofluor are maximum intensity projections of z-stacks. Bar = 5 µm. **(C)** Quantification of aggregate retention in cells from (B). Cells were scored for aggregate retention (no aggregates in small to medium sized buds without calcofluor staining). At least 100 cells were analyzed per strain. Bars represent the mean percentages of three technical replicates of three clones each and their SD over all values. **(D)** Quantification of aggregates associated with mitochondria in cells from (B). Colocalization was quantified by checking the planes of z-stacks manually. At least 100 Hsp104 foci were analyzed per strain. Bars represent the mean percentages of three technical replicates of three clones each and their SD over all values.

3.1.3 Reduced aggregate fusion does not lead to increased aggregate inheritance

Recently, Hansen et al. performed a genome-wide screen to find unknown factors involved in the early targeting of mitochondrial membrane proteins (2018). Based on a hit found in this screen they were able to identify a previously unknown pathway for the correct import of mitochondrial membrane proteins which they termed 'ER-SURF'. Alternatively, to direct import to mitochondria, this pathway describes a mode for the membrane precursor proteins to be moved along the surface of the ER with a subsequent handover to mitochondria. This pathway depends on the Hsp40/DnaJ protein Djp1 that was first described to be important specifically for peroxisomal protein import (Hettema et al., 1998) but was later also found to be involved in the import of the mitochondrial protein Mim1 (Papić et al., 2013). Since this pathway resembles the proposed route of protein aggregates which are supposedly first captured by the ER surface and later transferred to the mitochondrial surface, the hits found in this genome-wide screen were also considered good candidates to be involved in the capture and transfer of protein aggregates. Besides Djp1, the screen had 11 other hits.

3.1.3.1 Mutants displaying reduced aggregate fusion still display high aggregate-mitochondria association

Aggregate behavior was examined in deletion mutants of all hits (Δ*djp1*, Δ*ema17*, Δ*ema19*, Δ*ema35*, Δ*idp2*, Δ*age2*, Δ*aim32*, Δ*pex21*, Δ*set2* and Δ*arl1*) with the exception of the two essential genes *TIM50* and *IPA1*. For this the wildype *HSP104* allele in the genome was exchanged with *hsp104^{Y662A}GFP*, and the aggregate retention efficiency of these double mutants was evaluated (Figure 3A). None of the tested deletion strains displayed a different level of aggregate retention than the wild type. Despite this, a subset consisting of Δ*djp1* and deletion mutants of three ORFs of unknown function - Δ*ema17*, Δ*ema19* and Δ*ema35* - were characterized further. Looking at the percentageof protein aggregates marked by Hsp104^{Y662A}GFP foci and mitochondria, also no strong difference between the mutants and wild type cells was found (Figure 3B and C). Δ*ema17* and Δ*ema35* showed a moderate reduction of the percentage of association of about 15% compared to the wild type.

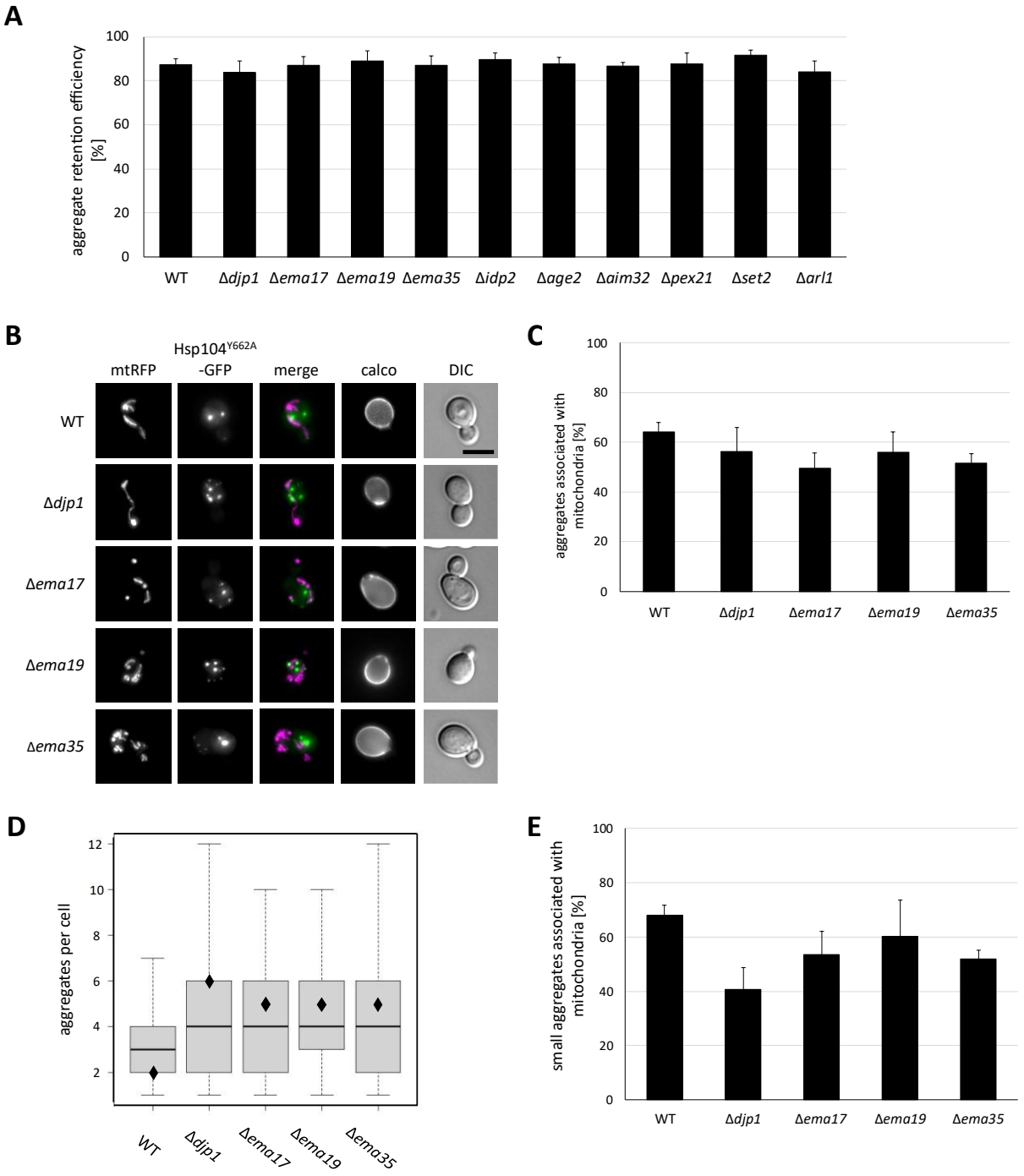

Figure 3: Deletion mutants with increased numbers of aggregates do not display disturbed aggregate retention or growth. (A) Analysis of the aggregate retention efficiency in deletion mutants of candidate genes for involvement in establishment of aggregate-mitochondria association. Deletion mutants expressing Hsp104^{Y662A}GFP and mtRFP were grown to logarithmic phase in SCD-L (selection for the mitochondrial marker), stained with calcofluor and subjected to heat shock for 5 min at 42°C. After 3 h of recovery the cells were harvested, fixed with formaldehyde, and analyzed using fluorescence microscopy. Cells were scored for aggregate retention (no aggregates in small to medium sized buds without calcofluor staining). At least 100 cells were analyzed per strain. Data represent the mean percentages of three technical replicates and the SD over all values. **(B)** Cells expressing Hsp104^{Y662A}-GFP and mtRFP were cultured as in (A) and analyzed by fluorescence microscopy. Pictures except calcofluor and DIC show maximum intensity projections. Bar = 5 µm. **(C)** Quantification of mitochondria-aggregate association of cells from (B). Colocalization was quantified by checking the planes of z-stacks manually. At least 200 cells were analyzed per strain. Bars represent the mean percentages

of two technical replicates of three clones each and their SD over all values. **(D)** Cells were cultivated as in (A) and the number of aggregates per cell was examined in at least 300 cells per strain. Data represent three technical replicates with three biological replicates. The black bar indicates the median and the whiskers indicate the first and third quartile of the data set. The mean values are indicated by the diamond. **(E)** The mitochondria-aggregate association rate of only small aggregates of (B) was analyzed. At least 100 cells were scored. Data represent three biological replicates and their SD.

Interestingly though, during evaluation of this experiment it was striking that the mutants seemed to display a noticeably higher number of Hsp104 foci per cell compared to the wild type (as seen in exemplary microscopy pictures in Figure 3B). This prompted a closer and systematic investigation which could confirm the observation (Figure 3D). All four mutants displayed a broader distribution with means of 5 (Δ*ema17*, Δ*ema19*, Δ*ema35*) and 6 (Δ*djp1*) aggregates per cell while the mean number of aggregates per cell in wild type cells is 2. This indicates that while the deletions did not have a direct impact on aggregate inheritance, the process of aggregate fusion seems to be disturbed either directly or indirectly. In accordance with this, the number of small aggregates appeared to be increased. The observed association between mitochondria and small aggregates was reduced in all deletion mutants (Figure 3E). This effect was especially strong in Δ*djp1* cells, where the rate of association was reduced to about 40% compared to a 68% association rate in the wild type.

3.1.3.2 Decreased aggregate fusion does not interfere with ER association

The model of aggregate retention by organellar binding describes a handover from the ER surface to the mitochondrial surface. The level of association of aggregates with mitochondria was not found to be increased even though a larger number of aggregates was observed in the cells. According to the model of organelle tethering of aggregates this should lead to a higher rate of aggregate association with the ER. Therefore, the level the association of protein aggregates with the ER was also examined in these deletion mutants (Figure 4A and B).

Surprisingly, all tested strains showed high colocalization with the ER. Since the ER covers a large area of the cell volume and the number of aggregates was high, one can expect a high level of overlapping signals, whether this is a reflection of an actual interaction or stochastic distribution is unclear. A drop dilution assay showed that regardless of the increased number of aggregates, the deletion mutants did not display a growth defect compared to the controls when grown at 25, 30 and 37°C (Figure 4C), so not even increased stress conditions at elevated temperatures which increase protein misfolding resulted in increased cytotoxicity. It is also worth mentioning that the sum of aggregates counted as colocalizing with mitochondria and ER is higher than 100%. This high level of presumed colocalization observed is most likely an artifact as protein aggregates are highly abundant in the stressed cells and a relatively large volume of the cell is taken up by the mitochondrial network and the ER. Due to the

limitations of fluorescence microscopy to distinguish between spatial proximity and actual interaction, an association could be suggested even if aggregates and mitochondria were merely in close spatial proximity. A substantial number of aggregates even seems to be associated with both organelles at the same time. This most likely results in an overestimation of the genuine associations. It was attempted to reduce the extent of this effect in this study by not evaluating maximum projections but rather evaluating fluorescence colocalization by monitoring the single planes of z-stacks.

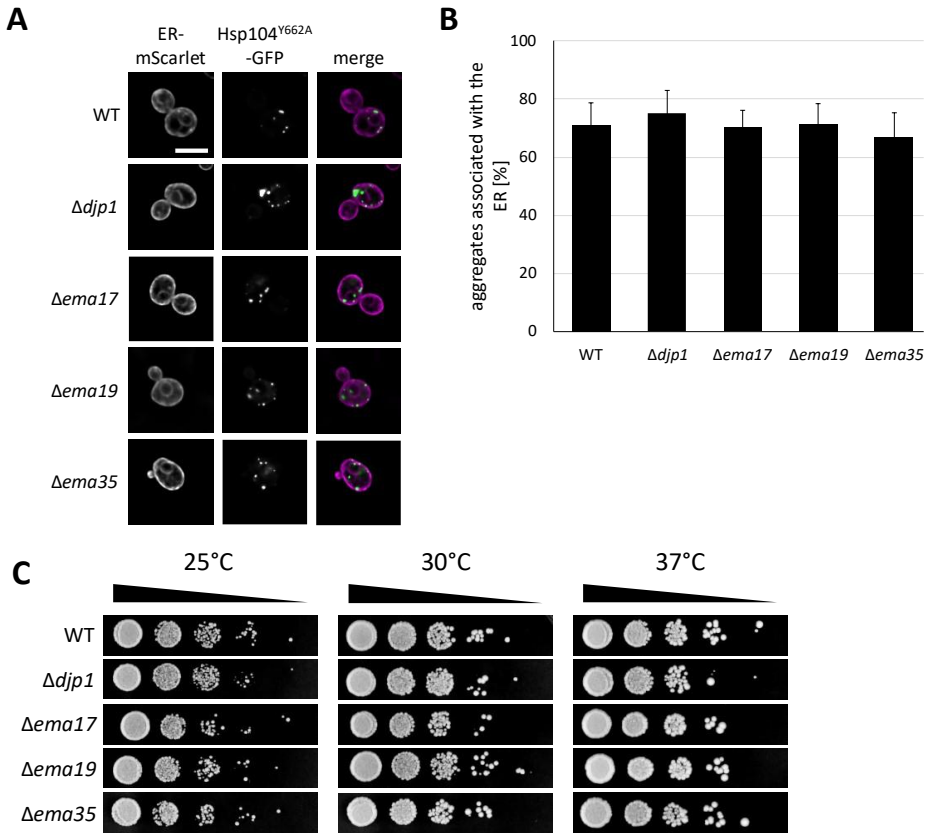

Figure 4: Deletion mutants with increased numbers of aggregates do not display reduced association to the ER or growth defects. (A) Fluorescence microscopy of the association of protein aggregates and the ER. Cells expressing Hsp104^{Y662A}-GFP and CPY-mScarlet-HDEL (ER-mScarlet) were to logarithmic phase in SCD-L (selection for ER marker), stained with calcofluor and subjected to heat shock for 5 min at 42°C. After 3 h of recovery the cells were harvested, fixed with formaldehyde, and analyzed using fluorescence microscopy. The pictures are maximum intensity projections of several central z-slices. Bar = 5 µm. **(B)** Quantification of (A). At least 50 cells per strain were evaluated. Bars represent the mean values of three technical replicates of three clones each and their SD over all values is shown. **(C)** Cells expressing Hsp104^{Y662A}GFP were adjusted to the same optical density and diluted in 1:10 serial steps. The dilutions were plated on YPD. Plates were incubated at 25°C, 30°C or 37°C for 2 days.

Taken together these findings cannot confirm an involvement of *EMA17*, *EMA19*, *EMA35* or *DJP1* in establishing organelle based aggregate retention. The deletion mutants of these genes did nonetheless

display an increase of the number of aggregates per cell with a lowered association rate of small aggregates to mitochondria compared to the wild type. These results indicate disturbed aggregate fusion. Unexpectedly, this did not result reduced aggregate retention during cell division as was previously described for fission yeast (Coelho et al., 2014).

3.1.4 Investigations regarding septins and mitochondrial inheritance

Another cellular complex that is a promising candidate for involvement in asymmetric inheritance of protein aggregates based on the current state of research and supported by findings of the Westermann group is the septin cytoskeleton. Septins are filament-forming members of a GTPase protein family which is conserved throughout most eukaryotic organisms with the exception of higher plants (Hartwell, 1971; Nishihama et al., 2011). In budding yeast, septins form a filament ring at the mother-bud neck which has been found to have dual function: as a scaffold for cytokinesis and, more importantly for this work, it serves as a diffusion barrier for asymmetrically inherited cellular components like nuclear pore complexes (Shcheprova et al., 2008) and misfolded proteins inside of the ER (Clay et al., 2014). This diffusion barrier is also involved in the correct assembly of the polarisome and the mitotic spindle during cell division (Chao et al., 2014). In addition to the described function as diffusion barrier, septins have been linked to mitochondrial inheritance through their regulators Cla4 and Bud6 as they were found to have a negative genetic interaction with *myo2(LQ)* (Böckler et al., 2017) and *myo2-fis1* (Hock, 2019). Since most septins are essential and viable mutants display strong morphological abnormalities in the form of pseudohyphal growth indicating cell division defects, two different types of conditional mutants were employed in this thesis to take a closer look at whether septins are involved in the asymmetric partitioning of mitochondria-associated cytosolic protein aggregates in *S. cerevisiae*.

3.1.4.1 The AID system allows rapid, inducible degradation of septins

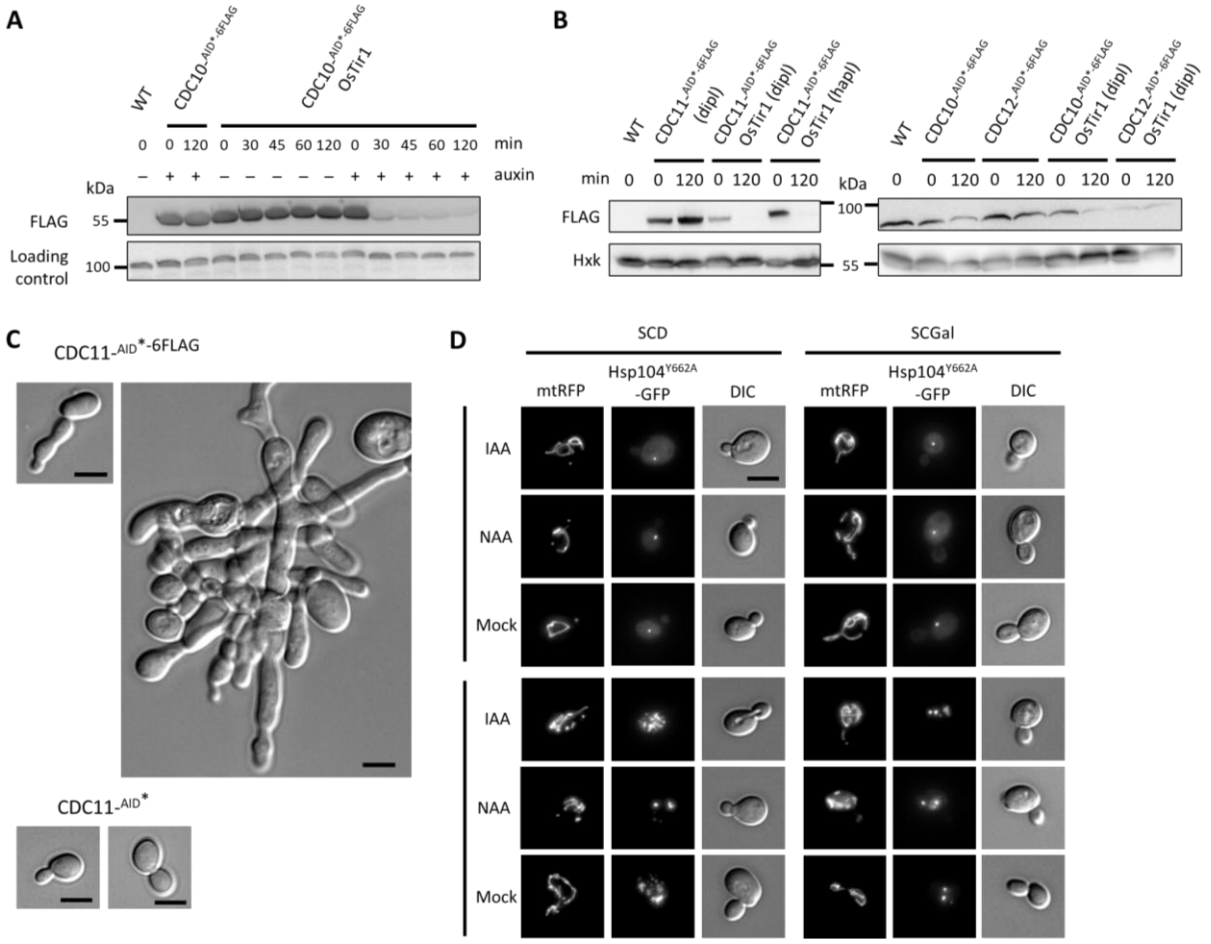

Figure 5: AID*-FLAG tag can be used for successful degradation of septins but causes reduced protein function. **(A)** Protein levels of Cdc10-$^{AID*-6FLAG}$ of whole cell lysates of strains treated with 0.5 mM auxin (NAA) or EtOH (p.a.) mock at the indicated time points after treatment analyzed by western blotting. The cells were logarithmically growing in YPD before AID induction. Cdc10 levels were detected using an antibody against the FLAG epitope tag. A strong, unspecific signal of the FLAG antibody was used as a loading control. **(B)** Protein levels of Cdc11-$^{AID*-6FLAG}$, Cdc10-$^{AID*-6FLAG}$ and Cdc12-$^{AID*-6FLAG}$ in whole cell lysates of heterozygous diploid or haploid strains before and 150 min after AID induction. The cells were treated as in (A). Hexokinase (Hxk) served as a loading control. **(C**) DIC microscopy of cells expressing Cdc11 tagged with AID*-6FLAG or AID*. Cells were grown to logarithmic growth phase and microscopy was performed using live cells. Bar = 5 µm. **(D)** Fluorescence microscopy of OsTIR1 Hsp104^{Y662A}-GFP cells (no AID tag). Mitochondria were stained with mitochondria-targeted RFP (mtRFP). Cells were grown in SCD-L or SCGal-L (both select for the mitochondrial marker) to logarithmic growth, then samples for T0 were harvested and fixed using formaldehyde. Remaining cells were heat shocked at 42°C for 5 min to induce aggregate formation. The cells were transferred to new medium which included 0.5 mM NAA, IAA, or equal amounts of EtOH (p.a.) as mock control to induce protein degradation. After 150 min of incubation at 30°C samples were taken, and cells were fixed with formaldehyde. Images except DIC are maximum intensity projections of z-stacks. Bar = 5 µm.

The auxin-inducible degron (AID) is a plant-derived system for the conditional and rapid depletion of proteins of interest (Nishimura et al., 2009). This allows the targeted degradation of essential proteins and has been optimized for use in yeast (Morawska and Ulrich, 2013). Here, a minimized degron

sequence (AID*) with a 6xFLAG epitope tag was fused to the C-terminal end of Cdc10, Cdc11 and Cdc12 in haploid or heterozygous diploid yeast cells. Additionally, the F-box protein TIR1 from *Oryza sativa* was integrated to the *HO* locus of the yeast genome (Papagiannakis et al., 2017). *CDC10* was chosen as a control for testing the system since it is a non-essential gene.

Indeed, as described previously Western blots could confirm a very rapid degradation of the protein of interest tagged with the AID tag in a OsTIR1 dependent manner (Figure 5A). 30 min after treatment with 0.5 mM of the auxin naphthaleneacetic acid (NAA) Cdc10 tagged with AID*6FLAG was already depleted. We could also confirm that the steady state level of Cdc10 was not impacted by the tag and the presence of OsTIR1 in the cells since the protein levels in untreated cells with and without OsTIR1 were comparable. This indicates that the system does not appear to be leaking. Similar results were found for another auxin molecule: Indole-3-acetic acid (IAA) (data not shown).

Since the tagging of the two essential septins used in this study, *CDC11* and *CDC12*, in haploid strains that already carried OsTIR1 was unsuccessful, the tagging was performed in diploid yeasts resulting in heterozygous diploids. Next these diploids were allowed to sporulate and dissected with a micromanipulator. This allowed the successful construction of a haploid *CDC11*-$^{AID*-6FLAG}$ OsTIR1 strain. However, no viable haploid tagged mutant of *CDC12* could be obtained. It can thus be assumed that the tagging resulted in a lethal loss or at least a reduction of function of Cdc12. A similar Cdc11 protein level could be found in the diploid and haploid yeasts, so the tag did not seem to destabilize the protein and the auxin induced protein degradation of tagged Cdc10 and Cdc11 occurred equally efficient in both haploid and diploid cells (Figure 5B). Likewise, it was also possible to deplete Cdc12 in heterozygous diploid cells.

While the successful degradation of all tested septins was confirmed using Western blotting, microscopy of the haploid strains with AID*-6FLAG tagged septins showed an alteration of cell morphology already without degron induction similar to *Δcdc10* or conditional septin mutants with pseudohyphal growth. Since the evaluation of aggregate retention efficiency with this cell morphology is not possible because mother and daughter cannot be distinguished and calcofluor staining did not lead to clear results, other AID tags were tested. Cells with the AID*-6HA tag also displayed the same phenotype (data not shown). These findings indicate that the tag negatively affects septin functionality resulting in defective cytokinesis. Next, a tag with only the AID* sequence without an epitope tag was tested to minimize the size of the tag. Haploid *CDC11*-^{AID*} cells were constructed by sporulation and tetrad dissection from heterozygous diploid yeasts. Light microscopy confirmed that the minimal tag did not interfere with cell division (Figure 5C). Therefore, further efforts to optimize a microscopy assay for the evaluation of the ARE were continued with the minimal AID* tag.

Pretests of a combined AID-ARE microscopy assay revealed that the addition of auxin or EtOH for the mock treatment to the culture medium lead to the fragmentation of mitochondria and a strong induction of the expression of Hsp104^{Y662A}-GFP. To optimize conditions OsTIR1 Hsp104^{Y662A}-GFP cells (without AID tag) were used, and the effect of different culture media and both NAA and IAA auxins were compared (Figure 5D). Since mitochondrial fragmentation was a problem and cells grown using galactose as a carbon source usually display a higher ratio of tubular mitochondria, cells were grown in SCGal-L and SCD-L for comparison. While there were indeed more tubular mitochondria observed in the SCGal cultures, the also expected increase in total mitochondrial mass made the evaluation of colocalization with protein aggregates difficult as the mitochondria cover such a large portion of the cell. Additionally, the auxin treated cultures after 150 min displayed high cytosolic background fluorescence of the mitochondrial marker, probably indicating an import defect. Another parameter that was changed was the used auxin chemical. NAA caused stronger mitochondrial fragmentation in SCD medium while IAA caused stronger aggregate formation which made evaluation of ARE impossible as new aggregates are constantly formed in mother and daughter. In SCD medium, the mock treatment with EtOH also caused aggregate formation but this was not the case in SCGal. Both NAA and IAA treated cells in SCGal display an expected amount of protein aggregates with some fused Hsp104 foci after 150 min. In conclusion all tested treatments have some drawbacks but the best results could be achieved using galactose as carbon source and IAA to induce the degradation.

In conclusion, the optimization of the culture medium and other experimental parameters could allow the use of the AID system in combination with ARE experiments, but these findings about the effects of IAA and most likely other auxin molecules must be taken into consideration during the planning of such experiments. Since the results investigating the role of septins in aggregate retention in temperature-sensitive septin mutants (see Figure 6) were more promising at the same time as these experiments were still being optimized, the approach using the AID system was not pursued any further.

3.1.4.2 Ambiguous findings using temperature-sensitive septin mutants

To investigate a potential role of septins in aggregate retention, experiments using temperature-sensitive (ts) yeast mutants were performed in parallel to the AID approach. For this the previously described *CDC12* ts mutants *cdc12-1* and *cdc12-6* were used (Barral et al., 1999; Barral et al., 2000). The *cdc12-6* mutant shows a stronger phenotype compared to *cdc12-1* with a higher number of cells without a septin ring at non-permissive temperatures. To investigate whether septins form a barrier that prohibits the inheritance of protein aggregates during budding, Hsp104^{Y662A}-GFP was used for the visualization of aggregates. In contrast to the previously described aggregate retention assays, the utilization of conditional ts mutants required a continuous heat shock at a restrictive temperature to inhibit septin ring formation. This also led to the constant formation of new protein aggregates throughout the entire cell. This assay can thus not be used to assess aggregate retention but can instead only give insights into aggregate movement and distribution. Another requirement for the assay was the formation and growth of daughter cells during restrictive conditions. Previously described assays utilizing the Hsp104^{Y662A}-GFP variant performed a 42°C heat shock and published experiments using these strains had used an incubation temperature of 38°C for prolonged time periods (Barral et al., 1999; Barral et al., 2000). However, a pretest showed that even at 38°C the cells already displayed such a high number of aggregates that single foci were not easily discernable, indicating that the cellular stress at this temperature level was too high to conduct this experiment. 35.5°C was determined to be an optimal temperature were aggregate foci formed but single foci could still be distinguished (data not shown).

Analogous to published observations the two *cdc12* mutant strains displayed a similar growth rate at permissive temperature (22°C) as wild type cells (Figure 6A). Both ts strains were unable to grow at the constant restrictive temperature of 35.5°C. In case of cells containing the *cdc12-6* allele, an incubation temperature of 30°C was already sufficient to prohibit growth completely while *cdc12-1* cells also displayed a strong growth defect. There was no discernable difference in the growth of ts mutants additionally expressing Hsp104^{Y662A}-GFP. In fluorescence microscopy the formation of aggregate foci at 35.5°C could be observed along with the formation and growth of new buds during the incubation at this restrictive temperature as indicated by the presence of buds lacking calcofluor stain (Figure 6B). After 4 h the morphology of the cells clearly showed that the septin ring was not functional at this temperature. The quantification of aggregate asymmetry displayed a strong reduction of mother-daughter asymmetry in *cdc12-6* with 35% and a smaller reduction with 52% in the *cdc12-1* mutant compared to 67% in WT cells (Figure 6C).

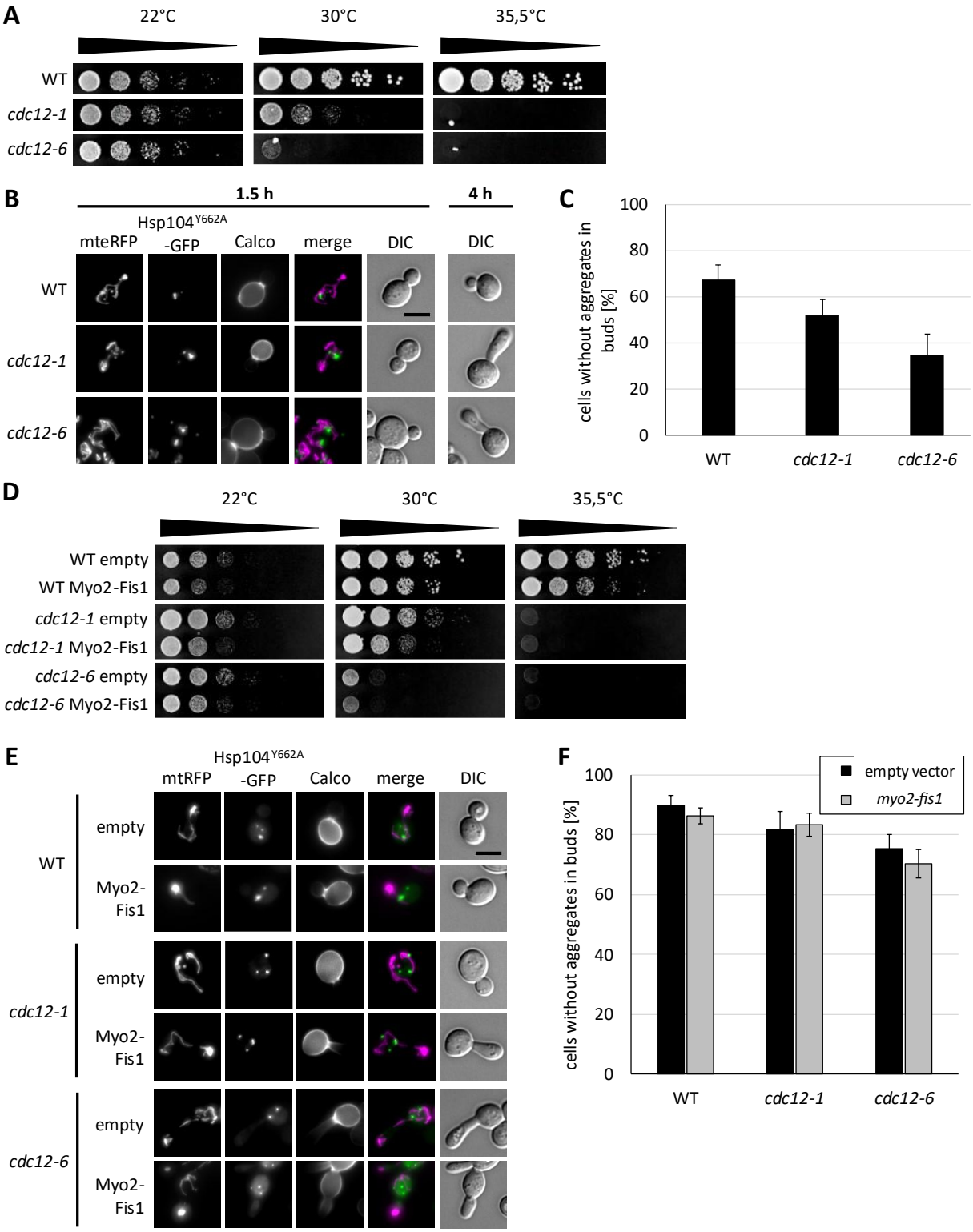

Figure 6: Ambiguous findings on the relationship between septins and protein aggregates. (A) Cells were adjusted to the same optical density and diluted in 1:10 serial steps. The dilutions were plated on YPD. Plates were incubated at 22°C, 30°C or 35.5°C for 2 days. **(B)** Cells expressing Hsp104^{Y662A}-GFP and mitochondrial targeted mtRFP were grown in logarithmic phase at 22°C in SCD-L (selection for mitochondrial marker), stained with calcofluor and resuspended in selection medium. The cultures were then incubated at 35.5°C. Samples were taken after 1.5 and 4 h and fixed with formaldehyde. Representative images of the analysis by fluorescence microscopy are shown. Pictures except calcofluor and DIC are maximum intensity projections. Bar = 5 µm. **(C)** Quantification of the number of cells without aggregates in buds of (B). At least 100 cells were analyzed per

strain. Bars represent the mean percentages of three technical replicates with three biological replicates and their SD over all values. **(D)** Cells expressing an empty vector control or Myo2-Fis1 were adjusted to the same optical density and diluted in 1:10 serial steps. The dilutions were plated on SCD-U (selection for myo2-fis1 containing plasmid). Plates were incubated at 22°C, 30°C or 35.5°C for 2 days. **(E)** Cells expressing $Hsp104^{Y662A}$-GFP and an empty vector control or Myo2-Ffis1 were cultured and treated as in (B). Mitochondria are visualized by mitochondrial targeted mtRFP. Representative images of the analysis by fluorescence microscopy are shown. Pictures except calcofluor and DIC are maximum intensity projections. Bar = 5 µm. **(F)** Quantification of the number of cells without aggregates in buds of (E). At least 100 cells were analyzed per strain. Data represents the mean percentages of three technical replicates with three biological replicates and the SD over all values.

As these findings suggest a potential involvement of septins in the maintenance of mother-daughter aggregate asymmetry, the next step was to test whether increased mitochondrial inheritance leads to an increased number of aggregates in buds as described in Böckler et al., 2017. In order to investigate this Myo2-Fis1, a fusion protein of the motor protein Myo2 with the cargo binding domain replaced by the transmembrane domain of the MOM protein Fis1, was expressed constitutively. An analysis of growth showed that the expression of the construct had a small negative impact compared to the empty vector regardless of incubation temperature in all three tested strains including the wild type (Figure 6D). As previously described, the construct led to a vast increase in mitochondrial mass in buds due to increased transport (Figure 6E). The percentage of cells without aggregates in the buds was comparably high in all tested strains regardless of whether the cells contained the empty vector or the myo2-fis1 construct (Figure 6F). This is a direct contradiction to the data in Figure 6C. The aggregate asymmetry in cells with empty vector was expected to correlate to those findings but instead no relevant difference between wild type and mutant cells could be found. Subsequent efforts to tightly control all experimental parameters like performing the heat shock in a water bath (data not shown) and synchronizing the cultures with mating factor alpha were unsuccessful (data now shown) and neither the strains expressing empty vector nor the strains without vector (same strains used in Figure 6C) displayed reliably reproducible differences between the wild type and the ts mutants.

3.2 Search for novel factors involved in mitochondrial inheritance

In *S. cerevisiae* mitochondrial inheritance has been found to depend on transport along actin cables mediated by the motor protein Myo2. The proteins Mmr1 and Ypt11 are involved in mediating the binding of Myo2 to mitochondria. Since Ypt11 is a cytosolic protein and Mmr1 is a protein that is merely peripherally associated to the mitochondrial outer membrane, it seems plausible that there are further currently undiscovered – particularly mitochondrial – factors involved in Myo2 recruitment to mitochondria. Further supporting this argument is the fact that single deletions of *MMR1* and *YPT11* only lead to a relatively small reduction in mitochondrial inheritance. Double mutants (at least in some strain backgrounds) however are inviable due to inability to transport mitochondria to the daughter during cell division (Itoh et al., 2004).

3.2.1 Educated-guess based microscopy screen of deletion mutants

A likely localization for proteins involved in mitochondrial transport and inheritance is the MOM. There, this protein would be able to directly interact with Mmr1, Ypt11 or even Myo2, thereby connecting them to the mitochondria. One approach to identify candidates for novel factors involved in mitochondrial inheritance is by looking at previous genomic screens finding genetic interactors with known components of mitochondrial inheritance. Thus, a list of candidates (see in Figure 7) was compiled based on (predicted) protein location in the MOM, aberrant mitochondrial morphology, negative genetic interaction in genome-wide screens with *myo2(LQ)*, Δ*mmr1* and Δ*ypt11* (Böckler et al., 2017; Costanzo et al., 2016).

Deletion mutants of the list of genes were either taken from the yeast deletion library and deletions were confirmed via PCR or mutants were constructed by homologous recombination. Subsequently, mitochondrial inheritance was evaluated in live cell microscopy. Of 30 tested strains only one (Δ*gem1*) showed a mild defect in mitochondrial inheritance. The deletion mutant has been described to have a slightly delayed mitochondrial transport during budding (Frederick et al., 2004) which could be confirmed here. There is no indication that Gem1 is involved in mitochondrial transport otherwise than causing a change in mitochondrial morphology which in turn has an influence on transportability.

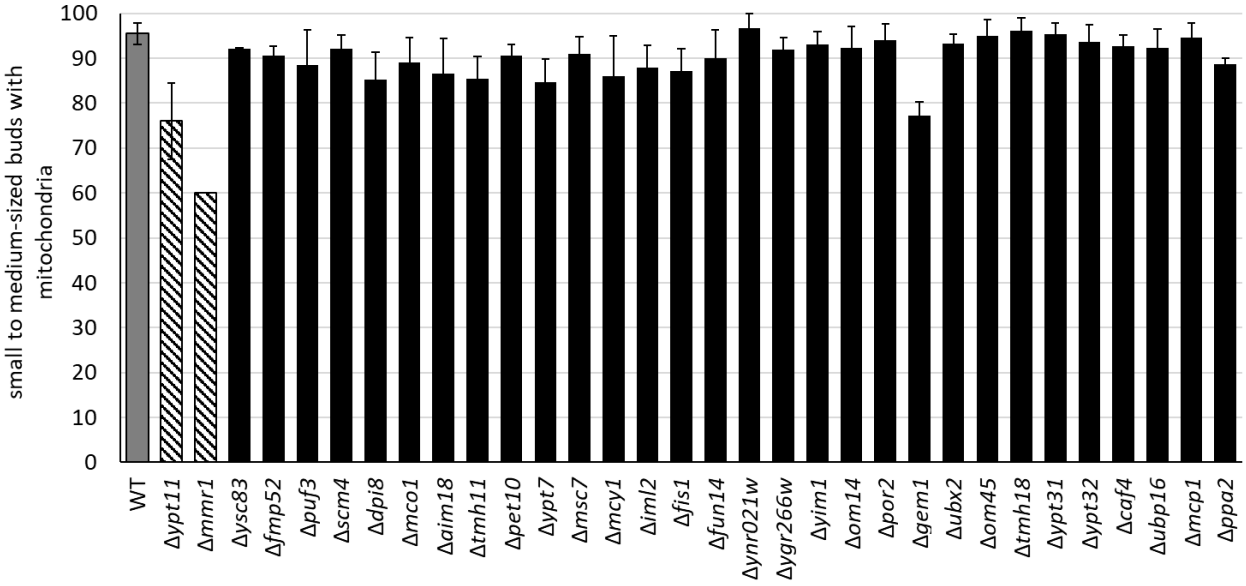

Figure 7: Analysis of mitochondrial inheritance via a microscopical screen in an educated-guess based set of deletion mutants. Yeast deletion mutants expressing a mitochondrial marker were grown in selective medium to logarithmic growth phase. Then mitochondrial inheritance was quantified in small to medium sized buds in live cells. Bars represent mean percentages of two replicates. At least 100 cells were analyzed per strain and the SD over all values are indicated. WT (grey), and Δ*ypt11* and Δ*mmr1* (striped) – mutants known to have a mitochondrial inheritance defect – were included for comparison.

3.2.2 Multicopy suppressor screen in Δ*mmr1* Δ*ypt11*

Since it has been shown that a strong promotion of mitochondrial transport, for example through the expression of the fusion protein Myo2-Fis1 that constitutes a constant tether between Myo2 transport protein and the MOM, can rescue insufficient mitochondrial transport in the Δ*mmr1* Δ*ypt11* double mutant (König, 2012), the overexpression of a potential, unknown factor assisting inheritance might similarly be able to rescue this lethal phenotype as well. In order to identify proteins involved in mitochondrial inheritance a multicopy suppressor screen in the Δ*mmr1* Δ*ypt11* strain was conducted (Figure 8A). This screen was referenced in 'A protein interaction map of the myosin Myo2 reveals a role of Alo1 in mitochondrial inheritance in yeast' by (Chelius et al., 2025).

The minimal tiling library, a sub-library of the yeast genomic tiling library, allows the quick and easy systematic overexpression screening of a large number of open reading frames (ORFs) (Jones et al., 2008). The library of 1588 multicopy vectors contains inserts consisting of segments of genomic DNA including three to five ORFs, potential ORFs and non-coding regions covering almost the entirety of the yeast genome (97.2%). In this screen, the pooled minimal tiling library was introduced into an otherwise inviable strain that carries a rescue plasmid carrying the *URA3* gene as a marker. Over several generations the cells are grown on media plates only selecting for the library plasmid in order to allow the loss of the rescue plasmid. Subsequently, the cells were transferred to plates containing

5-FOA to select against colonies carrying the rescue plasmid. 5-FOA selects against the expression of *URA3* which converts 5-FOA to the toxic metabolite 5-fluorouracil (Boeke et al., 1984). Cells able to grow on 5-FOA containing plates can therefore be rescued by the overexpression of one of the genes present on the respective library plasmid.

Here, a homozygous diploid Δ*mmr1* Δ*ypt11* strain was rescued with the plasmid pRS416-*MMR1* which carries the *MMR1* gene including its endogenous promoter and terminator sequences. A homozygous diploid strain was used since diploid cells possess a higher genomic stability compared to haploid strains which increased the probability of yeasts surviving the pRS416-*MMR1* counterselection were actually being rescued by the library plasmid instead of beneficial background mutations (Marad et al., 2018). After several pretests the amount of cells and DNA as well as their ratio in the transformation was adjusted in a way that yielded over 10,000 transformants. This was the target number of transformants in order to guarantee the covering of the entire library several times. After transfer to 5-FAO containing medium the 251 growing candidates were transferred to 5-FAO plates again for a second round of selection. 54 independent colonies grew reproducibly on 5-FOA containing medium plates. Most of them displayed growth comparable to the positive control (Figure 8B). For the positive control the homozygous diploid Δ*mmr1* Δ*ypt11* strain was transformed with the plasmid pAG415GDP-YPT11. This plasmid confers the constitutive overexpression of *YPT11*. A test on selective medium lacking uracil showed that all colonies contained subsets of cells still carrying the *MMR1* rescue plasmid alongside the library plasmid. After isolation from the yeast colonies, the library plasmids were amplified in *E. coli* and tested for the presence of *MMR1* and *YPT11* via PCR, 49 of 54 candidates carried plasmids containing one of these two genes. The remaining 5 candidates were sequenced for identification. One of the vectors was shown to be the empty library backbone while the other four were unique hits (Figure 8C).

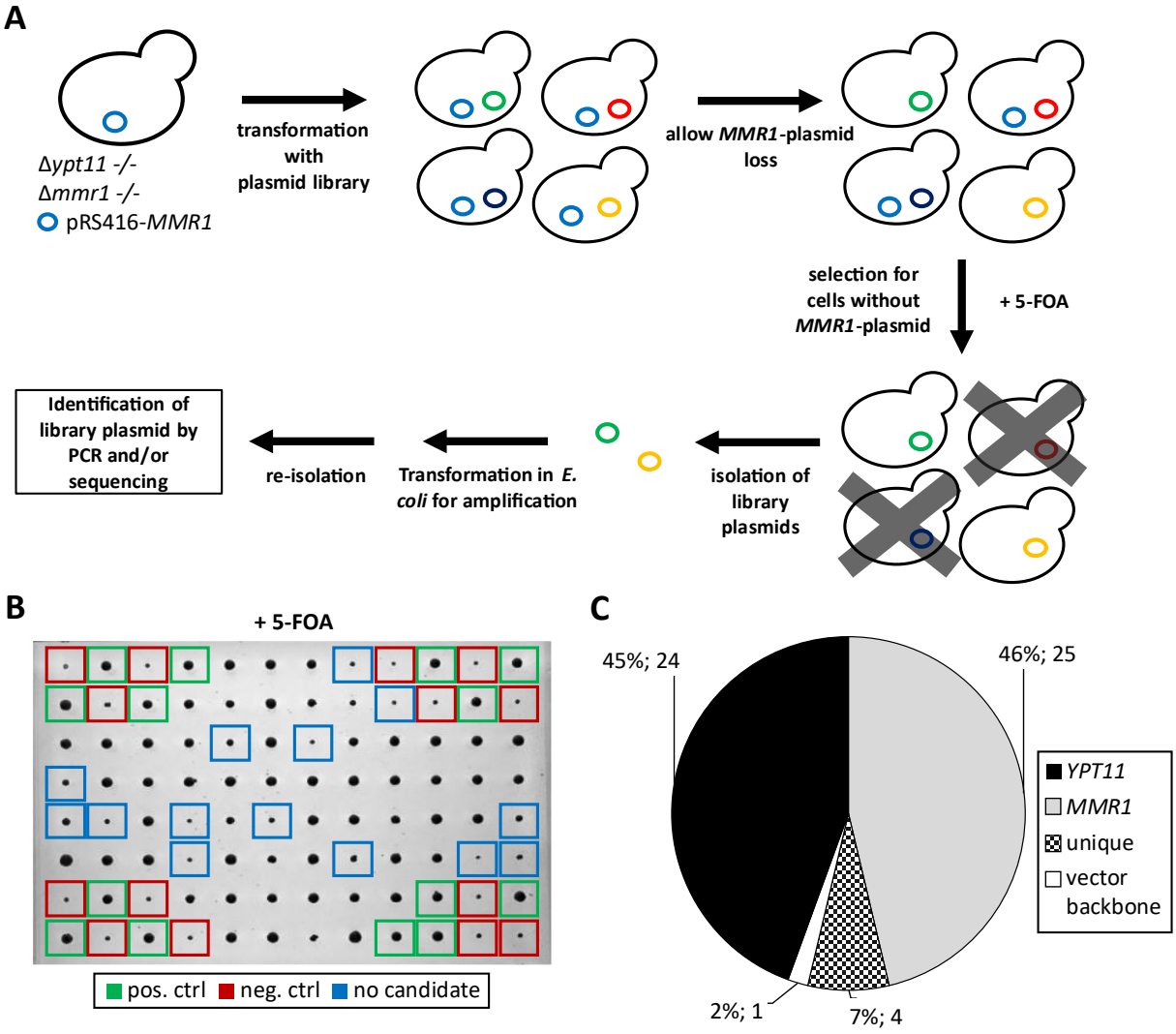

Figure 8: Multicopy suppressor screen in Δ*mmr1* Δ*ypt11*. (A) Homozygous diploid Δ*mmr1* Δ*ypt11* cells rescued by the expression of Mmr1 from pRS416-MMR1 (*URA3* marker) were transformed with the pooled minimal tiling plasmid library from the yeast genomic tiling library resulting in over 10.000 transformants. After growth on non-selective plates that allowed the loss of the rescue plasmid, the candidates were transferred to plates containing 5-FOA to select against the rescue plasmid. Library plasmids of the selected clones were isolated and transformed into *E. coli* for amplification and subsequently re-isolated. The identity of the plasmids was tested by PCR checking for *MMR1* and *YPT11* and in some cases sequencing. **(B)** Candidates growing on a 5-FAO selection plate along with the positive (green, pAG415GPD-YPT11) and negative controls (red, empty library vector). Blue box indicates growth comparable to negative control. Colonies marked with blue boxes were not analyzed further. **(C)** Identity of the library plasmids of the 54 candidates. Note that library plasmids contain genomic stretches usually including several ORFs as well as non-coding DNA, but for simplicity the plasmids are named "*YPT11*" and "*MMR1*" in this figure after the genes rescuing the Δ*mmr1* Δ*ypt11* phenotype.

In order to test the reproducibility of these candidates' ability to rescue the inviable Δ*mmr1* Δ*ypt11* strain, the extracted plasmids were re-transformed into the original double mutant strain, again carrying the rescue plasmid pRS416-MMR1. One extracted vector carrying *YPT11* and *MMR1*, respectively was chosen representatively. Again, after not selecting for the *URA3* plasmid for several

generations the cells were plated on medium containing 5-FAO (Figure 9A). Other than the cells containing plasmids containing *YPT11* and *MMR1* only one candidate containing the library plasmid "YGPM-32j02" was able to grow on 5-FOA medium in this drop dilution assay. These cells displayed growth comparable to the *YPT11* overexpressing positive control (pAG415GPD-*YPT11*). YGPM-32j02's insert contains three complete ORFs (*CSR2*, *NTO1* and *SRO7*) along with two partial ORFs (*APL4* and *HTS1*).

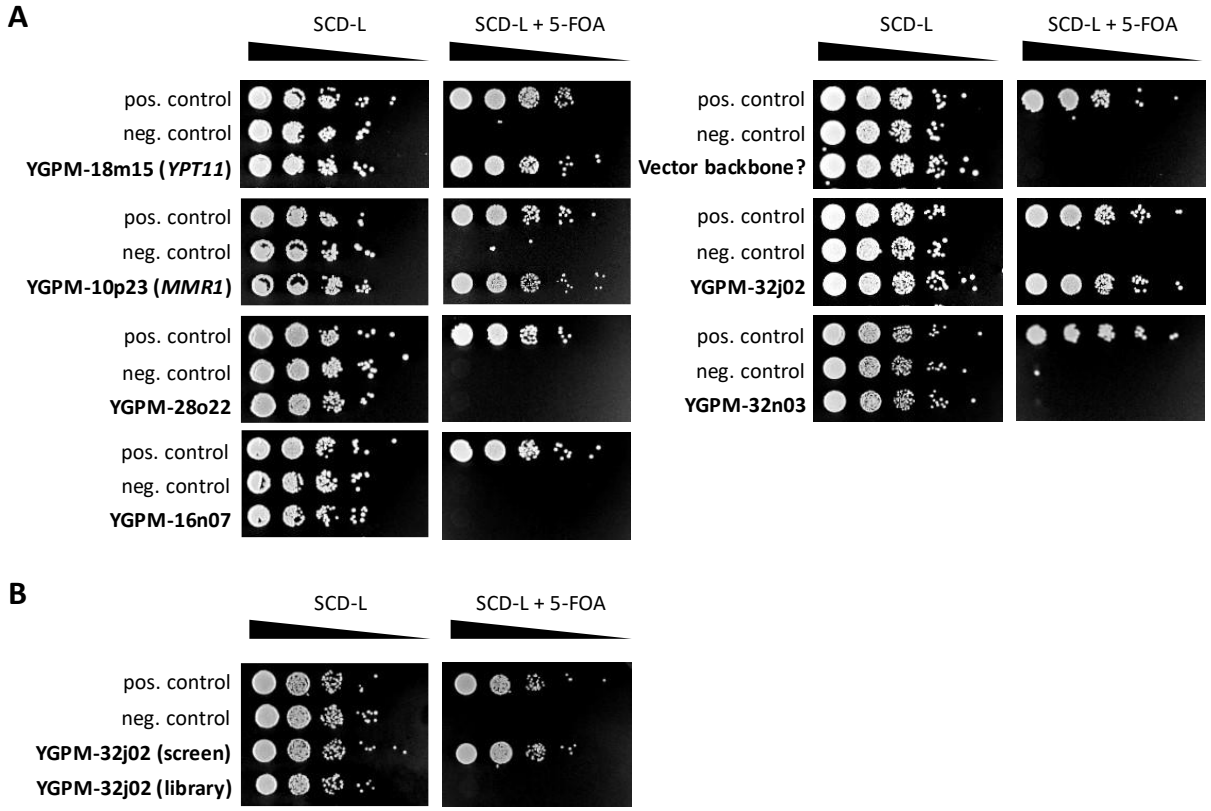

Figure 9: Candidate plasmids from multicopy suppressor screen cannot be confirmed manually. (A) The strain used in the multicopy suppressor screen (Δ*mmr1* Δ*ypt11* pRS416-*MMR1*) was transformed with the rescuing plasmids extracted during the screen and grown on plates not selecting for the *MMR1* plasmid twice to allow plasmid loss. For the assay cells were adjusted to the same optical density and diluted in 1:10 serial steps. The positive control was transformed with pAG415GPD-*YPT11*, and the negative control carries the empty library vector. The dilutions were plated on SCD-L (selection for library plasmid) and SCD-L + 5-FOA (selection fot library plasmid and against pRS416-*MMR1*) plates and incubated at 30°C for 3 days. **(B)** Δ*mmr1* Δ*ypt11* pRS416-*MMR1* was transformed with either YGPM-32j02 extracted in the multicopy suppressor screen or from the library stock. The assay was performed as described in (A).

To further validate its rescuing ability, the plasmid from the library's stock was extracted, purified and the query strain was transformed with it. Surprisingly, the plasmid from the library stock was not able to rescue Δ*mmr1* Δ*ypt11* unlike the plasmid extracted during the screen (Figure 9B). After re-isolation of the rescuing plasmid from the screen candidate both the library stock and the screen plasmid were compared by restriction digest and identified by sequencing. The identity of the library plasmid could

be confirmed but the extracted plasmid from the screen had been contaminated with a *MMR1* containing plasmid which apparently rescued the mutant phenotype.

Overall, the screen did not provide any more insights into mitochondrial inheritance and did not identify novel factors in mitochondrial inheritance as all potential hits except *MMR1* and *YPT11* themselves could not be confirmed. The high frequency with which *MMR1* and *YPT11* were found in the screen however demonstrated that the screen was highly successful from a technical perspective.

3.3 Selective inheritance of mitochondria and oxidative stress

Another factor that has been described to have a strong influence on mitochondrial transport and inheritance in higher eukaryotes is the production of ROS by mitochondria (Debattisti et al., 2017; Katajisto et al., 2015; Liao et al., 2017). Mitochondria naturally produce ROS which over time leads to a decline in mitochondrial fitness (Kauppila et al., 2017). Thus, mitochondria contribute substantially to cellular aging. In *S. cerevisiae* a couple of studies using mitochondrial membrane potential reporters have suggested asymmetric partitioning of high- and low-functioning organelles during cell division (Manzano-Lopez et al., 2019; McFaline-Figueroa et al., 2011). However, the data supporting this is limited and no information about the mechanism behind this process in yeast has been gathered yet. Here, the effect of externally applied as well as internally produced agents triggering oxidative stress on mitochondrial inheritance is assessed.

3.3.1 H_2O_2 treatment disturbs the actin cytoskeleton and abolishes mitochondrial movement

Hydrogen peroxide (H_2O_2) is naturally occurring in living cells as a toxic and short-lived byproduct of cellular metabolism but it also serves biological functions as a signaling molecule (Schieber and Chandel, 2014; Wong et al., 2017). Due to its production in mitochondria, H_2O_2 constantly contributes to the damaging of mitochondrial proteins, lipids, and DNA. Thus, hydrogen peroxide is thought to play a prominent role in the decline of mitochondrial fitness.

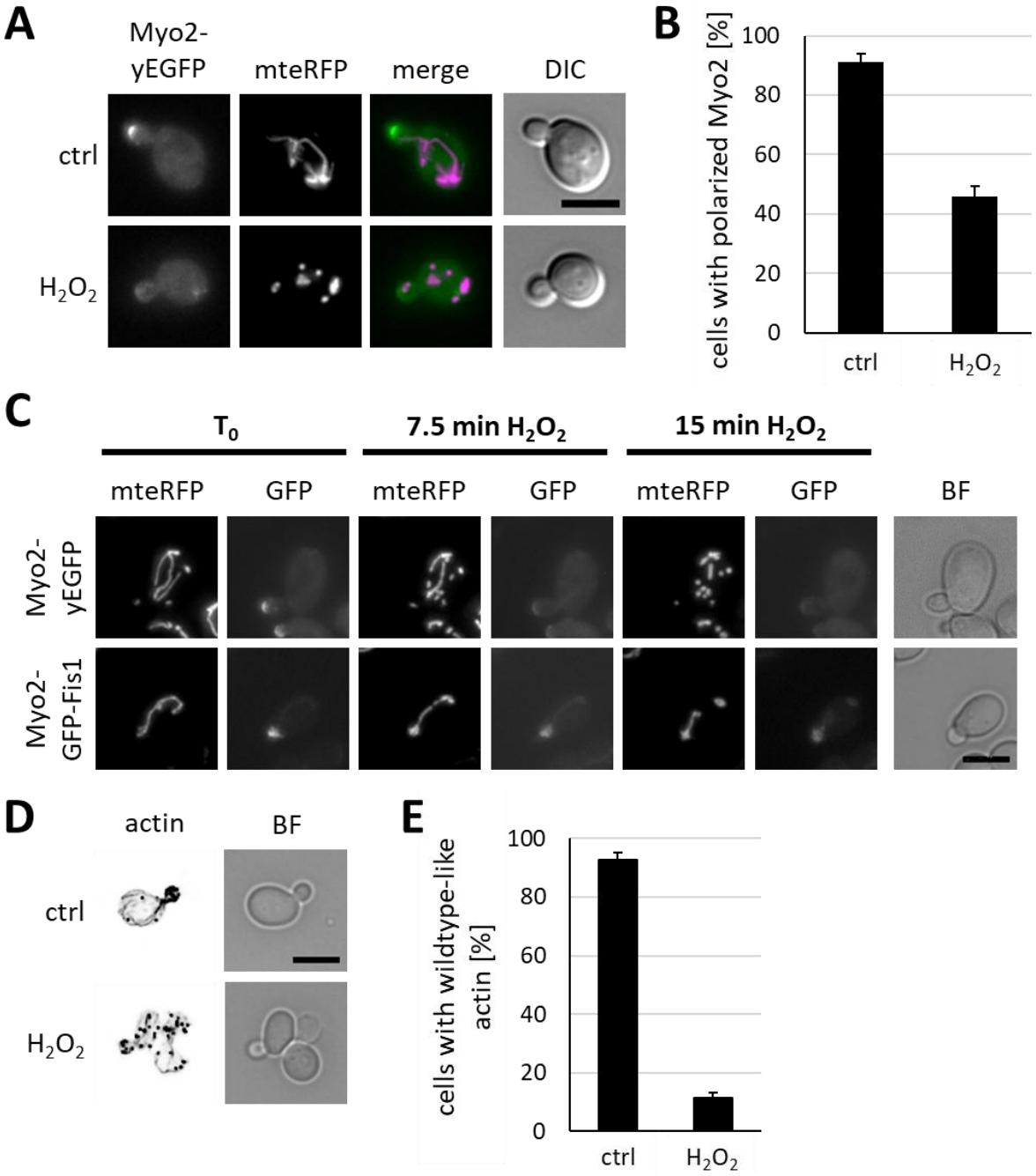

Figure 10: H_2O_2-induced oxidative stress alters Myo2 polarization and the actin cytoskeleton. (A) Cells expressing Myo2-yEGFP and a mitochondrial marker were grown to the logarithmic growth phase and were stressed by addition of 0.5 mM H_2O_2 to the culture medium. After 15 min the cells were harvested and analyzed by live cell fluorescence microscopy. Control samples (ctrl) were taken from the same culture before stress treatment. Fluorescence micrographs represent maximum intensity projections of deconvolved z-stacks. Bar = 5 µm. **(B)** Quantification of Myo2-yEGFP polarization in very small to small buds in (B). At least 100 cells were analyzed per strain. Data represents the mean percentages of three technical replicates with three biological replicates and the SD over all values. At least 100 cells were analyzed per replicate. **(C)** Cells expressing Myo2-yEGFP or pRS426-myo2-GFP-fis1 and a mitochondrial marker were grown in selective medium to logarithmic growth. Next, the cells were harvested and immobilized on an 8-well µ slide (ibidi) coated with concanavalin A. After unbound cells were washed away, the sample was covered with culture medium containing 0.5 mM H_2O_2 and immediately analyzed by fluorescence microscopy. Further pictures were taken 7.5 and 15 min after treatment. The brightfield (BF) picture was taken after 15 min. Fluorescence micrographs represent

maximum intensity projections of z-stacks. **(D)** WT cells were grown to the logarithmic growth phase and stressed by addition of 0.5 mM H_2O_2 to the culture medium. After 15 min cells were harvested, fixed, and analyzed by fluorescence microscopy. Control samples (ctrl) were taken from the same culture before the stress treatment. Next, the actin cytoskeleton was stained with rhodamine-phalloidin, and cells were analyzed by fluorescence microscopy. Fluorescence micrographs represent maximum intensity projections of z-stacks. Bar = 5 µm. **(E)** Quantification of the percentage of very small to small-budded cells containing wild type-like actin in (D). Data represents the mean values of three technical replicates and their SD over all values. At least 100 cells were analyzed per replicate.

To investigate the link of oxidative stress and mitochondrial damage to a reduction of mitochondrial transport, the effect of external treatment of cultures with H_2O_2 on factors relevant for mitochondrial inheritance was studied. First the localization of the mitochondrial transport motor protein Myo2 before and after H_2O_2 treatment was studied microscopically using yeast cells expressing Myo2-yEGFP. In smaller buds Myo2 was described to be localized in the bud and at the mother-bud neck and in larger budded cells closer to cytokinesis (Lillie and Brown, 1994). The same localizations were exhibited by Myo2-yEGFP in fluorescence microscopy in this study (Figure 10A). The number of small-budded cells displaying polarized Myo2 before and after 15 min incubation with 0.5 mM H_2O_2 was quantified and a strong reduction in polarization (by 45%) was observed following the treatment (Figure 10B). In these cells no bright foci were visible, only a cytosolic signal of comparable strength to untreated cells indicating a complete depolarization of Myo2. The observation that Myo2 polarization, which is necessary for a variety of cellular processes, was abolished due to the oxidative stress caused by H_2O_2 treatment is a strong indicator that H_2O_2 treatment has a too unspecific and strong effect on the cells to observe the selective effect on mitochondria. Furthermore, rapid mitochondrial fragmentation could be observed in cells treated with H_2O_2 similarly to descriptions in earlier studies concerning mitochondrial morphology during oxidative stress (Vowinckel et al., 2015).

Next it was tested whether the expression of Myo2-Fis1 which permanently attaches the motor protein to mitochondria and forces their transport into the bud, influenced the depolarization effect on Myo2. For this, cells either genomically expressing Myo2-yEGFP or constitutively expressing Myo2-GFP-Fis1 from a multicopy plasmid were compared in live cell microscopy over the course of 15 min after H_2O_2 addition to the medium (Figure 10C). As described in the previous experiment, small-budded cells expressing Myo2-yEGFP displayed polarized Myo2 in the beginning of the observation, but after 7.5 min the polarization was completely abolished. Similarly, cells expressing Myo2-GFP-Fis1 also showed polarized Myo2 in the beginning, but, differing from the WT protein, the fluorescence signal stayed polarized in the bud. The signal strength diminished over the time of 15 min. Whether this was caused by the protein's slow depolarization or bleaching of the fluorophores caused by the H_2O_2 (Alnuami et al., 2008) cannot be distinguished here. The remaining polarized Myo2, however, does not

seem to be functional but instead appeared to remain in the place it was in when the cells were subjected to the stress treatment. Overall, Myo2-GFP-Fis1 was not able to maintain a polarized localization during hydrogen peroxide treatment any more than the WT Myo2 protein. It is noteworthy that the mitochondria in cells expressing Myo2-GFP-Fis1 remained more tubular over the course of the observed timeframe compared to cells expressing Myo2-yEGFP but seemed to start fragmenting towards the end. Taken together these experiments show that the oxidative stress caused by the hydrogen peroxide treatment is unselectively affecting the whole cell in such a way that specific effects on mitochondrial inheritance cannot be examined.

This was further corroborated by staining the actin cytoskeleton with rhodamine-phalloidin (Figure 10D and E). Normally, similarly to the location of the motor protein Myo2 moving along the actin cables, actin patches that are part of the actin cytoskeleton can be found polarized at the bud and bud tip in smaller to medium sized buds (Adams and Pringle, 1984). Later, the patches are more evenly distributed throughout the connected mother and daughter cells. After H_2O_2 treatment the actin cytoskeleton was disorganized. This affected the actin cables which were strongly reduced compared to in control cells, as well as the actin patches which were no longer polarized but dispersed between mother and bud. The polarization of actin patches in very small to small buds was quantified in the control and compared to H_2O_2 treated samples and a strong reduction in polarization was found. While 93% of control cells displayed a wild type-like actin cytoskeleton, only 12% in the H_2O_2 stressed sample did. These findings are consistent with observations described by Vilella et al. (2005) and can provide an explanation why the Myo2-GFP-Fis1 foci observed in Figure 10C remained at the daughter cell tip. If there is no functional actin cytoskeleton available for Myo2 to move on, it remains in the same location.

Taken together these findings show that due to the unspecific stress induced in cells by H_2O_2 treatment it is not a suitable tool to study mitochondrial inheritance and its relationship to oxidative stress. Mitochondrial transport and mitochondrial inheritance are completely abolished as the actin cytoskeleton is disturbed and Myo2 localization is altered, making mitochondrial movement impossible. This, along with the disruption of the many other cellular processes both directly connected to Myo2 and the actin cytoskeleton as well as cellular metabolism in general, made it necessary to find a better tool to observe mitochondrial behavior during oxidative stress.

3.3.2 Selective inheritance of fit mitochondria during oxidative stress acts through Mmr1-mediated Myo2 recruitment

To specifically cause ROS formation and oxidative stress inside the mitochondrial matrix, the D-amino acid oxidase 1 (DAO) of the yeast *Rhodotorula gracilis* was inserted into the genome with the constitutive *TEF* promotor and the matrix targeting sequence of subunit 9 of the F_O-ATPase from *Neuropora crassa* (Su9) at the *HO* locus. This enzyme, Su9-DAO, allows organisms the utilization of D-amino acids for energy metabolism and produces hydrogen peroxide as a byproduct (Alonso et al., 1998; Tishkov and Khoronenkova, 2005). Importantly, while enzymes like this are present in a large number of organisms including humans, the genome of the baker's yeast does not contain a homolog. The construct used in this work was amplified from a previously described construct that has been shown to have measurable biological effects (Calabrese et al., 2019; Matlashov et al., 2014). It's ability to cause the H_2O_2 formation outside and inside of mitochondria at a level that can be considered oxidative stress has been shown before but has not been studied in this context and additionally has not previously been researched using microscopy. The most important results described in this chapter have been published in Chelius et al. (2023).

3.3.2.1 Intra-mitochondrial ROS production through Su9-DAO causes changes in mitochondrial morphology and inheritance

The expression of the Su9-DAO construct without induction by alanine addition does not elicit any observable cellular response. As no mitochondrial inheritance defect during DAO stress was observable in large buds, cell cycle synchronization of the culture was considered a possible improvement to increase the number of cells with small to medium sized buds in the sample. To determine the optimal experimental conditions for microscopy experiments using Su9-DAO in synchronized cell cultures different parameters were tested. First of all, it was a prerequisite to determine whether the cells were dividing when Su9-DAO induced ROS production was active. Naturally, this is necessary for investigations of mitochondrial inheritance. It was found that cells were indeed able to divide after induction with D-Ala and their division time was only reduced slightly compared cultures treated with L-Ala.

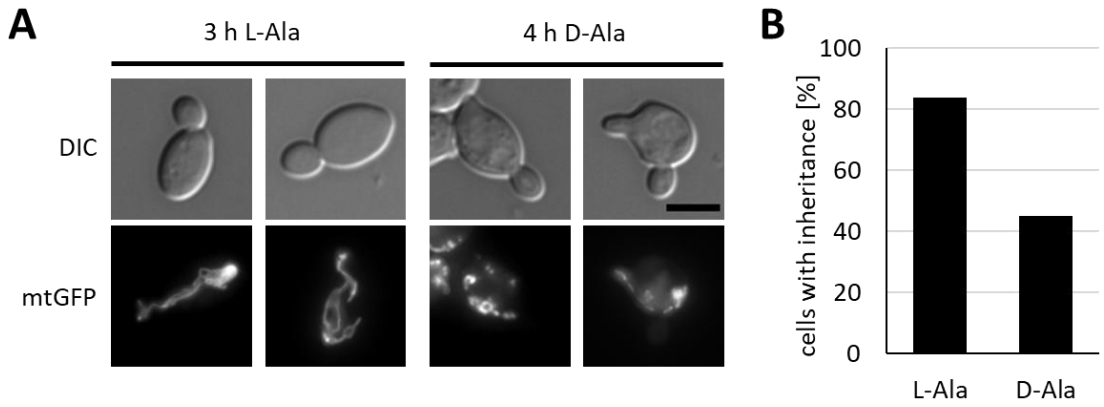

Figure 11: Induction of mitochondrial ROS production alters mitochondrial morphology and lowers mitochondrial inheritance. (A) Su9-DAO Δ*bar1* cells containing a mitochondrial marker were grown in selection medium (selection for mitochondrial marker) and kept in the logarithmic growth phase for at least 24 h. After 1.5 h of incubation with 5 µM mating factor alpha to synchronize the cultures' cell cycle, 100 mM L-alanine (L-Ala; control) or D-alanine (D-Ala) was added to the cells to induce ROS formation by DAO. 2.5 h after alpha factor addition the cells were washed three times to release them from the cell cycle arrest and further incubated in presence of L-Ala or D-Ala. After 2 h (L-Ala) and 3 h (D-Ala), when the newly formed buds had reached an appropriate size, cells were harvested, fixed and analyzed by fluorescence microscopy. GFP fluororescence micrographs represent maximum intensity projections of z-stacks. Bar = 5 µm. **(B)** Quantification of the proportion of cells of (A) with small to medium-sized buds with mitochondrial inheritance. Bars represent the mean value of 100 cells.

In order to achieve a higher level of cell cycle synchronization, Δ*bar1* cells expressing Su9-DAO were used. These mutants display an increased sensitivity to mating factor alpha with a prolonged cell cycle arrest as the Bar1 protein cleaves and thus inactivates mating factor alpha (Sprague and Herskowitz, 1981). According to preliminary experiments by Xenia Chelius, the strongest effects after DAO induction can be observed in selective growth medium without ammonium sulfate containing glucose as a carbon source and by keeping the cells in the logarithmic growth phase for at least 24 h which increases mitochondrial tubularity. To induce oxidative stress 100 mM D-Ala was added to the culture medium. The control was treated with equal amounts of L-Ala which is not metabolized by DAO and does not cause a stress response in the cells. To achieve a high level of synchronicity the cells were incubated with mating factor alpha and treated with D-Ala while in cell cycle arrest. After the release from cell cycle arrest, the cells were continuously incubated with D-Ala in the culture medium. Looking at the first buds formed after cell cycle release, a delay in mitochondrial inheritance could be seen along with a striking mitochondrial phenotype (Figure 11A). While the cells in the control treated with L-Ala showed a very high rate of tubular mitochondria after three hours, cells in the D-Ala treated sample displayed highly fragmented and aggregated mitochondria. The mitochondrial inheritance was also strongly reduced by the D-Ala treatment from over 80% of cells with small to medium buds containing mitochondria in the control compared to only about 45% in the stressed sample (Figure 11B).

Since similar results were observed in logarithmically growing cultures without synchronization and the synchronization altered the cell shape as well as prolonged the duration of the experiment significantly, the following experiments involving Su9-DAO were conducted without cell cycle synchronization. These experiments confirmed a mitochondrial inheritance defect of at least 30% in Su9-DAO expressing cultures treated with D-Ala. Notably, this effect is approximately as strong as the inheritance defect of small- to medium-budded cells lacking Mmr1 (Itoh et al., 2004).

3.3.2.2 Mitochondrial inheritance defect during Su9-DAO treatment is not caused by disturbance of the actin cytoskeleton or reduced Myo2 functionality

To further validate Su9-DAO as a suitable system for investigating mitochondrial inheritance during oxidative stress, we investigated its effect on the same factors involved in mitochondrial inheritance as in the experiments using hydrogen peroxide: Mmr1, Myo2 and the actin cytoskeleton. As changes of the actin cytoskeleton and Myo2 generally cause severe pleiotropic effects, they make experimental results very hard to interpret and insights into mechanisms of a potential quality control during mitochondrial inheritance nearly impossible. As described previously *MMR1* and *MYO2* were genomically tagged with yEGFP (see 3.3.1) in a strain also carrying Su9-DAO.

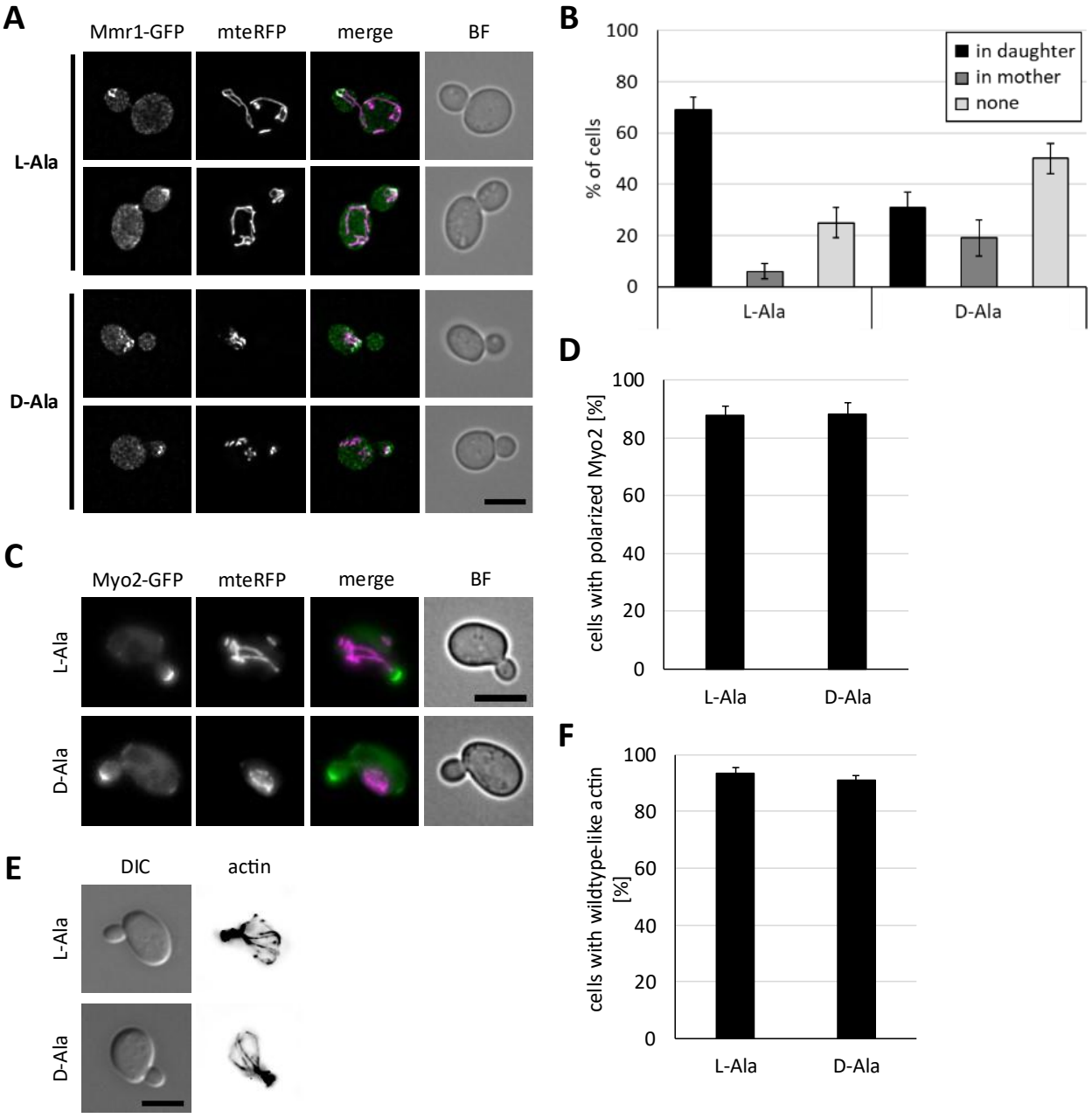

Figure 12: Su9-DAO stress alters Mmr1 localization but not Myo2 localization or actin cytoskeleton. (A) Cells expressing Mmr1-yEGFP and a mitochondrial marker were kept in the logarithmic growth phase for at least 24 h before DAO activity was induced by addition of 100 mM D-Ala (L-Ala for control). After 3 h cells were harvested, fixed, and analyzed by fluorescence microscopy. Fluorescence micrographs show maximum intensity projections of deconvolved z-stacks. Bar = 5 µm. **(B)** Quantification of the presence and existence of a Mmr1 focus in cells with small to medium-sized buds. If more than one focus was present with one being inside the bud, the cell was scored as 'in daughter'. Bars represent mean values of three technical replicates with their SD. At least 100 cells were analyzed per replicate. **(C)** Cells expressing Myo2-yEGFP and a mitochondrial marker were grown and treated as in (A). After 3 h L-/D-Ala treatment the cells were analyzed in live cell microscopy. Fluorescence micrographs represent maximum intensity projections of z-stacks. Bar = 5 µm. **(D)** Quantification of small-budded cells with polarized Myo2 in (C). Bars represent mean values of three technical replicates with their SD. At least 100 cells were scored per replicate. **(E)** Cells were grown, treated, and fixed as in (A). Next, the actin cytoskeleton was stained with rhodamine-phalloidin, and cells were analyzed in fluorescence microscopy. Fluorescence micrographs represent maximum intensity projections of z-stacks. Bar = 5 µm. **(F)** Quantification of cells with

wild type-like actin cytoskeleton with small buds in (E). Data represents the mean values of three technical replicates and their SD. At least 100 cells were analyzed per replicate.

In L-Ala treated cells, similarly as in untreated cells, most dividing cells displayed a Mmr1 focus inside of the daughter cell which was mostly located polarized at the bud tip (Figure 12A). This is indicative of Mmr1's relationship with Myo2. Expectedly, the Mmr1 focus also colocalized with mitochondria. When Su9-DAO expressing cells were treated with D-Ala, so ROS production was induced, an increase in the number of cells displaying a fluorescence focus in the mother could be observed. The number of cells without a Mmr1 focus more than doubled in comparison to the L-Ala treated sample (Figure 12B). At the same time the number of cells displaying a focus in the bud was considerably decreased. These observations could indicate a specific effect of ROS on Mmr1. This hypothesis is further supported by looking at the localization of Myo2 during Su9-DAO stress. Both in the L-Ala and the D-Ala treated samples, Myo2 localized to the bud tip in small-budded cells (Figure 12C and D) and to the mother-bud neck in large-budded cells (not shown), and thus was unaffected by the oxidative stress. Similarly, rhodamine-phalloidin staining demonstrated that the actin cytoskeleton remained unaltered and polarized after Su9-DAO induction when compared to the control (Figure 12E and F). Summarized, these findings point towards Su9-DAO being an excellent tool for studying the effect of mitochondrial damage especially as the mitochondrial transport mechanism is not damaged by it. Additionally, it shows that while mitochondrial inheritance was altered in ROS stressed samples, which supports the idea of quality control during inheritance. The oxidative stress did not result in a delocalization of Myo2. The location of Mmr1 on the other hand was altered after the induction of ROS production in the mitochondrial matrix. It is, however, yet unclear if this change in localization goes hand in hand with Mmr1 degradation and whether it is caused by a direct effect of Mmr1.

3.3.2.3 The mitochondrial inheritance defect during Su9-DAO stress can be overcome by artificially increasing Myo2-based transport

In order to investigate whether a direct link between reduced transport of mitochondria during oxidative stress and the observed mitochondrial inheritance defect exists, mitochondrial transport was enforced using different constructs. First, Mmr1, a known facilitator of mitochondrial inheritance, was overexpressed from a plasmid using the constitutive *GPD* promotor and the effect of DAO after D-Ala induction was evaluated. *MMR1* overexpression was shown to result in an increase of the mitochondrial volume inherited by the daughter cell (Itoh et al., 2004). If the reduced level of mitochondrial inheritance during ROS stress is caused by oxidative stress, *MMR1* overexpression could be able to increase mitochondrial inheritance. If the overexpression of *MMR1* indeed does have this

effect, it also gives an indication about the point of action for the mechanism behind the reduced mitochondrial inheritance during Su9-DAO caused oxidative stress. In Chelius et al. (2023) we showed that the growth of cells expressing Su9-DAO on plates containing D-Ala is severely decreased. So, it was tested whether *MMR1* overexpression can overcome this effect. Using fluorescence microscopy (Figure 13A), the overexpression of Mmr1 could be observed as an accumulation of mitochondrial mass in daughter cells and a comparatively earlier inheritance into smaller buds in accordance with published data (Itoh et al., 2004). *MMR1* overexpression led to an overall level of mitochondrial inheritance in small buds that surpassed the wild type-level and the empty vector control under non-stressed conditions (Figure 13B). In D-Ala treated cultures *MMR1* overexpression could completely offset the stress-induced mitochondrial inheritance defect. The cells even displayed a higher level of inheritance than unstressed cells containing the empty vector control. These results show that *MMR1* overexpression can overcome the negative effect of oxidative stress on mitochondrial inheritance. Although this seems to be only the case on a single cell level as there was no difference observable in the drop dilution assay. This indicates that reduced Myo2 recruitment could cause the reduction of mitochondrial inheritance during oxidative stress.

In accordance with this, similar effects were observed when Myo2-Fis1 was present. The fusion protein was constitutively expressed from a plasmid under the control of the endogenous *MYO2* promotor. This construct allows bypassing the recruitment of Myo2 to mitochondria by Mmr1 and Ypt11 and thus allows a closer examination of the reason for the reduction in mitochondrial inheritance in stressed cells. The Myo2-Fis1 expressing cells displayed the same strong growth impairment as cells with empty vector on plates inducing oxidative stress. The Myo2-Fis1 construct caused a large increase of mitochondrial transport which led to earlier mitochondrial inheritance to the bud along with an increase in the inherited mitochondrial mass (Figure 13C). This approach to bypass the wildtypical mitochondrial inheritance was also able to increase the portion of small to medium sized cells showing mitochondrial inheritance to a higher level than in the unstressed controls during DAO activity (Figure 13D). Taken together these findings indicate that reduced recruitment of the Myo2 motor protein might be the cause of the reduction of mitochondrial transport during ROS stress.

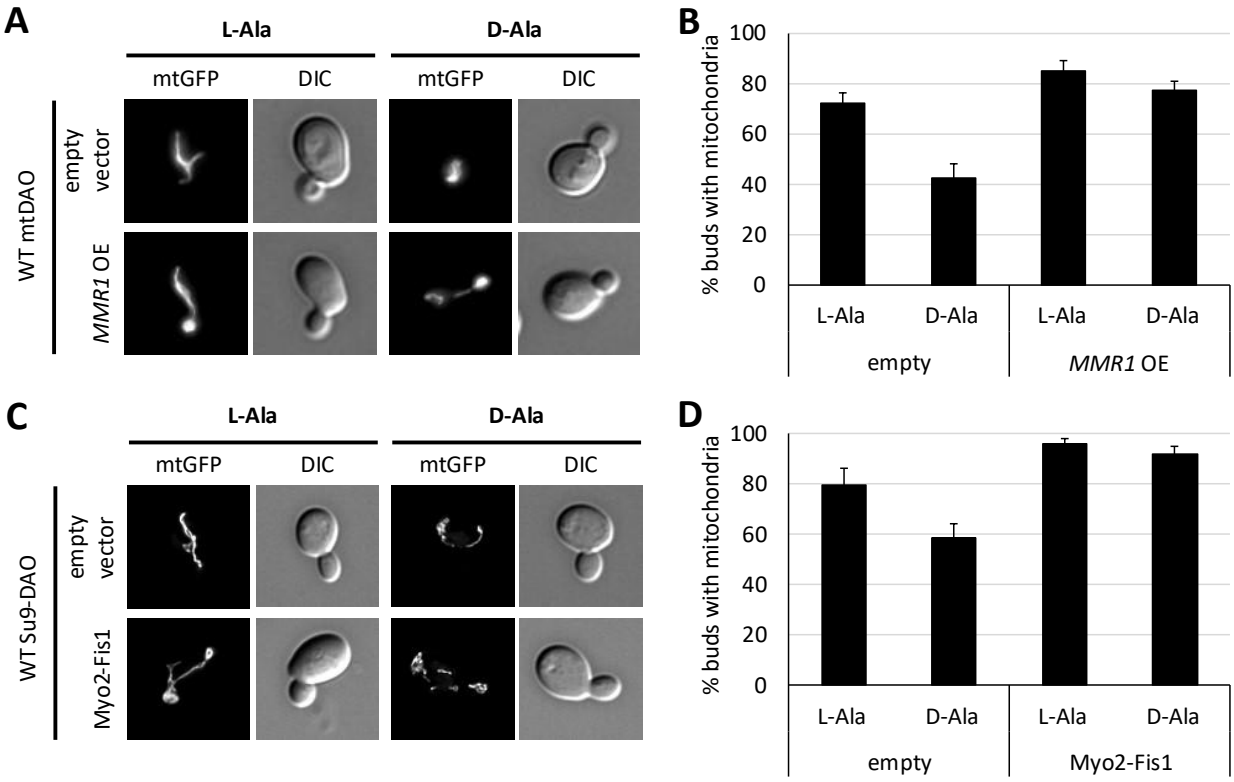

Figure 13: Overexpression of Mmr1 and the chimeric Myo2-Fis1 construct can rescue the mitochondrial inheritance defect caused by Su9-DAO. (A) Cells constitutively expressing *MMR1* from a single-copy plasmid or an empty vector control and a mitochondrial marker were kept in the logarithmic growth phase for at least 24 h before DAO activity was induced by addition of 100 mM L-Ala (control) or D-Ala. After 3 h cells were harvested, fixed, and analyzed by fluorescence microscopy. Fluorescence micrographs show maximum intensity projections of deconvolved z-stacks. Bar = 5 µm. **(B)** Quantification of the mitochondrial inheritance in small-budded cells in (A). Bars represent mean values of three technical replicates with their SD. At least 100 cells were scored per replicate. **(C)** Cells constitutively expressing Myo2-Fis1 or an empty vector control and a mitochondrial marker were kept in the logarithmic growth phase for at least 24 h before DAO activity was induced by addition of 100 mM L-Ala (control) or D-Ala. After 3 h cells were harvested, fixed, and analyzed by fluorescence microscopy. Fluorescence micrographs show maximum intensity projections of deconvolved z-stacks. Bar = 5 µm. **(D)** Quantification of the mitochondrial inheritance in small-budded cells in (C). Bars represent mean values of three technical replicates with three biological replicates and their SD over all values. At least 100 cells were scored per replicate.

3.3.2.4 Artificially anchoring the peroxisomal Myo2 receptor Inp2 to mitochondria can increase mitochondrial transport and counteract Su9-DAO stress

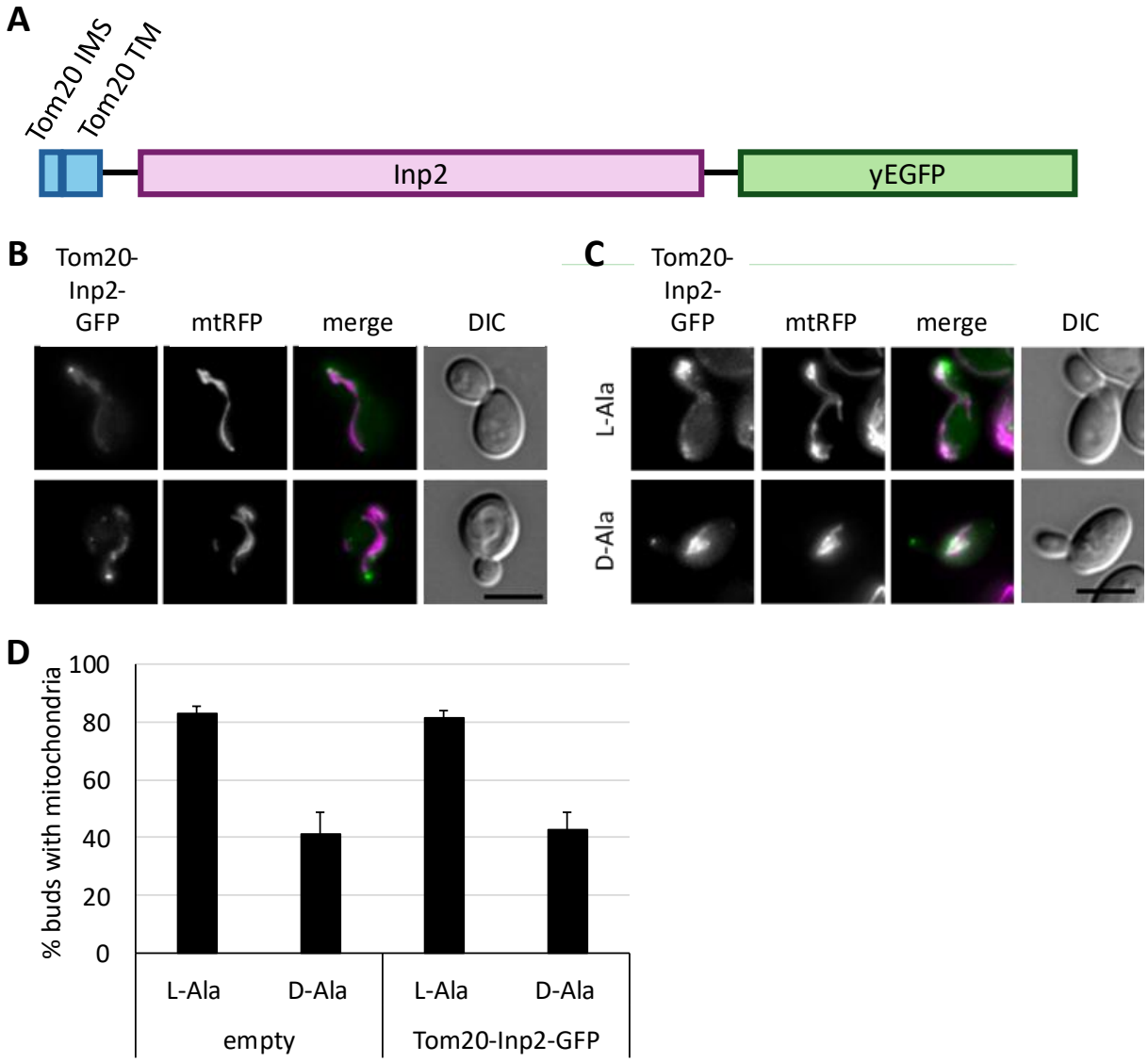

Figure 14: In unstressed and ROS-stressed WT cells Tom20-Inp2-GFP does not affect mitochondrial inheritance **(A)** Structure of the chimeric Tom20-Inp2-GFP protein. The inter- and transmembrane (IMS, TM) domains of Tom20 were fused to the C-terminal (CT) domain of Inp2 and yEGFP with small flexible linkers. This scheme is meant for purposes of visualization and fragments are not drawn to scale. **(B)** Cells expressing Tom20-Inp2-GFP and a mitochondrial marker were grown in selective medium (selection for mitochondrial marker) and fixed in logarithmic growth phase using formaldehyde and analyzed using fluorescence microscopy. Fluorescence micrographs represent maximum intensity projections of z-stacks. Bar = 5 µm. **(C)** Cells expressing Tom20-Inp2-GFP and a mitochondrial marker were kept in the logarithmic growth phase for at least 24 h before DAO activity was induced by addition of 100 mM L- or D-Ala. After 3 h cells were harvested, fixed, and analyzed by fluorescence microscopy. Fluorescence micrographs show maximum intensity projections of z-stacks. Bar = 5 µm. **(D)** Quantification of the mitochondrial inheritance in small- to medium-sized budded cells expressing an empty vector control or Tom20-Inp2-GFP treated as in (C). Bars represent mean values of three biological replicates with their SD. At least 100 cells were scored per replicate.

The observation that Su9-DAO does not affect the inheritance of all organelles since for example peroxisomes remain unaffected by the ROS stress (Chelius et al., 2023) could further point to Mmr1 as a target for mitochondrial quality control. To further investigate this idea, Tom20-Inp2-GFP, a chimeric protein that artificially recruits Myo2 to mitochondria, was constructed (Figure 14A). It consists of the C-terminal, cytosolic part of the peroxisomal Myo2 receptor Inp2, which was shown to be sufficient for binding the motor protein (Fagarasanu et al., 2006), fused to the N-terminal part of Tom20 including the transmembrane domain to target the protein to the MOM. Additionally, this chimeric protein was C-terminally tagged with yEGFP. This construct was cloned into a vector containing a prototrophic selection marker to select for cells containing the plasmid. The construct was expressed using the *TOM20* promotor and the whole construct was cloned into the pRS416 backbone by Verena Geiger as part of her bachelor thesis.

The yEGFP tag allowed quick and easy confirmation of the expression of the fusion protein and it's correct localization at the mitochondrial membrane. The GFP signal was observed colocalizing with mitochondria throughout the entire cell with low signal intensity and one or several stronger fluorescence foci (Figure 14B). Usually, a bright GFP focus was observable at the bud tip in dividing cells which suggests a successful interaction with the Myo2 motor protein. Overall, the localization of Tom20-Inp2-GFP under non-stress conditions appeared to be as intended: Colocalizing with mitochondria and polarization suggesting Myo2 binding. During Su9-DAO-caused oxidative stress an increase in polarized GFP foci that did colocalize with mitochondria as well as a general cytosolic signal could be observed, although a large portion of the protein remained mitochondrial (as visible in Figure 14C). The reduction of observable mitochondrial localization could indicate a reduction in mitochondrial import efficiency, at least to a level where Tom20-Inp2-GFP binding to Myo2 is faster than the import into the mitochondrial membrane. Expressing Tom20-Inp2-GFP in WT cells did not lead to an accumulation of mitochondria in the daughter cell as was observed for Myo2-Fis1 or Mmr1 overexpression. Additionally, the mitochondrial inheritance defect under Su9-DAO stress could not be overcome by the Tom20-Inp2-GFP construct (Figure 14C and D). While the localization of the GFP signal suggests that the Tom20-Inp2-GFP construct is expressed and its insertion into mitochondria is successful, it appears that the construct is either not functional so that it does not confer mitochondrial inheritance or is not expressed abundantly enough to carry mitochondrial inheritance alone while the Mmr1-, Ypt11- and Myo2-dependent transport machinery is affected by the oxidative stress. Other explanations for this could be that Tom20-Inp2-GFP is also affected by Su9-DAO stress or that the mitochondrial transport capacity of Myo2 is changed by oxidative stress in a specific fashion that does not affect the transport of other organelles.

To further investigate these possibilities as well as gain more insights into whether the Tom20-Inp2-GFP construct is able to mediate Myo2-dependent mitochondrial transport, it was tested whether Tom20-Inp2-GFP can rescue the inviable (in the BY strain background) Δ*mmr1* Δ*ypt11* double mutant. For this, the plasmid carrying Tom20-Inp2-GFP was introduced in a diploid heterozygous double mutant and the cells were sporulated on low-nutrient medium plates. The resulting tetrads were dissected, and their genotypes were analyzed by testing for selection markers and the alleles of interest were confirmed by colony PCR in relevant strains. While in the control carrying a pRS416 empty vector no double deletion mutants were viable, some double mutants carrying the Tom20-Inp2-GFP construct were able to form colonies and stably grow (Figure 15A). However, not all double mutants carrying Tom20-Inp2-GFP were rescued and the colonies that the rescued clones formed on the dissection plates were inhomogeneous in size, some being very small. After transfer to new agar plates, all viable double mutants displayed growth comparable to wild type cells, nonetheless. To confirm that the Tom20-Inp2-GFP construct and not another, secondary mutation was indeed responsible for rescuing the lethal phenotype, the ability of the double mutants to survive without the Tom20-Inp2-GFP plasmid was tested by transferring them to 5'FOA-containing medium plates which select against cells containing a plasmid with the *URA3* selection marker (Figure 15B). Neither Δ*mmr1* Δ*ypt11* cells with Tom20-Inp2-GFP nor Δ*mmr1* Δ*ypt11* Su9-DAO cells with Tom20-Inp2-GFP were able to grow on plates containing 5'FOA. This proves that the chimeric Tom20-Inp2-GFP construct is indeed functional and responsible for rescuing mitochondrial inheritance in the absence of Mmr1 and Ypt11.

When analyzing the Δ*mmr1* Δ*ypt11* Su9-DAO cells by fluorescence microscopy, it was of special note that the GFP fluorescence intensity and the number of cells showing expression of the construct compared to WT Su9-DAO cells was strongly increased compared to the previous experiments looking at Tom20-Inp2-GFP fluorescence (Figure 15C). The experiments cannot be compared to each other directly as it was necessary to decrease the exposure time for GFP excitation in order to not saturate the detector due to the brightness of the GFP signal and the contrast for the shown fluorescence micrographs was set to be consistent within each experiment but not between them. Taken together with the fact that not all double mutants were rescued by the Tom20-Inp2-GFP construct this can probably be explained by an upregulation of the expression of Tom20-Inp2-GFP. During Su9-DAO stress, an increase in Tom20-Inp2-GFP foci could again be observed as well as a higher amount of GFP fluorescence not colocalized with mitochondria (Figure 15C).

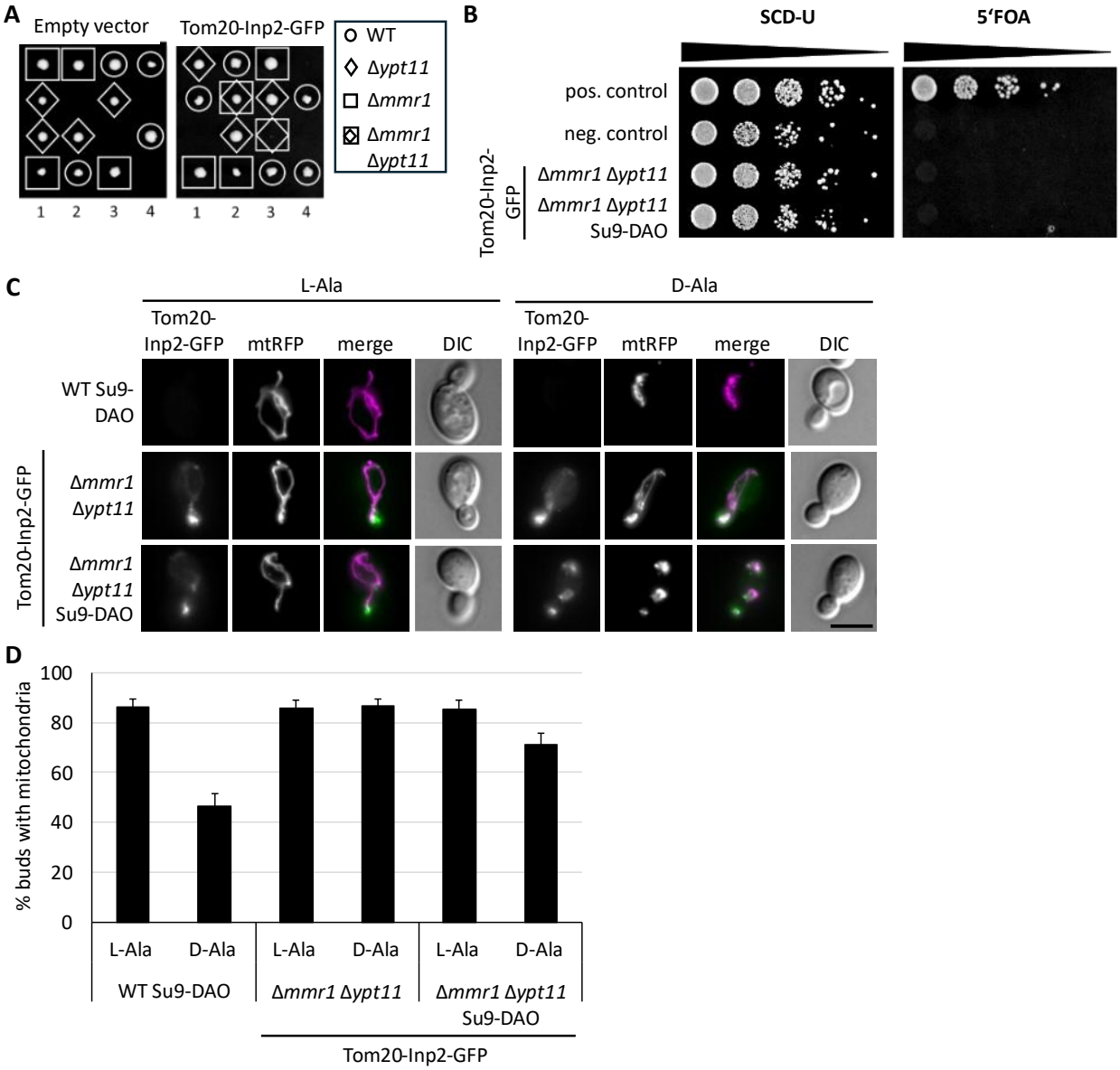

Figure 15: Tom20-Inp2-GFP can mediate mitochondrial transport under non-stressed and Su9-DAO -caused stress conditions in the absence of Mmr1 and Ypt11. (A) Heterozygous diploid Δ*mmr1* Δ*ypt11* cells containing either an empty vector control or expressing Tom20-Inp2-GFP were sporulated and tetrads were dissected on YPD medium plates. After 3 days of incubation, the genotypes of the resulting colonies were determined by plating on selection media and confirmed by PCR. **(B)** Cells were grown until stationary phase in non-selective SCD overnight to allow plasmid loss. The next day the cultures were adjusted to the same optical density. Then they were diluted in 1:10 serial steps and the dilutions were plated on SCD-U and SCD + 5'FOA plates and incubated at 30°C for 3 days. The positive control shows WT cells with an empty vector control. The negative control shows Δ*mmr1* Δ*ypt11* cells carrying pRS416-*MMR1*. **(C)** Cells containing either the empty vector control or Tom20-Inp2-GFP and a mitochondrial marker were kept in the logarithmic growth phase for at least 24 h before addition of 100 mM L- or D-Ala. After 3 h cells were harvested, fixed, and analyzed by fluorescence microscopy. Fluorescence micrographs show maximum intensity projections of z-stacks. Bar = 5 µm. **(D)** Quantification of the mitochondrial inheritance in small- to medium-sized budded cells in (D). Bars represent mean values of three technical replicates with three biological replicates and their SD over all values. At least 100 cells were scored per replicate.

Most importantly the expression of Tom20-Inp2-GFP during Su9-DAO stress in Δ*mmr1* Δ*ypt11* Su9-DAO mutant yeast cells did confer close to wild type like mitochondrial inheritance (Figure 15D) This is especially interesting as it can be assumed that the inviability of this double mutant is based on its inability to transport sufficient amounts of mitochondria during budding. Under non-stressed conditions mitochondrial inheritance was unchanged by Tom20-Inp2-GFP compared to WT Su9-DAO cells expressing the empty vector control. Additionally, this experiment shows that D-Ala treatment is not harmful in cells not expressing Su9-DAO (see Δ*mmr1* Δ*ypt11* cells) as it does neither alter mitochondrial morphology nor inheritance compared to the L-Ala control. These findings indicate that Mmr1 and/or Ypt11 are responsible for the mitochondrial quality control during inheritance caused by mitochondrial oxidative stress generated by Su9-DAO since mitochondrial inheritance can be restored by using an artificial mitochondrial Myo2 receptor.

3.3.2.5 Mmr1 is a key factor in mitochondrial quality control under oxidative stress

Since previously published data (Higuchi-Sanabria et al., 2016) as well as the findings in this project indicate an involvement of Mmr1 and Ypt11 or at least one of these proteins in the inheritance of specific mitochondria in a quality control mechanism during mitochondrial inheritance, the effect of Su9-DAO-caused oxidative stress in Δ*mmr1* or Δ*ypt11* deletion mutants was examined next. Additionally, the deletion mutant of *PTC1* was examined since this protein phosphorylates Mmr1 and thus regulates Mmr1´s activity and localization (Jin et al., 2009; Swayne et al., 2011).

In order to take a closer look at the Δ*ptc1* deletion mutant, it was analyzed by fluorescence microscopy with a focus on mitochondrial morphology and mitochondrial inheritance (Figure 16A and B). Δ*ptc1* cells displayed a strongly altered mitochondrial phenotype regardless of the presence of the Su9-DAO construct and its induction (cells without Su9-DAO construct not shown): A large population of Δ*ptc1* cells displayed a strong inheritance defect and an accumulation of mitochondria at the mother cell pole on the opposite side of the daughter as previously described (Roeder et al., 1998). The observed phenotype strongly resembles the phenotype conferred by the *myo2(LQ)* allele which possesses two point mutations in the cargo binding domain of the motor protein resulting in reduced mitochondrial inheritance (Förtsch et al., 2011). This resemblance with the *myo2(LQ)* phenotype could indicate that the deletion of *PTC1* leads to a similar inability to transport mitochondria through an alteration of Mmr1´s ability to establish Myo2 recruitment to mitochondria. Accordingly, the portion of small to medium sized buds containing mitochondria in Δ*ptc1* was only half of the WT control (43% and 86%). Su9-DAO -triggered intramitochondrial ROS production did not further lower the level of mitochondrial inheritance in the mutant. If these two mechanisms - the deletion and the stress - acted independently,

mitochondrial inheritance would be expected to be lowered by the simultaneous presence of both impairments. It seems likely however, that the effect of the deletion on mitochondrial inheritance was so strong that the level mitochondrial inheritance was already lowered to a minimum and Su9-DAO did not further impact the amount of inheritance.

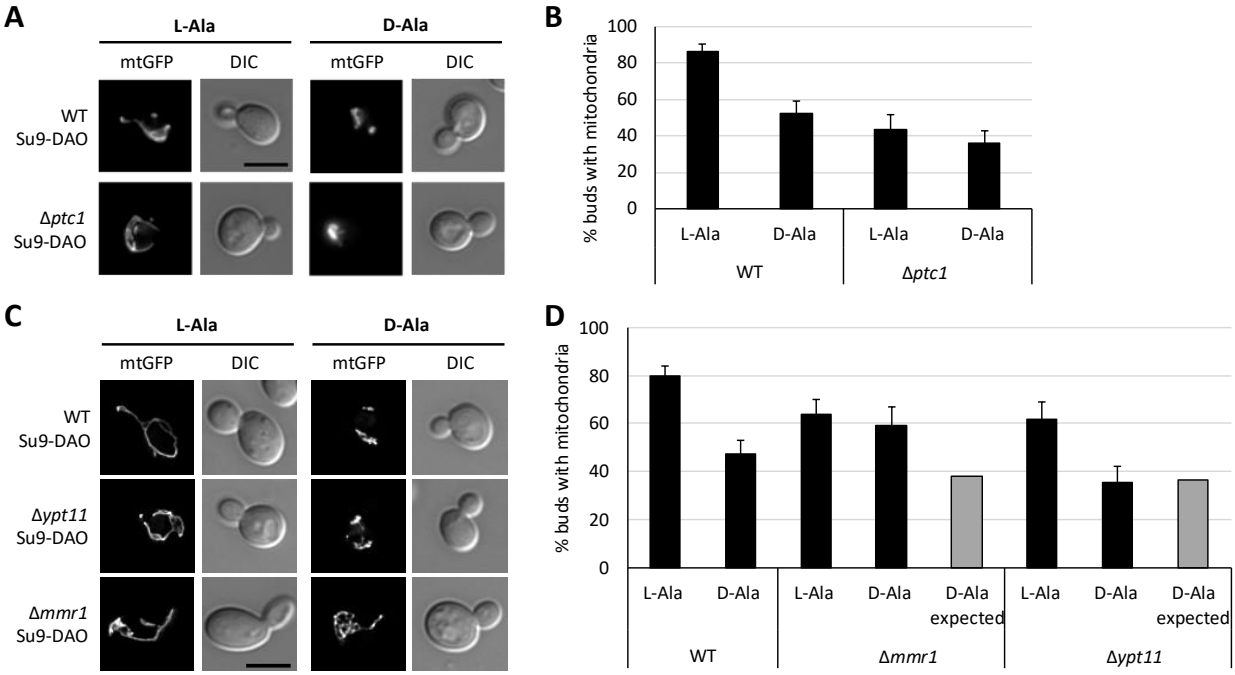

Figure 16: Quality control during mitochondrial inheritance under Su9-DAO stress requires Mmr1. (A) WT and Δ*ptc1* expressing Su9-DAO and a mitochondrial marker were kept in the logarithmic growth phase for at least 24 h before addition of 100 mM L- or D-Ala. After 3 h cells were harvested, fixed, and analyzed by fluorescence microscopy. Fluorescence images show maximum intensity projections of z-stacks. Bar = 5 µm. **(B)** Quantification of the mitochondrial inheritance in small- to medium-sized budded cells of (A). Bars represent mean values of three technical replicates with three biological replicates and their SD over all values. At least 100 cells were scored per replicate. **(C)** Fluorescence microscopy of Su9-DAO cells with a mitochondrial marker grown and treated as in (A). **(D)** Quantification of the mitochondrial inheritance in small- to medium-sized budded cells of (C). Bars represent mean values of three technical replicates with three biological replicates and their SD over all values. At least 100 cells were scored per replicate. The expected values for D-Ala treatment in Δ*mmr1* and Δ*ypt11* were calculated to display the expected % of buds with mitochondria if the mutation and stress treatment acted independently of each other.

Lastly, to investigate the involvement of the known Myo2 interactors Mmr1 and Ypt11 was tested directly by induction of intra-mitochondrial ROS stress in Δ*mmr1* and Δ*ypt11* single deletion mutants. If the reduction of mitochondrial transport and inheritance as a quality control mechanism during budding is dependent or acting on one or both of these proteins, Su9-DAO induction for intra-mitochondrial ROS production in the deletion mutants should not have an effect. To test this, Δ*mmr1* and Δ*ypt11* single deletion mutants genomically carrying the Su9-DAO construct were treated with L-

Ala or D-Ala and mitochondrial inheritance was evaluated microscopically and compared to wild type cells (Figure 16C and D). Under L-Ala control conditions both mutants displayed a moderately reduced level of mitochondrial inheritance. Under D-Ala stress conditions, Δ*ypt11* Su9-DAO cells displayed a reduced amount of mitochondrial inheritance that reflects the additive nature of the inheritance defect caused by Su9-DAO in WT and the deletion itself. Δ*mmr1* Su9-DAO cells on the other hand were completely unaffected by D-Ala treatment and had the same level of mitochondrial inheritance as the L-Ala control. Notably, Δ*mmr1* and Δ*mmr1* Su9-DAO cells had a strongly interconnected mitochondrial network, somewhat resembling a mutant of the mitochondrial fission machinery. This phenotype made it necessary to use GFP as a mitochondrial marker here while most other experiments involving DAO were performed using yEGFP as the brighter yEGFP did not allow the resolution of the net-like structures. These findings indicate that Mmr1 is an essential component in the mechanism behind preferential inheritance of higher functioning mitochondria. Since *MMR1* overexpression, Myo2-Fis1 and Tom20-Inp2-GFP, all constructs which allowed the bypassing or enhancement of the recruitment of the motor protein Myo2, proved to be successful in suppressing the mitochondrial inheritance defect during Su9-DAO -caused oxidative stress, it can be concluded that the mechanism discriminating mitochondrial fitness acts on this process. Ypt11 on the other hand, while able to compensate for the loss of Mmr1 in mitochondrial inheritance per se, does not seem to be involved in the process of fitness-based selective mitochondrial inheritance.

4 Discussion and outlook

4.1 Asymmetrical inheritance of protein aggregates

Baker´s yeast can replicate asexually by budding, performing an asymmetric division resulting in two non-identical cells. The newly formed cell – usually referred to as the 'daughter' –, is displaying full replicative potential while the other cell – typically called 'mother' – is exhibiting signs of aging and a limited capability to divide further (Higuchi-Sanabria et al., 2014). Mothers have been shown to retain cytotoxic agents like, for example ERCs (Sinclair and Guarente, 1997), damaged proteins (Aguilaniu et al., 2003), their sequestration sites (Miller et al., 2015b), and organelles associated with aggregates (Clay et al., 2014). With increasing lifetime and number of cell divisions, an accumulation of protein aggregates caused by external and intracellular factors increasing proteolytic stress takes place (Baldi et al., 2017; Denoth Lippuner et al., 2014; Kaeberlein, 2010; Klinger et al., 2010). A lot of research has attempted to discern whether aggregate asymmetry during cell division is driven by active retention mechanisms (Andrade-Restrepo, 2017; Coelho et al., 2014) or stochastic events (Paoletti et al., 2016). In recent years it has been largely agreed upon that this important feat is indeed accomplished by several cellular mechanisms in conjunction. One of the factors that have been linked to aggregate clearance (Ruan et al., 2017) and retention (Zhou et al., 2014) is the mitochondrial network by supposedly capturing smaller aggregates, tethering them to their outer surface and thus immobilizing them as well as its ability to import misfolded proteins. This connection would allow an elegant way for yeast cells to combine aggregate retention with the selective inheritance of high-functioning mitochondria if aggregates were preferentially attached to uninherited mitochondria. Furthermore, the observation that asymmetric inheritance of oxidatively damaged proteins and the level of aggregate association with organelles decline over the replicative lifespan of the mother cell has been made (Aguilaniu et al., 2003; Zhou et al., 2014). This coincides with a decline of overall mitochondrial fitness with an increased rate of ROS production and changes in morphology and dynamics in aged cells (Lam et al., 2011; Sharma et al., 2019). It was previously shown that increased mitochondrial inheritance, as forced through the expression of the Myo2-Fis1 construct, leads to a significant increase of inherited aggregates with more of them associated with mitochondria (Böckler et al., 2017). Likewise, reduced mitochondrial transport caused by the *myo2(LQ)* mutant allele led to a decreased aggregate retention level but aggregates present in daughters did appear to be not attached to mitochondria. This shows a close relationship between aggregates and mitochondria since disturbances of mitochondrial transport and dynamics leading to both decreased and increased mitochondrial transport both cause lower aggregate asymmetry between mother and daughter.

So far, only the mitochondrial fission protein Fis1 has been suggested to be involved in the attachment of protein aggregates to mitochondria as a potential anchor for aggregates on the mitochondrial surface, leading to increased aggregate leakage to the daughter (Zhou et al., 2014). The findings regarding the level of association could be confirmed in this study (Figure 1, page 38), however, even in the Δ*fis1* deletion mutant the levels of colocalization between Hsp104 foci and mitochondria observable in fluorescence microscopy remain fairly high. Notably, *FIS1* deletion did not lead to an increased rate of inheritance of aggregates by daughter cells. This suggests that the attachment of aggregates to mitochondria does not play an essential role in aggregate retention or that multiple parallel mechanisms to prevent aggregate inheritance are in place and potentially are able to compensate for each other's loss. Since the deletion of *FIS1* also influences mitochondrial dynamics which have been linked to aggregate retention, it is unclear whether the change in dynamics or the lack of the protein itself is causing the lowered aggregate association. It was verified, that the common secondary mutation in the *WHI2* gene in Δ*fis1* cells is not the cause of this effect. In line with previous results (Zhou et al., 2014) none of the strains tested for this thesis displayed a lower rate of aggregate retention but the Δ*fzo1* Δ*dnm1* double mutant displayed a lower rate of aggregate-mitochondria association. Since this mutant has both disturbed mitochondrial fusion and fission, this result further points towards a link between mitochondrial dynamics and movement and the capturing of aggregates as proposed in Böckler et al. (2017), where it was shown that the transport impaired *myo2(LQ)* mutant displays an increased level of aggregate inheritance and a higher level of free aggregates present in the bud.

One described mechanism for the detoxification of cytosolic misfolded proteins is their import into the mitochondrial intermembrane space and matrix where they are subsequently degraded by proteases in a process that was named MAGIC (mitochondria as guardian in cytosol) (Ruan et al., 2017). Additionally, a recent paper showed that intramitochondrial protein aggregates were retained in the mother by targeted mitochondrial fission (Sun et al., 2023). Similarly, it has been described that cytosolically translated mitochondrial proteins causing ribosomal stalling are translocated into mitochondria in a Vms1-dependent mechanism that is hindering protein aggregation (Izawa et al., 2017). Furthermore, IMiQ (intramitochondrial protein quality control compartment), an intra-mitochondrial protein deposit site, has been shown to be inherited asymmetrically and to detoxify aggregates dependent on mitochondrial fusion and fission (Bruderek et al., 2018). To test the relevance of mitochondrial import to aggregate retention and mother-daughter asymmetry, the 'clogger' constructs described by the Herrmann group were employed (Boos et al., 2019). Due to their inefficient and slow import, these constructs block the mitochondrial import pores and thus cause cellular and proteostatic stress and cell cycle arrest. It was possible to successfully develop an assay where the formation of heat induced protein aggregates could be triggered and observed in mitotically growing

cells while simultaneously inducing 'clogger' expression to lower mitochondrial import (Figure 2, page 41). However, a decrease of the mother cells' ability to retain protein aggregates due to the blockage of efficient mitochondrial import was not observed in this study. As previously mentioned, several other mechanisms to achieve asymmetric inheritance of aggregates, like sequestration into larger deposit sites, have been described (Miller et al., 2015b) and the redundancy of these mechanisms could very possibly be able to compensate for the loss of mitochondrial association to sustain a high level of aggregate retention. When looking at the effect of mitochondrial import clogging, a slight reduction on the level of association of aggregates to mitochondria could be observed. Interestingly, the cells expressing clogger proteins showed a higher number of aggregates with smaller size compared to the control, which aligns with the idea that smaller aggregates are captured on organelle surfaces in order to facilitate the formation of larger aggregates (Miller et al., 2015a; Zhou et al., 2014).

Contrastingly, another recent publication using the 'clogger' showed no increase in the number of aggregates based on clogger induction but an increase in Hsp104-GFP foci diameter (Krämer et al., 2023). It has to be noted, however, that the experimental setups differed in some important respects: the use of active versus inactive Hsp104, observation of heat shock induced aggregates versus the formation of aggregates after clogger induction, and raffinose versus lactate as carbon source in the medium. The increased number of fluorescent foci present in cells using the clogger constructs to block mitochondrial import could simply be a reflection of the increased proteostatic stress as more and more precursors and proteins cannot be imported and sorted to their correct location. It is highly probable that some of the Hsp104-GFP foci mark MitoStores (Krämer et al., 2023), protein granules storing mitochondrial precursors that cannot be imported, instead of misfolded proteins that formed larger aggregates from the heat stress. In conclusion, the effect might not be directly connected to mitochondrial import itself at all but caused by secondary effects due to the reduction of mitochondrial import.

Overall, it can be concluded that mitochondrial import does not seem to be essential for the upkeep of aggregate retention in *S. cerevisiae*, but it might affect it positively, albeit in a potentially indirect fashion. Other experiments with impaired mitochondrial import could help to elucidate this further. For example, oxidative phosphorylation could be blocked chemically using CCCP. Treatment with this chemical impairs mitochondrial import by breaking down the mitochondrial membrane potential that drives it (Martin et al., 1991). Alternatively, import mutants, for example conditional *ssc1* mutants, could be used for this purpose. Ssc1 (mtHsp70) is a chaperone involved in the import of mitochondrial matrix precursor proteins across the IMM that interacts with the TIM23 complex as well as many IMM and IMS proteins (Neupert and Herrmann, 2007).

A different approach to investigate the relationship between mitochondria and aggregates of misfolded proteins in this study was also based on the findings of the Herrmann group. In Hansen et al. they recently published a genome-wide screen aiming to identify an unknown mechanism for the import of mitochondrial membrane proteins (Hansen et al., 2018). As the pathway they discovered bears a close resemblance to the proposed route that aggregates follow (Zhou et al., 2014)– moving along the ER surface and being transported to mitochondria at ERMES (ER-mitochondria encounter structure) organelle-organelle contact sites – the pathway's key protein Djp1, as well as other hits found by Hansen et al. (2018) in their screen, were considered probable candidates to be involved in organellar tethering of aggregates . Deletion mutants of all non-essential genes found in the screen did not display altered levels of aggregate retention efficiency, but a subset of uncharacterized candidates (Δ*ema17*, Δ*ema19*, Δ*ema35*) and Δ*djp1* were analyzed further (Figure 3, page 43). These deletion mutants displayed normal to slightly reduced levels of mitochondria-aggregate association but a higher number of total aggregates per cell (often up to multiples of the amount in wild type cells). Additionally, it was striking that the increased number of aggregate foci was largely made up of small aggregates that to a larger extent did not colocalize with mitochondria. Since the level of aggregate inheritance during budding was not affected, this could signify that these smaller aggregates are either free or attached to the ER. According to the model, aggregate formation and fusion is taking place on the ER surface, but no increased level of colocalization with the ER could be detected either. This finding should be further investigated using live cell microscopy to assess whether the smaller aggregates are more mobile than larger ones, indicating that they might be free in the cytosol. Furthermore, no increased heat sensitivity or cytotoxicity could be observed in the deletion mutants in the drop dilution assay despite of the increased number of supposedly cytotoxic misfolded proteins. It has been known for a long time that cells can very successfully adapt to continuous heat stress by changing gene expression (Gasch et al., 2000; Piper, 1993). So, this result can be explained by adaptation to the permanently increased temperature. Taken together, these findings do not suggest an involvement of the observed proteins in mitochondria-aggregate association nor in the ER-aggregate association or in aggregate retention in general.

However, the fusion of aggregates was disturbed in some of the candidates (Figure 4, page 45). A question that should be addressed in further experiments concerning this, is whether the localization of the increased number of aggregates is different from a random distribution of a large number of foci in a limited area. Additionally, experiments investigating the nature of the interaction between mitochondria and misfolded proteins should be focused on. While protein aggregates are often observed in close proximity with mitochondria, the form of this interaction is largely unknown. It remains unclear whether protein aggregates are stably or transiently attached to the mitochondrial surface, for example through interaction with specific or unspecific proteins in the mitochondrial outer

membrane, or whether there even is an actual interaction. A possible attempt at this could be a bimolecular fluorescence complementation assay. Two fragments of a fluorescent reporter protein are merged to two proteins of interest. If the two proteins are in close contact and interact with each other, the fluorescent protein is able to fold properly and fluoresce. Hsp104^{Y662A} or other commonly used misfolding proteins like Ubc9ts, a temperature sensitive mutated variant of the ubiquitin-conjugating enzyme 9 (Ubc9) that misfolds above 30 °C (Kaganovich et al., 2008), could be used as aggregate markers along with abundant proteins of the mitochondrial outer membrane. Recently it was found that the mitochondrial outer membrane protein Tom70 is involved in the association of aggregates to the mitochondrial surface as well as aggregation itself (Liu et al., 2023). However, in these experiments Δ*tom70* mutants showed no increase in aggregate inheritance and only increased leakage was observed.

Based on published data that the septin ring at the mother-bud neck serves as a barrier for aging factors like aged nuclear pore complexes and protein aggregates in the ER (Clay et al., 2014; Shcheprova et al., 2008) and data from genome-wide screens conducted in the Westermann lab that found a negative genetic interaction with *myo2(LQ)* and Myo2-Fis1 amongst other (including unpublished) results (Böckler et al., 2017; Hock, 2019), septins were considered very interesting candidates for involvement in asymmetric inheritance of protein aggregates. Due to its interaction with altered *myo2* alleles, an involvement of the septins seems especially likely in combination with mitochondrial anchoring of aggregates. Thus, septins could possibly also be connected to mitochondrial quality control during inheritance. To combat the complications of studying essential genes as well as the strongly altered cell cycle and cellular morphology with cytokinesis defects in conditional or viable septin mutants, two different systems of conditional protein depletion were employed in this study: inducible degradation and temperature sensitive alleles. Tagging Cdc10, Cdc11 and Cdc12 with AID* or AID*-6FLAG, and the genomic integration of OsTIR1 allowed the quick, specific and easily confirmable depletion of septins in haploid and diploid cells (Figure 5, page 47). Contrary to other descriptions of the system (Morawska and Ulrich, 2013), the addition of the tag itself did not seem to lead to increased degradation, at least of tagged Cdc10 and Cdc11. As tagging of Cdc12 was unsuccessful in haploid yeast cells it is probable that the tag interfered with protein functionality. After confirming the AID system as a suitable tool for septin depletion, it was found that the smaller AID* tag without an additional epitope tag caused less defects in cellular morphology (mostly pseudohyphal growth). Nonetheless, the system turned out to be not optimal for microscopy studies with the goal of observing Hsp104^{Y662A}-GFP marked protein aggregates since the addition of auxin to the medium to induce degron activity caused an increased formation of aggregates and mitochondrial fragmentation. Others have also described that WT *S. cerevisiae* is affected by IAA regardless of the AID system's

presence as it has been found to inhibit growth and promote invasive growth (Nicastro et al., 2021; Prusty et al., 2004). Furthermore, IAA inhibits TORC1 (target of rapamycin complex 1) and thus majorly interferes with mitochondria – amongst many other cellular processes. It has previously been described that the deletion of a protein component of the TORC1 complex causes mitochondrial fission in fission yeast (Anjum et al., 2023). Therefore, a similar effect in *S. cerevisiae* can be expected. Additionally, yeasts are able to produce IAA themselves, although probably not in quantities required to induce protein degradation by the AID system (Spaepen et al., 2007).

In parallel, experiments using cells carrying the *cdc12-1* and *cdc12-6* mutant alleles (Barral et al., 1999; Barral et al., 2000) were conducted (Figure 6, page 51). The ARE protocol was adapted to allow simultaneous inactivation of the septin ring and an appropriate amount of aggregate formation while keeping the stress low enough to not cause cell cycle arrest by subjecting the cells to a continuous heat shock at a lowered temperature (compared to other heat shock experiments). It is important to note that this experiment cannot be used to determine aggregate retention as the continuous heat shock constantly triggers the formation of new heat-shock aggregates so it can only be used to investigate aggregate asymmetry. Furthermore, it allowed the investigation of aggregate mobility and whether retrograde transportation of aggregates from the bud to the mother cell is taking place at a substantial level through prolonged live-cell microscopy. At first, the results gathered showed a strong increase of aggregate inheritance under non-permissive temperature, but this could not be reproduced in follow-up experiments even when trying to control the experimental parameters like cell cycle synchronization and performing the heat shock in a water bath to make it more reproducible. Overall, it was not possible to investigate the role of septins in aggregate retention during budding since both approaches did not lead to reliable results. Nonetheless, septins remain a good candidate for functioning as a diffusion barrier for aggregates and further attempts to design and optimize experimental systems that allow the examination of septin mutants should be made.

Overall, no unknown mitochondrial factors that have an influence on aggregate retention could be identified in this study. However, a few proteins whose deletion increased the number of aggregate foci observable per cell or decreased colocalization of aggregates with mitochondria. Additionally, it was observed that a reduction of the mitochondrial import efficiency through the ‘Clogger’ constructs had a similar effect. For further studies in this field is imperative to employ methods to confirm a direct interaction between aggregates and mitochondria, whether it be in the form of tethering or otherwise, these findings however, remain somewhat speculative. As colocalization was only defined by the overlapping of fluorescence signals in a three-dimensional room through a subjective evaluation, a better data readout, for example automatization, is necessary to ensure reproducibility.

Furthermore, in this work, cells displaying a larger number of aggregates did not seem to suffer from any adverse effects. This raises the question whether aggregates disturb cellular function and are cytotoxic to as large an extent as previously assumed (Hipp et al., 2019). Yet, it seems most likely that the mothers harboring an increased number of aggregates display accelerated aging, dying after a smaller amount of cell divisions as they accumulate aggregates faster and proteostasis fails. The question whether an increased amount of protein aggregates per cell leads to increased stress or decreased stress tolerance is essential for this field of research. Based on the model that aggregate retention is necessary for the 'rejuvenation' of daughter cells, the examination of the effects on replicative lifespan in the tested candidates, but especially in Δ*fis1*, would be interesting. The analysis of this is time-consuming and can only be done in a limited number of strains at a time. This cannot be used as a method of screening for involved factors but to further characterize promising candidates that show strong effects in other experiments. Generally, it can be assumed that it is very difficult to observe strong effects on aggregate retention since cells have developed many different mechanisms to ensure proteostasis as well as methods to detoxify, store and retain protein aggregates. These mechanisms often serve redundant functions and can compensate for the loss of another, whether that is, for example, the sequestration of aggregates into larger deposit sites, import into and tethering on organelles, or increased activity of the chaperone system to prevent aggregation in the first place as well as the untangling of misfolded proteins followed by refolding or degradation.

4.2 Search for unknown factors involved in mitochondrial inheritance

Most recent literature agrees that mitochondrial inheritance in baker's yeast is powered by the Myo2 motor protein which carries mitochondria and a large variety of other cargoes including organelles (Eves et al., 2012; Fagarasanu et al., 2010; Förtsch et al., 2011) and mRNAs (Casolari et al., 2012) towards the daughter cell along the actin cytoskeleton. In order to recruit Myo2 to its multitude of cargoes, a variety of different adaptor and receptor proteins exist and their interactions with the cargo-binding domain of Myo2 have been studied intensely over the last decades. With Mmr1 and Ypt11 two important proteins involved in Myo2 recruitment have been described for mitochondria (Itoh et al., 2002; Itoh et al., 2004). The two proteins are not essential as they work in parallel and can compensate for the loss of one another (Chernyakov et al., 2013). This, along with the facts that Ypt11 is not exclusively involved in mitochondrial inheritance but also other organelles (Arai et al., 2008) and that knockouts of both genes show only small phenotypical changes (Itoh et al., 2002; Itoh et al., 2004), suggests the involvement of currently unknown factors in mitochondrial inheritance. It was considered rather likely at the beginning of this study that an unknown MOM membrane protein serves as a Myo2

anchor based on the transport mechanisms of other organelles (Fagarasanu et al., 2010) like Inp2 for peroxisomes or Vac8 for vacuoles (Tang et al., 2003). In order to find such an anchor, an educated guess approach was used (Figure 7, page 54), but none of the deletion mutants tested in this screen displayed a reduction of mitochondrial inheritance to an extent comparable to Δ*mmr1*. The only noteworthy strain was Δ*gem1*, which showed a smaller delay in inheritance, similar to Δ*ypt11*. Gem1 is a component of the ERMES (ER-mitochondria encounter structure) complex, an organelle contact site connecting the ER with mitochondria (Kornmann et al., 2011; Stroud et al., 2011), and its deletion leads to globular mitochondrial morphology (Frederick et al., 2004). The reduction of mitochondrial inheritance can probably be connected back to the observation that mitochondrial morphology has a direct impact on the effectivity of mitochondrial transport, where smaller units are transported less efficiently (Böckler et al., 2017). Since the reduction in inheritance is rather small and the deletion of a possible mitochondrial Myo2 receptor would be expected to at least cause a strong reduction if not even a complete block of mitochondrial transport to the bud, it is not likely that the effect observed here is a reflection of an involvement of Gem1 beyond its already known function.

In an attempt to also allow the examination of the involvement of essential genes in mitochondrial inheritance, a multicopy-suppressor screen was performed searching for ORFs whose overexpression can rescue the otherwise inviable Δ*mmr1* Δ*ypt11* double mutant (Figure 8, page 56). The initial screen identified four hits apart from the plasmids containing *MMR1* and *YPT11*. However, their ability to rescue the lethal phenotype could not be confirmed manually (Figure 9, page 57). As *MMR1* and *YPT11* themselves were found so often among the hits and only a small number of non-reproducible hits was found, the screen was successful on a technical level. Nonetheless, no unknown components of mitochondrial inheritance could be identified. This could be because unknown components involved in the inheritance require the interaction with Mmr1 or Ypt11 to perform their function. Additionally, this screen relies on the overexpression of larger genomic sections, using their endogenous promotors from a multicopy plasmid, but data from other overexpression screens suggest that the overexpression of several of these ORFs causes harmful effects on cellular function and survival (Stevenson et al., 2001). As evident by its name, Mmr1 (Mitochondrial Myo2 receptor-related) is itself considered by some to be the mitochondrial Myo2 receptor. While there are some arguments against that, like the fact Mmr1 is only peripherally attached and not inserted into the mitochondrial outer membrane and most convincingly the fact that mitochondrial inheritance is essential for cell survival (Förtsch et al., 2011) it seems likely that an essential gene is necessary for this process, it may very well be the case that Mmr1 and Ypt11 together are sufficient (Itoh et al., 2004). Nonetheless, it is obvious that there are still unknown factors and unanswered questions about the regulation and mechanism of mitochondrial inheritance.

4.3 Selective inheritance of mitochondria and oxidative stress

One of the larger remaining questions regarding mitochondrial inheritance in *S. cerevisiae* concerns the asymmetric partitioning during budding. While the asymmetric partitioning of mitochondria based on mitochondrial quality has often been described as a concept in review articles (Higuchi-Sanabria et al., 2014; Klecker and Westermann, 2020; Nystrom and Liu, 2014), the data supporting it has not been as abundant and limited. Asymmetric inheritance and altered distribution of mitochondria based on organelle fitness has been shown in higher eukaryotes, including rat neurons and human stem-like cell lines (Debattisti et al., 2017; Katajisto et al., 2015). In yeast, the data supporting this is mainly based on indirect measurements of mitochondrial membrane potential through redox-sensitive fluorescent dyes and comparing them between mothers and buds (McFaline-Figueroa et al., 2011). It is generally believed that asymmetric partitioning of mitochondria is achieved by selective transport into the bud along with cortex anchor-based retention at the mother and bud cell poles (Klecker et al., 2013; Lackner et al., 2013; Swayne et al., 2011). This process has been described as a driver of daughter rejuvenation and cellular aging processes (Hughes and Gottschling, 2012; Vevea et al., 2014). A major way in which mitochondria are thought to drive aging is through the production of ROS as a byproduct of cellular respiration (Wong et al., 2017). ROS are also the driver of mitochondrial decline over time due to their high reactivity with proteins and mitochondrial DNA (mtDNA) across different lifeforms (Breitenbach et al., 2014; Huang et al., 2020; Schieber and Chandel, 2014). With these damages accumulating over their lifespan a yeast cell's respiratory function and mitochondrial fitness declines over time. This is closely interconnected with mitochondrial fission and fusion as fusion has been shown to be necessary to maintain functional mtDNA (Rapaport et al., 1998) in yeast, while fission has been shown to help isolate low-functioning mitochondria in yeast and mammalian cells to allow their elimination through mitophagy (Kubli and Gustafsson, 2012; Okamoto et al., 2009). Likewise, it has been described previously that the external treatment of yeast cells with oxidative agents like hydrogen peroxide also causes an increased rate of mitochondrial fragmentation (Vowinckel et al., 2015). The same could be observed in this study (Figure 10, page 59). For Myo2, on the other hand, it could be determined that the oxidative stress treatment caused a large decrease of polarized Myo2 localization, indicating blockage of mitochondrial transport. Furthermore, staining of the actin cytoskeleton supported this assumption since almost all observed cells displayed an altered cytoskeleton. As this affects the cell on such a fundamental basis due to the ubiquitous functions of the actin cytoskeleton, it can be concluded that hydrogen peroxide treatment is not a suitable tool to investigate the effects of oxidative stress on mitochondria and specifically their transport and inheritance.

With the Su9-DAO system, which targets the DAO enzyme from another yeast species into the mitochondrial matrix and allows specific induction of ROS formation there, we identified an optimal system to study the effect of intramitochondrial ROS production on mitochondrial transport (Calabrese et al., 2019; Chelius et al., 2023). Here, the inducible production of ROS was employed to simulate the situation in aged mitochondria. We could observe a strong reduction of mitochondrial inheritance as well as a change in mitochondrial morphology towards fragmented and aggregated mitochondria as expected in stressed cells (Figure 11, page 63).

Furthermore, we observed that Su9-DAO -caused oxidative stress altered the localization of Mmr1, while the Myo2 motor protein was unaffected (Figure 12, page 65). Similarly, - and in contrast to hydrogen peroxide treatment – the actin cytoskeleton also remained unaltered during Su9-DAO treatment. This further shows that Su9-DAO is an appropriate tool to investigate questions of mitochondrial inheritance since the components required for mitochondrial transport are still intact and functional. Accordingly, the stimulation of mitochondrial transport through the overexpression of the adaptors Mmr1 (Figure 13, page 68) and Ypt11 (Chelius et al., 2023), as well as the permanent attachment of the Myo2 motor protein to the mitochondrial outer membrane through Myo2-Fis1 (Figure 13, page 68), increased mitochondrial inheritance levels to that of wildtype cells treated with L-Ala. These findings strongly suggest that mitochondrial quality control in this case acts on the level of transport and motor recruitment rather than through increased retrograde transport or on the level of a diffusion barrier at the mother-bud neck. In relation to this, we were able to design and implement another artificial chimeric mitochondrial Myo2 anchor with the Tom20-Inp2-GFP construct (Figure 14, page 69). This approach was based on the observation that peroxisomal inheritance was unaffected by Su9-DAO stress (Chelius et al., 2023). As Tom20-Inp2-GFP was able to rescue mitochondrial transport during Su9-DAO stress and bypassing of Mmr1 and Ypt11 renders mitochondrial inheritance unaltered by oxidative stress (Figure 15, page 72), oxidative stress affects either the mitochondrial Myo2 receptor or it's adaptors. Alternatively, posttranslational modifications could act on Myo2 itself, for example by blocking the binding site on the cargo binding domain necessary for mitochondrial transport. Alterations to Myo2 would have to act specifically at this site since we observed Myo2's ability to perform other functions during Su9-DAO stress. Supposedly, all mechanisms enforcing mitochondrial inheritance should also increase the amount of lower-functioning organelle components inherited. According to the model this should result in daughter cells with lower-than-wild type replicative potential due to accelerated aging or in two distinct populations of daughters displaying either increased or decreased replicative lifespans as has been described for Δ*mmr1* cells (McFaline-Figueroa et al., 2011). This hypothesis should be investigated further by determining replicative potential during DAO stress as well as through experiments involving aged cells, for example

through the mother enrichment program or by enriching old cells through magnetic labelling (Lindstrom and Gottschling, 2009).

Concerning the newly created Tom20-Inp2-GFP construct, it is unclear why there is no observable effect in mitochondrial inheritance in unstressed WT cells as well as L- and D-Ala treated WT Su9-DAO cells expressing the construct. Due to the strong increase in Tom20-Inp2-GFP fluorescence intensity in the Δ*mmr1* Δ*ypt11* Su9-DAO cells, compared to WT Tom20-Inp2-GFP cells, it seems rather likely that the expression level of the construct was altered due to selective pressure in the absence of the usually redundant pathways of Myo2 recruitment to mitochondria. This is further corroborated by the genotypical analysis of the dissected tetrads. It showed that not all Δ*mmr1* Δ*ypt11* double mutants were viable and the colonies formed by the viable clones were mostly small. Maybe this indicates that the *TOM20* promotor used for expression is not strong enough to cause an increase in mitochondrial bud directed transport under regular conditions. Similarly, the expression of Tom20-Inp2-GFP was not able to overcome the inheritance defect caused by Su9-DAO activity in WT cells. Most interestingly, the construct was nonetheless able to counteract the mitochondrial inheritance defect caused by the D-Ala induced intramitochondrial ROS stress in Δ*mmr1* Δ*ypt11* Su9-DAO cells in a similar manner as *MMR1* overexpression and Myo2-Fis 1 (Figure 13, page 68) were able to.

Most interestingly, we were able to detect a direct influence of the Mmr1 protein itself but not Ypt11 on the cell's susceptibility to oxidative stress caused by Su9-DAO activity (Figure 16, page 74). While the two proteins can compensate for the loss of each other under non-stress conditions regarding mitochondrial inheritance, the distinction of healthy mitochondria during inheritance seems to be solely dependent on one of them. Δ*mmr1* deletion mutants displayed equal levels of mitochondrial inheritance during intramitochondrial ROS production as the L-Ala control cells of the same genotype. Therefore, Δ*mmr1* cells are not sensitive to Su9-DAO induction, while the WT and Δ*ypt11* cells in the same experiment showed a strong reduction. This suggests an important role of Mmr1 during selective mitochondrial inheritance during ROS stress. This proposed role is further supported by the finding, that it was possible to counteract the negative effect on mitochondrial inheritance caused by Su9-DAO induction bypassing Mmr1 through the artificial Myo2-Fis1 or Tom20-Inp2-GFP constructs. Again, this finding connects nicely with the previously mentioned observation that Δ*mmr1* cells produced two differing populations of daughters with either enhanced or reduced replicative lifespans (McFaline-Figueroa et al., 2011). Mmr1 overexpression on the other hand, led to a decline of replicative lifespan, presumably due to the increased inheritance of lower functioning mitochondria (Higuchi-Sanabria et al., 2016). Recently it has also been described that cells with defective Mmr1 degradation produce elevated amounts of ROS (Obara et al., 2022). In order to further investigate Mmr1's involvement in mitochondrial quality control, the effect of the deletion of *PTC1* was examined. Ptc1 is a

serine/threonine phosphatase (Roeder et al., 1998) which targets Mmr1 as a substrate (Swayne et al., 2011) and its deletion mutant exhibits altered Mmr1 localization, as well as delayed mitochondrial inheritance. The Δ*ptc1* mutants displayed a very strong inheritance defect already under non-ROS-producing conditions which was not further elevated by Su9-DAO induction. Interestingly, the morphology of the mitochondria in these cells strongly resembled those in the *myo2(LQ)* mutant (Förtsch et al., 2011) as most mitochondrial mass formed a condensed clump at the mother cell pole. Using the brighter yEGFP fluorophore made the mitochondria in Δ*mmr1* appear to be aggregated while GFP allowed the differentiation of distinct mitochondrial tubules in a tight-knit net. Using a less bright fluorophore to visualize mitochondria in the Δ*ptc1* cells might reveal a similar situation.

Taken together, all these experiments utilizing the Su9-DAO construct to induce ROS stress specifically inside the mitochondrial matrix, along with the experiments conducted by other group members over the course of this project (see Chelius et al., 2023), were very successful in elucidating information about mitochondrial quality control during inheritance. We could show that unstressed mitochondria were preferentially inherited in newly formed buds by zygotes compared to Su9-DAO ROS stressed mitochondria. In an experiment using diploid mitochondrial fission and fusion deficient Δ*dnm1* Δ*fzo1* double mutants that contained two different mitochondria populations, one with and one without Su9-DAO. These two populations of mitochondria could directly be distinguished in fluorescence microscopy through differently colored fluorescent markers. While WT and Δ*ypt11* buds preferentially inherited unstressed mitochondria during D-Ala treatment, Δ*mmr1* daughters, on the other hand, were equally likely to inherit mitochondria from either population. Therefore, this project could show that Mmr1 plays an essential role in the distinction of the mitochondrial fitness levels during mitotic cell division. Δ*mmr1* cells were found to be unable to selectively retain damaged mitochondria. Thus, this project was able to show clear evidence for quality control during mitochondrial inheritance and that the decision about which mitochondria to retain or inherit is decided separately for each mitochondrium. Furthermore, we observed that this process appears to be driven by changes in Mmr1 protein localization. After DAO induction Mmr1-yeGFP relocalizes from mitochondria to a non-polar distribution throughout the cell. From these findings it can be concluded that Mmr1 relocalization during oxidative stress directly reduces Myo2 recruitment to the mitochondrial surface in the mother and thus reduces mitochondrial transport to the daughter and inheritance. As ROS stress leads to increased mitochondrial fragmentation dysfunctional mitochondria can effectively be separated. Mmr1 relocalization from those stressed, isolated mitochondria could allow the cell to selectively retain those organelles during budding. It remains unclear whether this mechanism occurs in parallel with the proposed mechanism of mitochondrial quality control through retrograde actin cable flow (Higuchi et al., 2013). To follow these experiments up, it should be examined whether Mmr1 itself is

altered post-translationally to induce the redistribution towards a general cytosolic localization, and if so, in which way, and what other proteins are involved in this mechanism.

5 References

Adams, A. E. and Pringle, J. R. (1984). Relationship of actin and tubulin distribution to bud growth in wild-type and morphogenetic-mutant Saccharomyces cerevisiae. *The Journal of cell biology*. **98**, 934–945. doi:10.1083/jcb.98.3.934.

Aguilaniu, H., Gustafsson, L., Rigoulet, M. and Nystrom, T. (2003). Asymmetric inheritance of oxidatively damaged proteins during cytokinesis. *Science (New York, N.Y.)*. **299**, 1751–1753. doi:10.1126/science.1080418.

Albakri, M. B., Jiang, Y., Genereaux, J. and Lajoie, P. (2018). Polyglutamine toxicity assays highlight the advantages of mScarlet for imaging in Saccharomyces cerevisiae. *F1000Research*. **7**, 1242. doi:10.12688/f1000research.15829.2.

Alberti, S., Gitler, A. D. and Lindquist, S. (2007). A suite of Gateway cloning vectors for high-throughput genetic analysis in Saccharomyces cerevisiae. *Yeast (Chichester, England)*. **24**, 913–919. doi:10.1002/yea.1502.

Alnuami, A. A., Zeedi, B., Qadri, S. M. and Ashraf, S. S. (2008). Oxyradical-induced GFP damage and loss of fluorescence. *International Journal of Biological Macromolecules*. **43**, 182–186. doi:10.1016/j.ijbiomac.2008.05.002.

Alonso, J., Barredo, J. L., Díez, B., Mellado, E., Salto, F., García, J. L. and Cortés, E. (1998). D-amino-acid oxidase gene from Rhodotorula gracilis (Rhodosporidium toruloides) ATCC 26217. *Microbiology (Reading, England)*. **144 (Pt 4)**, 1095–1101. doi:10.1099/00221287-144-4-1095.

Altmann, K., Frank, M., Neumann, D., Jakobs, S. and Westermann, B. (2008). The class V myosin motor protein, Myo2, plays a major role in mitochondrial motility in Saccharomyces cerevisiae. *The Journal of cell biology*. **181**, 119–130. doi:10.1083/jcb.200709099.

Andrade-Restrepo, M. (2017). Is Aggregate-Dependent Yeast Aging Fortuitous? A Model of Damage Segregation and Aggregate Dynamics. *Biophysical journal*. **113**, 2464–2476. doi:10.1016/j.bpj.2017.09.033.

Anjum, S., Srivastava, S., Panigrahi, L., Ansari, U. A., Trivedi, A. K. and Ahmed, S. (2023). TORC1 mediated regulation of mitochondrial integrity and calcium ion homeostasis by Wat1/mLst8 in S. pombe. *International Journal of Biological Macromolecules*. **253**, 126907. doi:10.1016/j.ijbiomac.2023.126907.

Arai, S., Noda, Y., Kainuma, S., Wada, I. and Yoda, K. (2008). Ypt11 functions in bud-directed transport of the Golgi by linking Myo2 to the coatomer subunit Ret2. *Current biology : CB*. **18**, 987–991. doi:10.1016/j.cub.2008.06.028.

Babazadeh, R., Ahmadpour, D., Jia, S., Hao, X., Widlund, P., Schneider, K., Eisele, F., Edo, L. D., Smits, G. J. and Liu, B. et al. (2019). Syntaxin 5 Is Required for the Formation and Clearance of Protein Inclusions during Proteostatic Stress. *Cell reports*. **28**, 2096-2110.e8. doi:10.1016/j.celrep.2019.07.053.

Baldi, S., Bolognesi, A., Meinema, A. C. and Barral, Y. (2017). Heat stress promotes longevity in budding yeast by relaxing the confinement of age-promoting factors in the mother cell. *eLife*. **6**. doi:10.7554/eLife.28329.

Barral, Y., Mermall, V., Mooseker, M. S. and Snyder, M. (2000). Compartmentalization of the cell cortex by septins is required for maintenance of cell polarity in yeast. *Molecular cell*. **5**, 841–851. doi:10.1016/s1097-2765(00)80324-x.

Barral, Y., Parra, M., Bidlingmaier, S. and Snyder, M. (1999). Nim1-related kinases coordinate cell cycle progression with the organization of the peripheral cytoskeleton in yeast. *Genes Dev*. **13**, 176–187. doi:10.1101/gad.13.2.176.

Bassett, D. E., Boguski, M. S. and Hieter, P. (1996). Yeast genes and human disease. *Nature*. **379**, 589–590. doi:10.1038/379589a0.

Beach, D. L., Thibodeaux, J., Maddox, P., Yeh, E. and Bloom, K. (2000). The role of the proteins Kar9 and Myo2 in orienting the mitotic spindle of budding yeast. *Current biology : CB*. **10**, 1497–1506. doi:10.1016/s0960-9822(00)00837-x.

Ben-Aroya, S., Coombes, C., Kwok, T., O'Donnell, K. A., Boeke, J. D. and Hieter, P. (2008). Toward a comprehensive temperature-sensitive mutant repository of the essential genes of Saccharomyces cerevisiae. *Molecular cell*. **30**, 248–258. doi:10.1016/j.molcel.2008.02.021.

Berman, S. B., Pineda, F. J. and Hardwick, J. M. (2008). Mitochondrial fission and fusion dynamics: the long and short of it. *Cell death and differentiation*. **15**, 1147–1152. doi:10.1038/cdd.2008.57.

Bertin, A., McMurray, M. A., Pierson, J., Thai, L., McDonald, K. L., Zehr, E. A., García, G., Peters, P., Thorner, J. and Nogales, E. (2011). Three-dimensional ultrastructure of the septin filament network in Saccharomyces cerevisiae. *Molecular Biology of the Cell*. **23**, 423–432. doi:10.1091/mbc.e11-10-0850.

Bhatia-Kissova, I. and Camougrand, N. (2021). Mitophagy in Yeast: Decades of Research. *Cells*. **10**. doi:10.3390/cells10123541.

Böckler, S., Chelius, X., Hock, N., Klecker, T., Wolter, M., Weiss, M., Braun, R. J. and Westermann, B. (2017). Fusion, fission, and transport control asymmetric inheritance of mitochondria and protein aggregates. *The Journal of cell biology*. **216**, 2481–2498. doi:10.1083/jcb.201611197.

Boeke, J. D., LaCroute, F. and Fink, G. R. (1984). A positive selection for mutants lacking orotidine-5'-phosphate decarboxylase activity in yeast: 5-fluoro-orotic acid resistance. *Molecular & general genetics : MGG*. **197**, 345–346. doi:10.1007/BF00330984.

Boldogh, I., Vojtov, N., Karmon, S. and Pon, L. A. (1998). Interaction between mitochondria and the actin cytoskeleton in budding yeast requires two integral mitochondrial outer membrane proteins, Mmm1p and Mdm10p. *The Journal of cell biology*. **141**, 1371–1381. doi:10.1083/jcb.141.6.1371.

Boldogh, I. R., Yang, H. C., Nowakowski, W. D., Karmon, S. L., Hays, L. G., Yates, J. R. 3. and Pon, L. A. (2001). Arp2/3 complex and actin dynamics are required for actin-based mitochondrial motility in yeast. *Proceedings of the National Academy of Sciences of the United States of America*. **98**, 3162–3167. doi:10.1073/pnas.051494698.

Boldogh, I. R., Nowakowski, D. W., Yang, H.-C., Chung, H., Karmon, S., Royes, P. and Pon, L. A. (2003). A Protein Complex Containing Mdm10p, Mdm12p, and Mmm1p Links Mitochondrial Membranes and DNA to the Cytoskeleton-based Segregation Machinery. *Molecular Biology of the Cell*. **14**, 4618–4627. doi:10.1091/mbc.e03-04-0225.

Boldogh, I. R., Ramcharan, S. L., Yang, H.-C. and Pon, L. A. (2004). A type V myosin (Myo2p) and a Rab-like G-protein (Ypt11p) are required for retention of newly inherited mitochondria in yeast cells during cell division. *Molecular Biology of the Cell*. **15**, 3994–4002. doi:10.1091/mbc.E04-01-0053.

Boos, F., Kramer, L., Groh, C., Jung, F., Haberkant, P., Stein, F., Wollweber, F., Gackstatter, A., Zoller, E. and van der Laan, M. et al. (2019). Mitochondrial protein-induced stress triggers a global adaptive transcriptional programme. *Nature Cell Biology*. **21**, 442–451. doi:10.1038/s41556-019-0294-5.

Botstein, D. and Fink, G. R. (2011). Yeast: an experimental organism for 21st Century biology. *Genetics*. **189**, 695–704. doi:10.1534/genetics.111.130765.

Brachmann, C. B., Davies, A., Cost, G. J., Caputo, E., Li, J., Hieter, P. and Boeke, J. D. (1998). Designer deletion strains derived from Saccharomyces cerevisiae S288C: a useful set of strains and plasmids for PCR-mediated gene disruption and other applications. *Yeast (Chichester, England)*. **14**, 115–132. doi:10.1002/(SICI)1097-0061(19980130)14:2<115::AID-YEA204>3.0.CO;2-2.

Breitenbach, M., Rinnerthaler, M., Hartl, J., Stincone, A., Vowinckel, J., Breitenbach-Koller, H. and Ralser, M. (2014). Mitochondria in ageing: there is metabolism beyond the ROS. *FEMS yeast research*. **14**, 198–212. doi:10.1111/1567-1364.12134.

Bruderek, M., Jaworek, W., Wilkening, A., Rüb, C., Cenini, G., Förtsch, A., Sylvester, M. and Voos, W. (2018). IMiQ: a novel protein quality control compartment protecting mitochondrial functional integrity. *Molecular Biology of the Cell*. **29**, 256–269. doi:10.1091/mbc.E17-01-0027.

Buttery, S. M., Kono, K., Stokasimov, E. and Pellman, D. (2012). Regulation of the formin Bnr1 by septins anda MARK/Par1-family septin-associated kinase. *Molecular Biology of the Cell*. **23**, 4041–4053. doi:10.1091/mbc.E12-05-0395.

Byers, B. and Goetsch, L. (1976). A highly ordered ring of membrane-associated filaments in budding yeast. *The Journal of cell biology*. **69**, 717–721. doi:10.1083/jcb.69.3.717.

Calabrese, G., Peker, E., Amponsah, P. S., Hoehne, M. N., Riemer, T., Mai, M., Bienert, G. P., Deponte, M., Morgan, B. and Riemer, J. (2019). Hyperoxidation of mitochondrial peroxiredoxin limits H2O2-induced cell death in yeast. *The EMBO journal*. **38**, e101552. doi:10.15252/embj.2019101552.

Casamayor, A. and Snyder, M. (2003). Molecular dissection of a yeast septin: distinct domains are required for septin interaction, localization, and function. *Molecular and cellular biology*. **23**, 2762–2777. doi:10.1128/MCB.23.8.2762-2777.2003.

Casolari, J. M., Thompson, M. A., Salzman, J., Champion, L. M., Moerner, W. E. and Brown, P. O. (2012). Widespread mRNA association with cytoskeletal motor proteins and identification and dynamics of myosin-associated mRNAs in S. cerevisiae. *PloS one*. **7**, e31912. doi:10.1371/journal.pone.0031912.

Catlett, N. L. and Weisman, L. S. (1998). The terminal tail region of a yeast myosin-V mediates its attachment to vacuole membranes and sites of polarized growth. *Proceedings of the National Academy of Sciences of the United States of America*. **95**, 14799–14804.

Cavalier-Smith, T. (1987). The simultaneous symbiotic origin of mitochondria, chloroplasts, and microbodies. *Annals of the New York Academy of Sciences*. **503**, 55–71. doi:10.1111/j.1749-6632.1987.tb40597.x.

Caviston, J. P., Longtine, M., Pringle, J. R. and Bi, E. (2003). The role of Cdc42p GTPase-activating proteins in assembly of the septin ring in yeast. *Molecular Biology of the Cell*. **14**, 4051–4066. doi:10.1091/mbc.e03-04-0247.

Cerveny, K. L., Studer, S. L., Jensen, R. E. and Sesaki, H. (2007). Yeast Mitochondrial Division and Distribution Require the Cortical Num1 Protein. *Developmental cell*. **12**, 363–375. doi:10.1016/j.devcel.2007.01.017.

Chao, J. T., Wong, A. K. O., Tavassoli, S., Young, B. P., Chruscicki, A., Fang, N. N., Howe, L. J., Mayor, T., Foster, L. J. and Loewen, C. J. R. (2014). Polarization of the endoplasmic reticulum by ER-septin tethering. *Cell*. **158**, 620–632. doi:10.1016/j.cell.2014.06.033.

Chelius, X., Bartosch, V., Rausch, N., Haubner, M., Schramm, J., Braun, R. J., Klecker, T. and Westermann, B. (2023). Selective retention of dysfunctional mitochondria during asymmetric cell division in yeast. *PLoS biology*. **21**, e3002310. doi:10.1371/journal.pbio.3002310.

Chelius, X., Rausch, N., Bartosch, V., Klecker, M., Klecker, T. and Westermann, B. (2025). A protein interaction map of the myosin Myo2 reveals a role of Alo1 in mitochondrial inheritance in yeast. *Journal of cell science*; **138 (3)**, JCS263678. doi:10.1242/jcs.263678

Chen, W., Ping, H. A. and Lackner, L. L. (2018). Direct membrane binding and self-interaction contribute to Mmr1 function in mitochondrial inheritance. *Molecular Biology of the Cell*. **29**, 2346–2357. doi:10.1091/mbc.E18-02-0122.

Chen, X. J. and Butow, R. A. (2005). The organization and inheritance of the mitochondrial genome. *Nature reviews. Genetics*. **6**, 815–825. doi:10.1038/nrg1708.

Chen, Y., McMillan-Ward, E., Kong, J., Israels, S. J. and Gibson, S. B. (2007). Mitochondrial electron-transport-chain inhibitors of complexes I and II induce autophagic cell death mediated by reactive oxygen species. *Journal of cell science*. **120**, 4155–4166. doi:10.1242/jcs.011163.

Cheng, W.-C., Teng, X., Park, H. K., Tucker, C. M., Dunham, M. J. and Hardwick, J. M. (2008). Fis1 deficiency selects for compensatory mutations responsible for cell death and growth control defects. *Cell death and differentiation*. **15**, 1838–1846. doi:10.1038/cdd.2008.117.

Chernyakov, I., Santiago-Tirado, F. and Bretscher, A. (2013). Active segregation of yeast mitochondria by Myo2 is essential and mediated by Mmr1 and Ypt11. *Current biology : CB*. **23**, 1818–1824. doi:10.1016/j.cub.2013.07.053.

Chou, C.-C., Patel, M. T. and Gartenberg, M. R. (2015). A series of conditional shuttle vectors for targeted genomic integration in budding yeast. *FEMS yeast research*. **15**. doi:10.1093/femsyr/fov010.

Clay, L., Caudron, F., Denoth-Lippuner, A., Boettcher, B., Buvelot Frei, S., Snapp, E. L. and Barral, Y. (2014). A sphingolipid-dependent diffusion barrier confines ER stress to the yeast mother cell. *eLife*. **3**, e01883. doi:10.7554/eLife.01883.

Coelho, M., Lade, S. J., Alberti, S., Gross, T. and Tolić, I. M. (2014). Fusion of Protein Aggregates Facilitates Asymmetric Damage Segregation. *PLoS biology*. **12**, e1001886. doi:10.1371/journal.pbio.1001886.

Collins, Y., Chouchani, E. T., James, A. M., Menger, K. E., Cochemé, H. M. and Murphy, M. P. (2012). Mitochondrial redox signalling at a glance. *Journal of cell science*. **125**, 801–806. doi:10.1242/jcs.098475.

Colombi, P., Webster, B. M., Fröhlich, F. and Lusk, C. P. (2013). The transmission of nuclear pore complexes to daughter cells requires a cytoplasmic pool of Nsp1. *The Journal of cell biology*. **203**, 215–232. doi:10.1083/jcb.201305115.

Connor, O. M., Matta, S. K. and Friedman, J. R. (2023). Completion of mitochondrial division requires the intermembrane space protein Mdi1/Atg44. *The Journal of cell biology*. **222**, e202303147. doi:10.1083/jcb.202303147.

Cooper, K. F., Khakhina, S., Kim, S. K. and Strich, R. (2014). Stress-induced nuclear-to-cytoplasmic translocation of cyclin C promotes mitochondrial fission in yeast. *Developmental cell*. **28**, 161–173. doi:10.1016/j.devcel.2013.12.009.

Costanzo, M., VanderSluis, B., Koch, E. N., Baryshnikova, A., Pons, C., Tan, G., Wang, W., Usaj, M., Hanchard, J. and Lee, S. D. et al. (2016). A global genetic interaction network maps a wiring diagram of cellular function. *Science (New York, N.Y.)*. **353**. doi:10.1126/science.aaf1420.

Debattisti, V., Gerencser, A. A., Saotome, M., Das, S. and Hajnóczky, G. (2017). ROS Control Mitochondrial Motility through p38 and the Motor Adaptor Miro/Trak. *Cell reports*. **21**, 1667–1680. doi:10.1016/j.celrep.2017.10.060.

Denoth Lippuner, A., Julou, T. and Barral, Y. (2014). Budding yeast as a model organism to study the effects of age. *FEMS microbiology reviews*. **38**, 300–325. doi:10.1111/1574-6976.12060.

Dimmer, K. S., Fritz, S., Fuchs, F., Messerschmitt, M., Weinbach, N., Neupert, W. and Westermann, B. (2002). Genetic basis of mitochondrial function and morphology in Saccharomyces cerevisiae. *Molecular Biology of the Cell*. **13**, 847–853. doi:10.1091/mbc.01-12-0588.

Dobbelaere, J., Gentry, M. S., Hallberg, R. L. and Barral, Y. (2003). Phosphorylation-Dependent Regulation of Septin Dynamics during the Cell Cycle. *Developmental cell*. **4**, 345–357. doi:10.1016/S1534-5807(03)00061-3.

Dong, F., Zhu, M., Zheng, F. and Fu, C. (2022). Mitochondrial fusion and fission are required for proper mitochondrial function and cell proliferation in fission yeast. *FEBS J*. **289**, 262–278. doi:10.1111/febs.16138.

Douglas, L. M., Alvarez, F. J., McCreary, C. and Konopka, J. B. (2005). Septin function in yeast model systems and pathogenic fungi. *Eukaryotic cell*. **4**, 1503–1512. doi:10.1128/EC.4.9.1503-1512.2005.

Drake, T., Yusuf, E. and Vavylonis, D. (2012). A Systems-Biology Approach to Yeast Actin Cables. In *Advances in Systems Biology* (ed. I. I. Goryanin and A. B. Goryachev), pp. 325–335. New York, NY: Springer New York.

Drubin, D. G., Jones, H. D. and Wertman, K. F. (1993). Actin structure and function: roles in mitochondrial organization and morphogenesis in budding yeast and identification of the phalloidin-binding site. *Molecular Biology of the Cell*. **4**, 1277–1294. doi:10.1091/mbc.4.12.1277.

Egner, A., Jakobs, S. and Hell, S. W. (2002). Fast 100-nm resolution three-dimensional microscope reveals structural plasticity of mitochondria in live yeast. *Proceedings of the National Academy of Sciences of the United States of America*. **99**, 3370–3375. doi:10.1073/pnas.052545099.

Erjavec, N., Larsson, L., Grantham, J. and Nyström, T. (2007). Accelerated aging and failure to segregate damaged proteins in Sir2 mutants can be suppressed by overproducing the protein aggregation-remodeling factor Hsp104p. *Genes Dev*. **21**, 2410–2421. doi:10.1101/gad.439307.

Erjavec, N. and Nyström, T. (2007). Sir2p-dependent protein segregation gives rise to a superior reactive oxygen species management in the progeny of Saccharomyces cerevisiae. *Proceedings of the National Academy of Sciences*. **104**, 10877–10881. doi:10.1073/pnas.0701634104.

Estrada, P., Kim, J., Coleman, J., Walker, L., Dunn, B., Takizawa, P., Novick, P. and Ferro-Novick, S. (2003). Myo4p and She3p are required for cortical ER inheritance in Saccharomyces cerevisiae. *The Journal of cell biology*. **163**, 1255–1266. doi:10.1083/jcb.200304030.

Eves, P. T., Jin, Y., Brunner, M. and Weisman, L. S. (2012). Overlap of cargo binding sites on myosin V coordinates the inheritance of diverse cargoes. *The Journal of cell biology*. **198**, 69–85. doi:10.1083/jcb.201201024.

Fagarasanu, A., Fagarasanu, M., Eitzen, G. A., Aitchison, J. D. and Rachubinski, R. A. (2006). The peroxisomal membrane protein Inp2p is the peroxisome-specific receptor for the myosin V motor Myo2p of Saccharomyces cerevisiae. *Developmental cell*. **10**, 587–600. doi:10.1016/j.devcel.2006.04.012.

Fagarasanu, A., Mast, F. D., Knoblach, B. and Rachubinski, R. A. (2010). Molecular mechanisms of organelle inheritance: Lessons from peroxisomes in yeast. *Nature reviews. Molecular cell biology*. **11**, 644–654. doi:10.1038/nrm2960.

Farkasovsky, M. and Küntzel, H. (2001). Cortical Num1p Interacts with the Dynein Intermediate Chain Pac11p and Cytoplasmic Microtubules in Budding Yeast. *The Journal of cell biology*. **152**, 251–262. doi:10.1083/jcb.152.2.251.

Fehrenbacher, K. L., Boldogh, I. R. and Pon, L. A. (2005). A Role for Jsn1p in Recruiting the Arp2/3 Complex to Mitochondria in Budding Yeast. *Molecular Biology of the Cell*. **16**, 5094–5102. doi:10.1091/mbc.e05-06-0590.

Fehrenbacher, K. L., Yang, H.-C., Gay, A. C., Huckaba, T. M. and Pon, L. A. (2004). Live cell imaging of mitochondrial movement along actin cables in budding yeast. *Current biology : CB*. **14**, 1996–2004. doi:10.1016/j.cub.2004.11.004.

Fekkes, P., Shepard, K. A. and Yaffe, M. P. (2000). Gag3p, an Outer Membrane Protein Required for Fission of Mitochondrial Tubules. *The Journal of cell biology*. **151**, 333–340. doi:10.1083/jcb.151.2.333.

Feng, Z., Okada, S., Cai, G., Zhou, B. and Bi, E. (2015). Myosin-II heavy chain and formin mediate the targeting of myosin essential light chain to the division site before and during cytokinesis. *Molecular Biology of the Cell*. **26**, 1211–1224. doi:10.1091/mbc.E14-09-1363.

Fletcher, D. A. and Mullins, R. D. (2010). Cell mechanics and the cytoskeleton. *Nature*. **463**, 485–492. doi:10.1038/nature08908.

Förtsch, J., Hummel, E., Krist, M. and Westermann, B. (2011). The myosin-related motor protein Myo2 is an essential mediator of bud-directed mitochondrial movement in yeast. *The Journal of cell biology*. **194**, 473–488. doi:10.1083/jcb.201012088.

Foury, F., Roganti, T., Lecrenier, N. and Purnelle, B. (1998). The complete sequence of the mitochondrial genome of Saccharomyces cerevisiae. *FEBS Letters*. **440**, 325–331. doi:10.1016/s0014-5793(98)01467-7.

Frederick, R. L., McCaffery, J. M., Cunningham, K. W., Okamoto, K. and Shaw, J. M. (2004). Yeast Miro GTPase, Gem1p, regulates mitochondrial morphology via a novel pathway. *The Journal of cell biology*. **167**, 87–98. doi:10.1083/jcb.200405100.

Frederick, R. L., Okamoto, K. and Shaw, J. M. (2008). Multiple pathways influence mitochondrial inheritance in budding yeast. *Genetics*. **178**, 825–837. doi:10.1534/genetics.107.083055.

Frey, T. G. and Mannella, C. A. (2000). The internal structure of mitochondria. *Trends in biochemical sciences*. **25**, 319–324. doi:10.1016/s0968-0004(00)01609-1.

Friedman, J. R., Lackner, L. L., West, M., DiBenedetto, J. R., Nunnari, J. and Voeltz, G. K. (2011). ER tubules mark sites of mitochondrial division. *Science (New York, N.Y.)*. **334**, 358–362. doi:10.1126/science.1207385.

Fukuda, T., Furukawa, K., Maruyama, T., Yamashita, S., Noshiro, D., Song, C., Ogasawara, Y., Okuyama, K., Alam, J. M. and Hayatsu, M. et al. (2023). The mitochondrial intermembrane space protein mitofissin drives mitochondrial fission required for mitophagy. *Molecular cell*. **83**, 2045-2058.e9. doi:10.1016/j.molcel.2023.04.022.

Furukawa, K., Hayatsu, M., Okuyama, K., Fukuda, T., Yamashita, S. I., Inoue, K., … Kanki, T. (2024). Atg44/Mdi1/mitofissin facilitates Dnm1-mediated mitochondrial fission. *Autophagy*, 20(10), 2314–2322. https://doi.org/10.1080/15548627.2024.2360345

Futcher, B. (1999). Cell cycle synchronization. *Methods in cell science: an official journal of the Society for In Vitro Biology*. **21**, 79–86. doi:10.1023/a:1009872403440.

Galletta, B. J. and Cooper, J. A. (2009). Actin and endocytosis: mechanisms and phylogeny. *Current opinion in cell biology*. **21**, 20–27. doi:10.1016/j.ceb.2009.01.006.

Gallina, I., Colding, C., Henriksen, P., Beli, P., Nakamura, K., Offman, J., Mathiasen, D. P., Silva, S., Hoffmann, E. and Groth, A. et al. (2015). Cmr1/WDR76 defines a nuclear genotoxic stress body linking genome integrity and protein quality control. *Nature Communications*. **6**, 6533. doi:10.1038/ncomms7533.

García-Rodríguez, L. J., Gay, A. C. and Pon, L. A. (2007). Puf3p, a Pumilio family RNA binding protein, localizes to mitochondria and regulates mitochondrial biogenesis and motility in budding yeast. *The Journal of cell biology*. **176**, 197–207. doi:10.1083/jcb.200606054.

Gasch, A. P., Spellman, P. T., Kao, C. M., Carmel-Harel, O., Eisen, M. B., Storz, G., Botstein, D. and Brown, P. O. (2000). Genomic Expression Programs in the Response of Yeast Cells to Environmental Changes. *Molecular Biology of the Cell*. **11**, 4241–4257. doi:10.1091/mbc.11.12.4241.

Giaever, G., Chu, A. M., Ni, L., Connelly, C., Riles, L., Véronneau, S., Dow, S., Lucau-Danila, A., Anderson, K. and André, B. et al. (2002). Functional profiling of the Saccharomyces cerevisiae genome. *Nature*. **418**, 387–391. doi:10.1038/nature00935.

Gietz, R. D. and Schiestl, R. H. (2007). High-efficiency yeast transformation using the LiAc/SS carrier DNA/PEG method. *Nature protocols*. **2**, 31–34. doi:10.1038/nprot.2007.13.

Gladyshev, V. N. (2014). The free radical theory of aging is dead. Long live the damage theory! *Antioxidants & redox signaling*. **20**, 727–731. doi:10.1089/ars.2013.5228.

Goffeau, A., Barrell, B. G., Bussey, H., Davis, R. W., Dujon, B., Feldmann, H., Galibert, F., Hoheisel, J. D., Jacq, C. and Johnston, M. et al. (1996). Life with 6000 genes. *Science (New York, N.Y.)*. **274**, 546, 563-7. doi:10.1126/science.274.5287.546.

Goley, E. D. and Welch, M. D. (2006). The ARP2/3 complex: an actin nucleator comes of age. *Nature reviews. Molecular cell biology*. **7**, 713–726. doi:10.1038/nrm2026.

Gouin, E., Gantelet, H., Egile, C., Lasa, I., Ohayon, H., Villiers, V., Gounon, P., Sansonetti, P. J. and Cossart, P. (1999). A comparative study of the actin-based motilities of the pathogenic bacteria Listeria monocytogenes, Shigella flexneri and Rickettsia conorii. *Journal of cell science*. **112 (Pt 11)**, 1697–1708. doi:10.1242/jcs.112.11.1697.

Govindan, B., Bowser, R. and Novick, P. (1995). The role of Myo2, a yeast class V myosin, in vesicular transport. *The Journal of cell biology*. **128**, 1055–1068. doi:10.1083/jcb.128.6.1055.

Griffin, E. E., Graumann, J. and Chan, D. C. (2005). The WD40 protein Caf4p is a component of the mitochondrial fission machinery and recruits Dnm1p to mitochondria. *The Journal of cell biology*. **170**, 237–248. doi:10.1083/jcb.200503148.

Grousl, T., Ungelenk, S., Miller, S., Ho, C.-T., Khokhrina, M., Mayer, M. P., Bukau, B. and Mogk, A. (2018). A prion-like domain in Hsp42 drives chaperone-facilitated aggregation of misfolded proteins. *The Journal of cell biology*. **217**, 1269–1285. doi:10.1083/jcb.201708116.

Haber, J. E. (2012). Mating-type genes and MAT switching in Saccharomyces cerevisiae. *Genetics*. **191**, 33–64. doi:10.1534/genetics.111.134577.

Hammer, J. A. and Sellers, J. R. (2012). Walking to work: roles for class V myosins as cargo transporters. *Nature Reviews Molecular Cell Biology*. **13**, 13–26. doi:10.1038/nrm3248.

Hammermeister, M., Schödel, K. and Westermann, B. (2010). Mdm36 is a mitochondrial fission-promoting protein in Saccharomyces cerevisiae. *Molecular Biology of the Cell*. **21**, 2443–2452. doi:10.1091/mbc.e10-02-0096.

Hanscho, M., Ruckerbauer, D. E., Chauhan, N., Hofbauer, H. F., Krahulec, S., Nidetzky, B., Kohlwein, S. D., Zanghellini, J. and Natter, K. (2012). Nutritional requirements of the BY series of Saccharomyces cerevisiae strains for optimum growth. *FEMS yeast research*. **12**, 796–808. doi:10.1111/j.1567-1364.2012.00830.x.

Hansen, K. G., Aviram, N., Laborenz, J., Bibi, C., Meyer, M., Spang, A., Schuldiner, M. and Herrmann, J. M. (2018). An ER surface retrieval pathway safeguards the import of mitochondrial membrane proteins in yeast. *Science (New York, N.Y.)*. **361**, 1118–1122. doi:10.1126/science.aar8174.

Harman, D. (1956). Aging: a theory based on free radical and radiation chemistry. *Journal of gerontology*. **11**, 298–300. doi:10.1093/geronj/11.3.298.

Hartwell, L. H. (1971). Genetic control of the cell division cycle in yeast: IV. Genes controlling bud emergence and cytokinesis. *Experimental Cell Research*. **69**, 265–276. doi:10.1016/0014-4827(71)90223-0.

Henderson, K. A. and Gottschling, D. E. (2008). A mother's sacrifice: What is she keeping for herself? *Current opinion in cell biology*. **20**, 723–728. doi:10.1016/j.ceb.2008.09.004.

Herlan, M., Vogel, F., Bornhovd, C., Neupert, W. and Reichert, A. S. (2003). Processing of Mgm1 by the rhomboid-type protease Pcp1 is required for maintenance of mitochondrial morphology and of mitochondrial DNA. *The Journal of biological chemistry*. **278**, 27781–27788. doi:10.1074/jbc.M211311200.

Hermann, G. J., Thatcher, J. W., Mills, J. P., Hales, K. G., Fuller, M. T., Nunnari, J. and Shaw, J. M. (1998). Mitochondrial fusion in yeast requires the transmembrane GTPase Fzo1p. *The Journal of cell biology*. **143**, 359–373. doi:10.1083/jcb.143.2.359.

Hettema, E. H., Ruigrok, C. C., Koerkamp, M. G., van den Berg, M., Tabak, H. F., Distel, B. and Braakman, I. (1998). The Cytosolic DnaJ-like Protein Djp1p Is Involved Specifically in Peroxisomal Protein Import. *The Journal of cell biology*. **142**, 421–434. doi:10.1083/jcb.142.2.421.

Higuchi, R., Vevea, J. D., Swayne, T. C., Chojnowski, R., Hill, V., Boldogh, I. R. and Pon, L. A. (2013). Actin Dynamics Affect Mitochondrial Quality Control and Aging in Budding Yeast. *Current biology : CB*. **23**, 2417–2422. doi:10.1016/j.cub.2013.10.022.

Higuchi-Sanabria, R., Charalel, J. K., Viana, M. P., Garcia, E. J., Sing, C. N., Koenigsberg, A., Swayne, T. C., Vevea, J. D., Boldogh, I. R. and Rafelski, S. M. et al. (2016). Mitochondrial anchorage and fusion contribute to mitochondrial inheritance and quality control in the budding yeast Saccharomyces cerevisiae. *Molecular Biology of the Cell*. **27**, 776–787. doi:10.1091/mbc.E15-07-0455.

Higuchi-Sanabria, R., Pernice, W. M. A., Vevea, J. D., Alessi Wolken, D. M., Boldogh, I. R. and Pon, L. A. (2014). Role of asymmetric cell division in lifespan control in Saccharomyces cerevisiae. *FEMS yeast research*. **14**, 1133–1146. doi:10.1111/1567-1364.12216.

Hill, K. L., Catlett, N. L. and Weisman, L. S. (1996). Actin and myosin function in directed vacuole movement during cell division in Saccharomyces cerevisiae. *The Journal of cell biology*. **135**, 1535–1549. doi:10.1083/jcb.135.6.1535.

Hill, S. M., Hao, X., Gronvall, J., Spikings-Nordby, S., Widlund, P. O., Amen, T., Jorhov, A., Josefson, R., Kaganovich, D. and Liu, B. et al. (2016). Asymmetric Inheritance of Aggregated Proteins and Age Reset in Yeast Are Regulated by Vac17-Dependent Vacuolar Functions. *Cell reports*. **16**, 826–838. doi:10.1016/j.celrep.2016.06.016.

Hipp, M. S., Kasturi, P. and Hartl, F. U. (2019). The proteostasis network and its decline in ageing. *Nature reviews. Molecular cell biology*. **20**, 421–435. doi:10.1038/s41580-019-0101-y.

Hock, N. S. (2019). Untersuchung des Myo2-abhängigen Transports von Mitochondrien in Saccharomyces cerevisiae, Universität Bayreuth, Bayreuth.

Huang, Z., Chen, Y. and Zhang, Y. (2020). Mitochondrial reactive oxygen species cause major oxidative mitochondrial DNA damages and repair pathways. *Journal of Biosciences*. **45**, 84. doi:10.1007/s12038-020-00055-0.

Huffaker, T. C., Thomas, J. H. and Botstein, D. (1988). Diverse effects of beta-tubulin mutations on microtubule formation and function. *The Journal of cell biology*. **106**, 1997–2010. doi:10.1083/jcb.106.6.1997.

Hughes, A. L. and Gottschling, D. E. (2012). An early age increase in vacuolar pH limits mitochondrial function and lifespan in yeast. *Nature*. **492**, 261–265. doi:10.1038/nature11654.

Huh, W.-K., Falvo, J. V., Gerke, L. C., Carroll, A. S., Howson, R. W., Weissman, J. S. and O'Shea, E. K. (2003). Global analysis of protein localization in budding yeast. *Nature*. **425**, 686–691. doi:10.1038/nature02026.

Ingerman, E., Perkins, E. M., Marino, M., Mears, J. A., McCaffery, J. M., Hinshaw, J. E. and Nunnari, J. (2005). Dnm1 forms spirals that are structurally tailored to fit mitochondria. *The Journal of cell biology*. **170**, 1021–1027. doi:10.1083/jcb.200506078.

Itoh, T., Toh-E, A. and Matsui, Y. (2004). Mmr1p is a mitochondrial factor for Myo2p-dependent inheritance of mitochondria in the budding yeast. *The EMBO journal*. **23**, 2520–2530. doi:10.1038/sj.emboj.7600271.

Itoh, T., Watabe, A., Toh-E, A. and Matsui, Y. (2002). Complex formation with Ypt11p, a rab-type small GTPase, is essential to facilitate the function of Myo2p, a class V myosin, in mitochondrial distribution in Saccharomyces cerevisiae. *Molecular and cellular biology*. **22**, 7744–7757.

Izawa, T., Park, S.-H., Zhao, L., Hartl, F. U. and Neupert, W. (2017). Cytosolic Protein Vms1 Links Ribosome Quality Control to Mitochondrial and Cellular Homeostasis. *Cell*. **171**, 890-903.e18. doi:10.1016/j.cell.2017.10.002.

Jacobs, C. W., Adams, A. E., Szaniszlo, P. J. and Pringle, J. R. (1988). Functions of microtubules in the Saccharomyces cerevisiae cell cycle. *The Journal of cell biology*. **107**, 1409–1426. doi:10.1083/jcb.107.4.1409.

Jakobs, S., Martini, N., Schauss, A. C., Egner, A., Westermann, B. and Hell, S. W. (2003). Spatial and temporal dynamics of budding yeast mitochondria lacking the division component Fis1p. *Journal of cell science*. **116**, 2005–2014. doi:10.1242/jcs.00423.

Janke, C., Magiera, M. M., Rathfelder, N., Taxis, C., Reber, S., Maekawa, H., Moreno-Borchart, A., Doenges, G., Schwob, E. and Schiebel, E. et al. (2004). A versatile toolbox for PCR-based tagging of yeast genes: new fluorescent proteins, more markers and promoter substitution cassettes. *Yeast (Chichester, England)*. **21**, 947–962. doi:10.1002/yea.1142.

Jazwinski, S. M. (2004). Yeast replicative life span--the mitochondrial connection. *FEMS yeast research*. **5**, 119–125. doi:10.1016/j.femsyr.2004.04.005.

Jin, Y., Taylor Eves, P., Tang, F. and Weisman, L. S. (2009). PTC1 is required for vacuole inheritance and promotes the association of the myosin-V vacuole-specific receptor complex. *Molecular Biology of the Cell*. **20**, 1312–1323. doi:10.1091/mbc.e08-09-0954.

Johnston, J. R. (1966). Reproductive capacity and mode of death of yeast cells. *Antonie van Leeuwenhoek*. **32**, 94–98. doi:10.1007/BF02097448.

Jones, G. M., Stalker, J., Humphray, S., West, A., Cox, T., Rogers, J., Dunham, I. and Prelich, G. (2008). A systematic library for comprehensive overexpression screens in Saccharomyces cerevisiae. *Nature methods*. **5**, 239–241. doi:10.1038/nmeth.1181.

Juan, C. A., Pérez de la Lastra, José Manuel, Plou, F. J. and Pérez-Lebeña, E. (2021). The Chemistry of Reactive Oxygen Species (ROS) Revisited: Outlining Their Role in Biological Macromolecules (DNA, Lipids and Proteins) and Induced Pathologies. *International journal of molecular sciences*. **22**. doi:10.3390/ijms22094642.

Kaeberlein, M. (2010). Lessons on longevity from budding yeast. *Nature*. **464**, 513–519. doi:10.1038/nature08981.

Kaganovich, D., Kopito, R. and Frydman, J. (2008). Misfolded proteins partition between two distinct quality control compartments. *Nature*. **454**, 1088–1095. doi:10.1038/nature07195.

Kaksonen, M., Sun, Y. and Drubin, D. G. (2003). A Pathway for Association of Receptors, Adaptors, and Actin during Endocytic Internalization. *Cell*. **115**, 475–487. doi:10.1016/S0092-8674(03)00883-3.

Kaksonen, M., Toret, C. P. and Drubin, D. G. (2005). A modular design for the clathrin- and actin-mediated endocytosis machinery. *Cell*. **123**, 305–320. doi:10.1016/j.cell.2005.09.024.

Katajisto, P., Dohla, J., Chaffer, C. L., Pentinmikko, N., Marjanovic, N., Iqbal, S., Zoncu, R., Chen, W., Weinberg, R. A. and Sabatini, D. M. (2015). Stem cells. Asymmetric apportioning of aged mitochondria between daughter cells is required for stemness. *Science (New York, N.Y.)*. **348**, 340–343. doi:10.1126/science.1260384.

Kauppila, T. E. S., Kauppila, J. H. K. and Larsson, N.-G. (2017). Mammalian Mitochondria and Aging: An Update. *Cell metabolism*. **25**, 57–71. doi:10.1016/j.cmet.2016.09.017.

Kennedy, B. K., Austriaco, N R, Jr and Guarente, L. (1994). Daughter cells of Saccharomyces cerevisiae from old mothers display a reduced life span. *The Journal of cell biology*. **127**, 1985–1993. doi:10.1083/jcb.127.6.1985.

Kikyo, M., Tanaka, K., Kamei, T., Ozaki, K., Fujiwara, T., Inoue, E., Takita, Y., Ohya, Y. and Takai, Y. (1999). An FH domain-containing Bnr1p is a multifunctional protein interacting with a variety of cytoskeletal proteins in Saccharomyces cerevisiae. *Oncogene*. **18**, 7046–7054. doi:10.1038/sj.onc.1203184.

Klecker, T., Scholz, D., Fortsch, J. and Westermann, B. (2013). The yeast cell cortical protein Num1 integrates mitochondrial dynamics into cellular architecture. *Journal of cell science*. **126**, 2924–2930. doi:10.1242/jcs.126045.

Klecker, T. and Westermann, B. (2020). Asymmetric inheritance of mitochondria in yeast. *Biological chemistry*. **401**, 779–791. doi:10.1515/hsz-2019-0439.

Klinger, H., Rinnerthaler, M., Lam, Y. T., Laun, P., Heeren, G., Klocker, A., Simon-Nobbe, B., Dickinson, J. R., Dawes, I. W. and Breitenbach, M. (2010). Quantitation of (a)symmetric inheritance of functional and of oxidatively damaged mitochondrial aconitase in the cell division of old yeast mother cells. *Experimental gerontology*. **45**, 533–542. doi:10.1016/j.exger.2010.03.016.

König, J. (2012). *Untersuchungen zur anterograden Bewegung und Vererbung von Mitochondrien in Saccharomyces cerevisiae*. Bayreuth.

Kornmann, B., Currie, E., Collins, S. R., Schuldiner, M., Nunnari, J., Weissman, J. S. and Walter, P. (2009). An ER-mitochondria tethering complex revealed by a synthetic biology screen. *Science (New York, N.Y.)*. **325**, 477–481. doi:10.1126/science.1175088.

Kornmann, B., Osman, C. and Walter, P. (2011). The conserved GTPase Gem1 regulates endoplasmic reticulum–mitochondria connections. *Proceedings of the National Academy of Sciences*. **108**, 14151–14156. doi:10.1073/pnas.1111314108.

Kowaltowski, A. J. and Vercesi, A. E. (1999). Mitochondrial damage induced by conditions of oxidative stress. *Free Radical Biology and Medicine*. **26**, 463–471. doi:10.1016/S0891-5849(98)00216-0.

Krämer, L., Dalheimer, N., Räschle, M., Storchová, Z., Pielage, J., Boos, F. and Herrmann, J. M. (2023). MitoStores: chaperone-controlled protein granules store mitochondrial precursors in the cytosol. *The EMBO journal*, e112309. doi:10.15252/embj.2022112309.

Kubli, D. A. and Gustafsson, Å. B. (2012). Mitochondria and mitophagy: the yin and yang of cell death control. *Circulation research*. **111**, 1208–1221. doi:10.1161/CIRCRESAHA.112.265819.

Kurihara, Y., Kanki, T., Aoki, Y., Hirota, Y., Saigusa, T., Uchiumi, T. and Kang, D. (2012). Mitophagy plays an essential role in reducing mitochondrial production of reactive oxygen species and mutation of mitochondrial DNA by maintaining mitochondrial quantity and quality in yeast. *The Journal of biological chemistry*. **287**, 3265–3272. doi:10.1074/jbc.M111.280156.

Kushnirov, V. V. (2000). Rapid and reliable protein extraction from yeast. *Yeast (Chichester, England)*. **16**, 857–860. doi:10.1002/1097-0061(20000630)16:9<857::AID-YEA561>3.0.CO;2-B.

Lackner, L. L., Ping, H., Graef, M., Murley, A. and Nunnari, J. (2013). Endoplasmic reticulum-associated mitochondria-cortex tether functions in the distribution and inheritance of mitochondria. *Proceedings of the National Academy of Sciences of the United States of America*. **110**, E458-E467. doi:10.1073/pnas.1215232110.

Lai, C.-Y., Jaruga, E., Borghouts, C. and Jazwinski, S. M. (2002). A Mutation in the ATP2 Gene Abrogates the Age Asymmetry Between Mother and Daughter Cells of the Yeast Saccharomyces cerevisiae. *Genetics*. **162**, 73–87. doi:10.1093/genetics/162.1.73.

Lam, Y. T., Aung-Htut, M. T., Lim, Y. L., Yang, H. and Dawes, I. W. (2011). Changes in reactive oxygen species begin early during replicative aging of Saccharomyces cerevisiae cells. *Free Radical Biology and Medicine*. **50**, 963–970. doi:10.1016/j.freeradbiomed.2011.01.013.

Lasserre, J.-P., Dautant, A., Aiyar, R. S., Kucharczyk, R., Glatigny, A., Tribouillard-Tanvier, D., Rytka, J., Blondel, M., Skoczen, N. and Reynier, P. et al. (2015). Yeast as a system for modeling mitochondrial disease mechanisms and discovering therapies. *Disease models & mechanisms*. **8**, 509–526. doi:10.1242/dmm.020438.

Laun, P., Pichova, A., Madeo, F., Fuchs, J., Ellinger, A., Kohlwein, S., Dawes, I., Fröhlich, K. U. and Breitenbach, M. (2001). Aged mother cells of Saccharomyces cerevisiae show markers of oxidative stress and apoptosis. *Molecular microbiology*. **39**, 1166–1173.

Lazzarino, D. A., Boldogh, I., Smith, M. G., Rosand, J. and Pon, L. A. (1994). Yeast mitochondria contain ATP-sensitive, reversible actin-binding activity. *Molecular Biology of the Cell*. **5**, 807–818. doi:10.1091/mbc.5.7.807.

Lewandowska, A., Macfarlane, J. and Shaw, J. M. (2013). Mitochondrial association, protein phosphorylation, and degradation regulate the availability of the active Rab GTPase Ypt11 for mitochondrial inheritance. *Molecular Biology of the Cell*. **24**, 1185–1195. doi:10.1091/mbc.E12-12-0848.

Li, K. W., Lu, M. S., Iwamoto, Y., Drubin, D. G. and Pedersen, R. T. A. (2021). A preferred sequence for organelle inheritance during polarized cell growth. *Journal of cell science*. **134**. doi:10.1242/jcs.258856.

Liao, P.-C., Tandarich, L. C. and Hollenbeck, P. J. (2017). ROS regulation of axonal mitochondrial transport is mediated by Ca2+ and JNK in Drosophila. *PloS one*. **12**, e0178105. doi:10.1371/journal.pone.0178105.

Lill, R. and Mühlenhoff, U. (2005). Iron-sulfur-protein biogenesis in eukaryotes. *Trends in biochemical sciences*. **30**, 133–141. doi:10.1016/j.tibs.2005.01.006.

Lillie, S. H. and Brown, S. S. (1994). Immunofluorescence localization of the unconventional myosin, Myo2p, and the putative kinesin-related protein, Smy1p, to the same regions of polarized growth in Saccharomyces cerevisiae. *The Journal of cell biology*. **125**, 825–842. doi:10.1083/jcb.125.4.825.

Lindstrom, D. L. and Gottschling, D. E. (2009). The mother enrichment program: a genetic system for facile replicative life span analysis in Saccharomyces cerevisiae. *Genetics*. **183**, 413-22, 1SI-13SI. doi:10.1534/genetics.109.106229.

Liu, B., Larsson, L., Caballero, A., Hao, X., Oling, D., Grantham, J. and Nystrom, T. (2010). The polarisome is required for segregation and retrograde transport of protein aggregates. *Cell*. **140**, 257–267. doi:10.1016/j.cell.2009.12.031.

Liu, B., Larsson, L., Franssens, V., Hao, X., Hill, S. M., Andersson, V., Höglund, D., Song, J., Yang, X. and Öling, D. et al. (2011). Segregation of protein aggregates involves actin and the polarity machinery. *Cell*. **147**, 959–961. doi:10.1016/j.cell.2011.11.018.

Liu, Q., Fong, B., Yoo, S., Unruh, J. R., Guo, F., Yu, Z., Chen, J., Si, K., Li, R. and Zhou, C. (2023). Nascent mitochondrial proteins initiate the localized condensation of cytosolic protein aggregates on the mitochondrial surface. *Proceedings of the National Academy of Sciences*. **120**, e2300475120. doi:10.1073/pnas.2300475120.

Longtine, M. S., McKenzie, A. 3., Demarini, D. J., Shah, N. G., Wach, A., Brachat, A., Philippsen, P. and Pringle, J. R. (1998). Additional modules for versatile and economical PCR-based gene deletion and modification in Saccharomyces cerevisiae. *Yeast (Chichester, England)*. **14**, 953–961. doi:10.1002/(SICI)1097-0061(199807)14:10<953::AID-YEA293>3.0.CO;2-U.

Longtine, M. S., DeMarini, D. J., Valencik, M. L., Al-Awar, O. S., Fares, H., Virgilio, C. de and Pringle, J. R. (1996). The septins: roles in cytokinesis and other processes. *Current opinion in cell biology*. **8**, 106–119. doi:10.1016/S0955-0674(96)80054-8.

Lum, R., Tkach, J. M., Vierling, E. and Glover, J. R. (2004). Evidence for an Unfolding/Threading Mechanism for Protein Disaggregation by *Saccharomyces cerevisiae* Hsp104 *. *The Journal of biological chemistry*. **279**, 29139–29146. doi:10.1074/jbc.M403777200.

Malina, C., Larsson, C. and Nielsen, J. (2018). Yeast mitochondria: an overview of mitochondrial biology and the potential of mitochondrial systems biology. *FEMS yeast research*. **18**, foy040. doi:10.1093/femsyr/foy040.

Manford, A. G., Stefan, C. J., Yuan, H. L., Macgurn, J. A. and Emr, S. D. (2012). ER-to-plasma membrane tethering proteins regulate cell signaling and ER morphology. *Developmental cell*. **23**, 1129–1140. doi:10.1016/j.devcel.2012.11.004.

Manzano-Lopez, J., Matellan, L., Alvarez-Llamas, A., Blanco-Mira, J. C. and Monje-Casas, F. (2019). Asymmetric inheritance of spindle microtubule-organizing centres preserves replicative lifespan. *Nature Cell Biology*. **21**, 952–965. doi:10.1038/s41556-019-0364-8.

Marad, D. A., Buskirk, S. W. and Lang, G. I. (2018). Altered access to beneficial mutations slows adaptation and biases fixed mutations in diploids. *Nature Ecology & Evolution*. **2**, 882–889. doi:10.1038/s41559-018-0503-9.

Marquardt, J., Chen, X. and Bi, E. (2019). Architecture, remodeling, and functions of the septin cytoskeleton. *Cytoskeleton*. **76**, 7–14. doi:10.1002/cm.21475.

Martin, J., Mahlke, K. and Pfanner, N. (1991). Role of an energized inner membrane in mitochondrial protein import. Delta psi drives the movement of presequences. *The Journal of biological chemistry*. **266**, 18051–18057.

Mathew, V., Tam, A. S., Milbury, K. L., Hofmann, A. K., Hughes, C. S., Morin, G. B., Loewen, C. J. R. and Stirling, P. C. (2017). Selective aggregation of the splicing factor Hsh155 suppresses splicing upon genotoxic stress. *The Journal of cell biology*. **216**, 4027–4040. doi:10.1083/jcb.201612018.

Matlashov, M. E., Belousov, V. V. and Enikolopov, G. (2014). How much H(2)O(2) is produced by recombinant D-amino acid oxidase in mammalian cells? *Antioxidants & redox signaling*. **20**, 1039–1044. doi:10.1089/ars.2013.5618.

McFaline-Figueroa, J. R., Vevea, J., Swayne, T. C., Zhou, C., Liu, C., Leung, G., Boldogh, I. R. and Pon, L. A. (2011). Mitochondrial quality control during inheritance is associated with lifespan and mother-daughter age asymmetry in budding yeast. *Aging cell*. **10**, 885–895. doi:10.1111/j.1474-9726.2011.00731.x.

Meeusen, S., McCaffery, J. M. and Nunnari, J. (2004). Mitochondrial fusion intermediates revealed in vitro. *Science (New York, N.Y.)*. **305**, 1747–1752. doi:10.1126/science.1100612.

Melkov, A. and Abdu, U. (2018). Regulation of long-distance transport of mitochondria along microtubules. *Cellular and Molecular Life Sciences*. **75**, 163–176. doi:10.1007/s00018-017-2590-1.

Mesquita, A., Weinberger, M., Silva, A., Sampaio-Marques, B., Almeida, B., Leão, C., Costa, V., Rodrigues, F., Burhans, W. C. and Ludovico, P. (2010). Caloric restriction or catalase inactivation extends yeast chronological lifespan by inducing H2O2 and superoxide dismutase activity. *Proceedings of the National Academy of Sciences*. **107**, 15123–15128. doi:10.1073/pnas.1004432107.

Miller, S. B. M., Ho, C.-T., Winkler, J., Khokhrina, M., Neuner, A., Mohamed, M. Y. H., Guilbride, D. L., Richter, K., Lisby, M. and Schiebel, E. et al. (2015a). Compartment-specific aggregases direct distinct nuclear and cytoplasmic aggregate deposition. *The EMBO journal*. **34**, 778–797. doi:10.15252/embj.201489524.

Miller, S. B. M., Mogk, A. and Bukau, B. (2015b). Spatially organized aggregation of misfolded proteins as cellular stress defense strategy. *Journal of molecular biology*. **427**, 1564–1574. doi:10.1016/j.jmb.2015.02.006.

Mishra, M., Huang, J. and Balasubramanian, M. K. (2014). The yeast actin cytoskeleton. *FEMS microbiology reviews*. **38**, 213–227. doi:10.1111/1574-6976.12064.

Mnaimneh, S., Davierwala, A. P., Haynes, J., Moffat, J., Peng, W.-T., Zhang, W., Yang, X., Pootoolal, J., Chua, G. and Lopez, A. et al. (2004). Exploration of essential gene functions via titratable promoter alleles. *Cell*. **118**, 31–44. doi:10.1016/j.cell.2004.06.013.

Morawska, M. and Ulrich, H. D. (2013). An expanded tool kit for the auxin-inducible degron system in budding yeast. *Yeast (Chichester, England)*. **30**, 341–351. doi:10.1002/yea.2967.

Moreau, C. A., Bhargav, S. P., Kumar, H., Quadt, K. A., Piirainen, H., Strauss, L., Kehrer, J., Streichfuss, M., Spatz, J. P. and Wade, R. C. et al. (2017). A unique profilin-actin interface is important for malaria parasite motility. *PLOS Pathogens*. **13**, e1006412. doi:10.1371/journal.ppat.1006412.

Mozdy, A. D., McCaffery, J. M. and Shaw, J. M. (2000). Dnm1p GTPase-mediated mitochondrial fission is a multi-step process requiring the novel integral membrane component Fis1p. *The Journal of cell biology*. **151**, 367–380. doi:10.1083/jcb.151.2.367.

Mumberg, D., Müller, R. and Funk, M. (1995). Yeast vectors for the controlled expression of heterologous proteins in different genetic backgrounds. *Gene*. **156**, 119–122. doi:10.1016/0378-1119(95)00037-7.

Murley, A., Lackner, L. L., Osman, C., West, M., Voeltz, G. K., Walter, P., Nunnari, J. and Youle, R. J. (2013). ER-associated mitochondrial division links the distribution of mitochondria and mitochondrial DNA in yeast. *eLife*. **2**, e00422. doi:10.7554/eLife.00422.

Murphy, M. P. (2009). How mitochondria produce reactive oxygen species. *The Biochemical journal*. **417**, 1–13. doi:10.1042/BJ20081386.

Neupert, W. and Herrmann, J. M. (2007). Translocation of proteins into mitochondria. *Annual review of biochemistry*. **76**, 723–749. doi:10.1146/annurev.biochem.76.052705.163409.

Ng, R. and Abelson, J. (1980). Isolation and sequence of the gene for actin in Saccharomyces cerevisiae. *Proceedings of the National Academy of Sciences of the United States of America*. **77**, 3912–3916. doi:10.1073/pnas.77.7.3912.

Nicastro, R., Raucci, S., Michel, A. H., Stumpe, M., Garcia Osuna, G. M., Jaquenoud, M., Kornmann, B. and Virgilio, C. de (2021). Indole-3-acetic acid is a physiological inhibitor of TORC1 in yeast. *PLOS Genetics*. **17**, e1009414. doi:10.1371/journal.pgen.1009414.

Nishihama, R., Onishi, M. and Pringle, J. R. (2011). New insights into the phylogenetic distribution and evolutionary origins of the septins. *Biological chemistry*. **392**, 681–687. doi:10.1515/BC.2011.086.

Nishimura, K., Fukagawa, T., Takisawa, H., Kakimoto, T. and Kanemaki, M. (2009). An auxin-based degron system for the rapid depletion of proteins in nonplant cells. *Nature methods*. **6**, 917–922. doi:10.1038/nmeth.1401.

Nystrom, T. and Liu, B. (2014). The mystery of aging and rejuvenation - a budding topic. *Current opinion in microbiology*. **18**, 61–67. doi:10.1016/j.mib.2014.02.003.

Obara, K., Yoshikawa, T., Yamaguchi, R., Kuwata, K., Nakatsukasa, K., Nishimura, K. and Kamura, T. (2022). Proteolysis of adaptor protein Mmr1 during budding is necessary for mitochondrial homeostasis in Saccharomyces cerevisiae. *Nature Communications*. **13**, 2005. doi:10.1038/s41467-022-29704-8.

Okamoto, K., Kondo-Okamoto, N. and Ohsumi, Y. (2009). Mitochondria-anchored receptor Atg32 mediates degradation of mitochondria via selective autophagy. *Developmental cell*. **17**, 87–97. doi:10.1016/j.devcel.2009.06.013.

Omer, S., Brock, K., Beckford, J. and Lee, W.-L. (2020). Overexpression of Mdm36 reveals Num1 foci that mediate dynein-dependent microtubule sliding in budding yeast. *Journal of cell science*. **133**, jcs246363. doi:10.1242/jcs.246363.

Otsuga, D., Keegan, B. R., Brisch, E., Thatcher, J. W., Hermann, G. J., Bleazard, W. and Shaw, J. M. (1998). The dynamin-related GTPase, Dnm1p, controls mitochondrial morphology in yeast. *The Journal of cell biology*. **143**, 333–349. doi:10.1083/jcb.143.2.333.

Ozaki-Kuroda, K., Yamamoto, Y., Nohara, H., Kinoshita, M., Fujiwara, T., Irie, K. and Takai, Y. (2001). Dynamic localization and function of Bni1p at the sites of directed growth in Saccharomyces cerevisiae. *Molecular and cellular biology*. **21**, 827–839. doi:10.1128/MCB.21.3.827-839.2001.

Paoletti, C., Quintin, S., Matifas, A. and Charvin, G. (2016). Kinetics of Formation and Asymmetrical Distribution of Hsp104-Bound Protein Aggregates in Yeast. *Biophysical journal*. **110**, 1605–1614. doi:10.1016/j.bpj.2016.02.034.

Papagiannakis, A., Niebel, B., Wit, E. C. and Heinemann, M. (2017). Autonomous Metabolic Oscillations Robustly Gate the Early and Late Cell Cycle. *Molecular cell*. **65**, 285–295. doi:10.1016/j.molcel.2016.11.018.

Papić, D., Elbaz-Alon, Y., Koerdt, S. N., Leopold, K., Worm, D., Jung, M., Schuldiner, M. and Rapaport, D. (2013). The Role of Djp1 in Import of the Mitochondrial Protein Mim1

Demonstrates Specificity between a Cochaperone and Its Substrate Protein. *Molecular and cellular biology*. **33**, 4083–4094. doi:10.1128/MCB.00227-13.

Pernice, W. M., Vevea, J. D. and Pon, L. A. (2016). A role for Mfb1p in region-specific anchorage of high-functioning mitochondria and lifespan in Saccharomyces cerevisiae. *Nature Communications*. **7**, 10595. doi:10.1038/ncomms10595.

Ping, H. A., Kraft, L. M., Chen, W., Nilles, A. E. and Lackner, L. L. (2016). Num1 anchors mitochondria to the plasma membrane via two domains with different lipid binding specificities. *The Journal of cell biology*. **213**, 513–524. doi:10.1083/jcb.201511021.

Piper, P. W. (1993). Molecular events associated with acquisition of heat tolerance by the yeast Saccharomyces cerevisiae. *FEMS microbiology reviews*. **11**, 339–355. doi:10.1111/j.1574-6976.1993.tb00005.x.

Pollard, T. D. (2007). Regulation of actin filament assembly by Arp2/3 complex and formins. *Annual review of biophysics and biomolecular structure*. **36**, 451–477. doi:10.1146/annurev.biophys.35.040405.101936.

Pollard, T. D. (2016). Actin and Actin-Binding Proteins. *Cold Spring Harbor perspectives in biology*. **8**. doi:10.1101/cshperspect.a018226.

Pollegioni, L., Diederichs, K., Molla, G., Umhau, S., Welte, W., Ghisla, S. and Pilone, M. S. (2002). Yeast D-amino acid oxidase: structural basis of its catalytic properties. *Journal of molecular biology*. **324 3**, 535–546.

Poveda-Huertes, D., Matic, S., Marada, A., Habernig, L., Licheva, M., Myketin, L., Gilsbach, R., Tosal-Castano, S., Papinski, D. and Mulica, P. et al. (2020). An Early mtUPR: Redistribution of the Nuclear Transcription Factor Rox1 to Mitochondria Protects against Intramitochondrial Proteotoxic Aggregates. *Molecular cell*. **77**, 180-188.e9. doi:10.1016/j.molcel.2019.09.026.

Prusty, R., Grisafi, P. and Fink, G. R. (2004). The plant hormone indoleacetic acid induces invasive growth in Saccharomyces cerevisiae. *Proceedings of the National Academy of Sciences of the United States of America*. **101**, 4153–4157. doi:10.1073/pnas.0400659101.

Pruyne, D., Gao, L., Bi, E. and Bretscher, A. (2004a). Stable and Dynamic Axes of Polarity Use Distinct Formin Isoforms in Budding Yeast. *Molecular Biology of the Cell*. **15**, 4971–4989. doi:10.1091/mbc.e04-04-0296.

Pruyne, D., Legesse-Miller, A., Gao, L., Dong, Y. and Bretscher, A. (2004b). Mechanisms of polarized growth and organelle segregation in yeast. *Annual review of cell and developmental biology*. **20**, 559–591. doi:10.1146/annurev.cellbio.20.010403.103108.

Rafelski, S. M., Viana, M. P., Zhang, Y., Chan, Y.-H. M., Thorn, K. S., Yam, P., Fung, J. C., Li, H., Costa, L. d. F. and Marshall, W. F. (2012). Mitochondrial network size scaling in budding yeast. *Science (New York, N.Y.)*. **338**, 822–824. doi:10.1126/science.1225720.

Rapaport, D., Brunner, M., Neupert, W. and Westermann, B. (1998). Fzo1p Is a Mitochondrial Outer Membrane Protein Essential for the Biogenesis of Functional Mitochondria in *Saccharomyces cerevisiae**. *The Journal of biological chemistry*. **273**, 20150–20155. doi:10.1074/jbc.273.32.20150.

Redza-Dutordoir, M. and Averill-Bates, D. A. (2016). Activation of apoptosis signalling pathways by reactive oxygen species. *Biochimica et biophysica acta*. **1863**, 2977–2992. doi:10.1016/j.bbamcr.2016.09.012.

Rhee, S. G., Bae, Y. S., Lee, S. R. and Kwon, J. (2000). Hydrogen peroxide: a key messenger that modulates protein phosphorylation through cysteine oxidation. *Science's STKE : signal transduction knowledge environment*. **2000**, pe1. doi:10.1126/stke.2000.53.pe1.

Richter, C., Park, J. W. and Ames, B. N. (1988). Normal oxidative damage to mitochondrial and nuclear DNA is extensive. *Proceedings of the National Academy of Sciences of the United States of America*. **85**, 6465–6467. doi:10.1073/pnas.85.17.6465.

Roeder, A. D., Hermann, G. J., Keegan, B. R., Thatcher, S. A. and Shaw, J. M. (1998). Mitochondrial Inheritance Is Delayed in Saccharomyces cerevisiae Cells Lacking the Serine/Threonine PhosphatasePTC1. *Molecular Biology of the Cell*. **9**, 917–930. doi:10.1091/mbc.9.4.917.

Rossanese, O. W., Reinke, C. A., Bevis, B. J., Hammond, A. T., Sears, I. B., O'Connor, J. and Glick, B. S. (2001). A role for actin, Cdc1p, and Myo2p in the inheritance of late Golgi elements in Saccharomyces cerevisiae. *The Journal of cell biology*. **153**, 47–62. doi:10.1083/jcb.153.1.47.

Ruan, L., Zhou, C., Jin, E., Kucharavy, A., Zhang, Y., Wen, Z., Florens, L. and Li, R. (2017). Cytosolic proteostasis through importing of misfolded proteins into mitochondria. *Nature*. **543**, 443–446. doi:10.1038/nature21695.

Saarikangas, J., Caudron, F., Prasad, R., Moreno, D. F., Bolognesi, A., Aldea, M. and Barral, Y. (2017). Compartmentalization of ER-Bound Chaperone Confines Protein Deposit Formation to the Aging Yeast Cell. *Current biology*. **27**, 773–783. doi:10.1016/j.cub.2017.01.069.

Scheckhuber, C. Q., Erjavec, N., Tinazli, A., Hamann, A., Nyström, T. and Osiewacz, H. D. (2007). Reducing mitochondrial fission results in increased life span and fitness of two fungal ageing models. *Nature Cell Biology*. **9**, 99–105. doi:10.1038/ncb1524.

Schieber, M. and Chandel, N. S. (2014). ROS Function in Redox Signaling and Oxidative Stress. *Current biology : CB*. **24**, R453-R462. doi:10.1016/j.cub.2014.03.034.

Schindelin, J., Arganda-Carreras, I., Frise, E., Kaynig, V., Longair, M., Pietzsch, T., Preibisch, S., Rueden, C., Saalfeld, S. and Schmid, B. et al. (2012). Fiji: an open-source platform for biological-image analysis. *Nature methods*. **9**, 676–682. doi:10.1038/nmeth.2019.

Scholz, D., Förtsch, J., Böckler, S., Klecker, T. and Westermann, B. (2013). Analyzing membrane dynamics with live cell fluorescence microscopy with a focus on yeast mitochondria. *Methods in molecular biology (Clifton, N.J.)*. **1033**, 275–283. doi:10.1007/978-1-62703-487-6_17.

Schott, D., Ho, J., Pruyne, D. and Bretscher, A. (1999). The COOH-terminal domain of Myo2p, a yeast myosin V, has a direct role in secretory vesicle targeting. *The Journal of cell biology*. **147**, 791–808. doi:10.1083/jcb.147.4.791.

Sesaki, H. and Jensen, R. E. (2004). Ugo1p Links the Fzo1p and Mgm1p GTPases for Mitochondrial Fusion *. *The Journal of biological chemistry*. **279**, 28298–28303. doi:10.1074/jbc.M401363200.

Sharma, A., Smith, H. J., Yao, P. and Mair, W. B. (2019). Causal roles of mitochondrial dynamics in longevity and healthy aging. *EMBO reports*. **20**, e48395. doi:10.15252/embr.201948395.

Shcheprova, Z., Baldi, S., Frei, S. B., Gonnet, G. and Barral, Y. (2008). A mechanism for asymmetric segregation of age during yeast budding. *Nature*. **454**, 728–734. doi:10.1038/nature07212.

Sheff, M. A. and Thorn, K. S. (2004). Optimized cassettes for fluorescent protein tagging in Saccharomyces cerevisiae. *Yeast (Chichester, England)*. **21**, 661–670. doi:10.1002/yea.1130.

Shepard, K. A., Gerber, A. P., Jambhekar, A., Takizawa, P. A., Brown, P. O., Herschlag, D., DeRisi, J. L. and Vale, R. D. (2003). Widespread cytoplasmic mRNA transport in yeast: Identification of 22 bud-localized transcripts using DNA microarray analysis. *Proceedings of the National Academy of Sciences*. **100**, 11429–11434. doi:10.1073/pnas.2033246100.

Sherman, F. (2002). Getting started with yeast. *Methods in enzymology*. **350**, 3–41. doi:10.1016/s0076-6879(02)50954-x.

Sies, H., Belousov, V. V., Chandel, N. S., Davies, M. J., Jones, D. P., Mann, G. E., Murphy, M. P., Yamamoto, M. and Winterbourn, C. (2022). Defining roles of specific reactive oxygen species (ROS) in cell biology and physiology. *Nature reviews. Molecular cell biology*. **23**, 499–515. doi:10.1038/s41580-022-00456-z.

Sikorski, R. S. and Hieter, P. (1989). A system of shuttle vectors and yeast host strains designed for efficient manipulation of DNA in Saccharomyces cerevisiae. *Genetics*. **122**, 19–27. doi:10.1093/genetics/122.1.19.

Simon, V. R., Karmon, S. L. and Pon, L. A. (1997). Mitochondrial inheritance: Cell cycle and actin cable dependence of polarized mitochondrial movements in Saccharomyces cerevisiae. *Cell Motil. Cytoskeleton*. **37**, 199–210. doi:10.1002/(SICI)1097-0169(1997)37:3<199::AID-CM2>3.0.CO;2-2.

Sinclair, D. A. and Guarente, L. (1997). Extrachromosomal rDNA circles--a cause of aging in yeast. *Cell*. **91**, 1033–1042. doi:10.1016/s0092-8674(00)80493-6.

Song, J., Yang, Q., Yang, J., Larsson, L., Hao, X., Zhu, X., Malmgren-Hill, S., Cvijovic, M., Fernandez-Rodriguez, J. and Grantham, J. et al. (2014). Essential Genetic Interactors of SIR2 Required for Spatial Sequestration and Asymmetrical Inheritance of Protein Aggregates. *PLOS Genetics*. **10**, e1004539. doi:10.1371/journal.pgen.1004539.

Sontag, E. M., Morales-Polanco, F., Chen, J.-H., McDermott, G., Dolan, P. T., Gestaut, D., Le Gros, M. A., Larabell, C. and Frydman, J. (2023). Nuclear and cytoplasmic spatial protein quality control is coordinated by nuclear–vacuolar junctions and perinuclear ESCRT. *Nature Cell Biology*. **25**, 699–713. doi:10.1038/s41556-023-01128-6.

Spaepen, S., Vanderleyden, J. and Remans, R. (2007). Indole-3-acetic acid in microbial and microorganism-plant signaling. *FEMS microbiology reviews*. **31**, 425–448. doi:10.1111/j.1574-6976.2007.00072.x.

Spokoini, R., Moldavski, O., Nahmias, Y., England, J. L., Schuldiner, M. and Kaganovich, D. (2012). Confinement to organelle-associated inclusion structures mediates asymmetric inheritance of aggregated protein in budding yeast. *Cell reports*. **2**, 738–747. doi:10.1016/j.celrep.2012.08.024.

Sprague, G. F. and Herskowitz, I. (1981). Control of yeast cell type by the mating type locus. I. Identification and control of expression of the a-specific gene BAR1. *Journal of molecular biology*. **153**, 305–321. doi:10.1016/0022-2836(81)90280-1.

Stevenson, L. F., Kennedy, B. K. and Harlow, E. (2001). A large-scale overexpression screen in Saccharomyces cerevisiae identifies previously uncharacterized cell cycle genes. *Proceedings of the National Academy of Sciences*. **98**, 3946–3951. doi:10.1073/pnas.051013498.

Stroud, D. A., Oeljeklaus, S., Wiese, S., Bohnert, M., Lewandrowski, U., Sickmann, A., Guiard, B., van der Laan, M., Warscheid, B. and Wiedemann, N. (2011). Composition and topology of the endoplasmic reticulum-mitochondria encounter structure. *Journal of molecular biology*. **413**, 743–750. doi:10.1016/j.jmb.2011.09.012.

Sun, G., Hwang, C., Jung, T., Liu, J. and Li, R. (2023). Biased placement of Mitochondria fission facilitates asymmetric inheritance of protein aggregates during yeast cell division. *PLOS Computational Biology*. **19**, e1011588. doi:10.1371/journal.pcbi.1011588.

Swayne, T. C., Zhou, C., Boldogh, I. R., Charalel, J. K., McFaline-Figueroa, J. R., Thoms, S., Yang, C., Leung, G., McInnes, J. and Erdmann, R. et al. (2011). Role for cER and Mmr1p in anchorage of mitochondria at sites of polarized surface growth in budding yeast. *Current biology : CB*. **21**, 1994–1999. doi:10.1016/j.cub.2011.10.019.

Tamborrini, D., Juanes, M. A., Ibanes, S., Rancati, G. and Piatti, S. (2018). Recruitment of the mitotic exit network to yeast centrosomes couples septin displacement to actomyosin constriction. *Nature Communications*. **9**, 4308. doi:10.1038/s41467-018-06767-0.

Tang, F., Kauffman, E., Novak, J., Nau J. J., Catlett N. L. and Weisman L. S. (2003) Regulated degradation of a class V myosin receptor directs movement of the yeast vacuole. *Nature* **422**, 87–92 https://doi.org/10.1038/nature01453

Tang, K., Li, Y., Yu, C. and Wei, Z. (2019). Structural mechanism for versatile cargo recognition by the yeast class V myosin Myo2. *The Journal of biological chemistry*. **294**, 5896–5906. doi:10.1074/jbc.RA119.007550.

Tartakoff, A. M., Aylyarov, I. and Jaiswal, P. (2013). Septin-containing barriers control the differential inheritance of cytoplasmic elements. *Cell reports*. **3**, 223–236. doi:10.1016/j.celrep.2012.11.022.

Teysseire, N., Chiche-Portiche, C. and Raoult, D. (1992). Intracellular movements of Rickettsia conorii and R. typhi based on actin polymerization. *Research in microbiology*. **143**, 821–829. doi:10.1016/0923-2508(92)90069-z.

Tieu, Q. and Nunnari, J. (2000). Mdv1p Is a Wd Repeat Protein That Interacts with the Dynamin-Related Gtpase, Dnm1p, to Trigger Mitochondrial Division. *The Journal of cell biology*. **151**, 353–366. doi:10.1083/jcb.151.2.353.

Tishkov, V. I. and Khoronenkova, S. V. (2005). D-Amino acid oxidase: structure, catalytic mechanism, and practical application. *Biochemistry. Biokhimiia*. **70**, 40–54.

Tong, A. H. Y. and Boone, C. (2006). Synthetic genetic array analysis in Saccharomyces cerevisiae. *Methods in molecular biology (Clifton, N.J.)*. **313**, 171–192. doi:10.1385/1-59259-958-3:171.

Tzagoloff, A. and Dieckmann, C. L. (1990). PET genes of Saccharomyces cerevisiae. *Microbiological reviews*. **54**, 211–225. doi:10.1128/mr.54.3.211-225.1990.

Versele, M. and Thorner, J. (2004). Septin collar formation in budding yeast requires GTP binding and direct phosphorylation by the PAK, Cla4. *The Journal of cell biology*. **164**, 701–715. doi:10.1083/jcb.200312070.

Vevea, J. D., Swayne, T. C., Boldogh, I. R. and Pon, L. A. (2014). Inheritance of the fittest mitochondria in yeast. *Trends in cell biology*. **24**, 53–60. doi:10.1016/j.tcb.2013.07.003.

Vilella, F., Herrero, E., Torres, J. and de La Torre-Ruiz, M. A. (2005). Pkc1 and the upstream elements of the cell integrity pathway in Saccharomyces cerevisiae, Rom2 and Mtl1, are required for cellular responses to oxidative stress. *The Journal of biological chemistry*. **280**, 9149–9159. doi:10.1074/jbc.M411062200.

Vowinckel, J., Hartl, J., Butler, R. and Ralser, M. (2015). MitoLoc: A method for the simultaneous quantification of mitochondrial network morphology and membrane potential in single cells. *Mitochondrion*. **24**, 77–86. doi:10.1016/j.mito.2015.07.001.

Wallace, D. C. (2010). Mitochondrial DNA mutations in disease and aging. *Environmental and molecular mutagenesis*. **51**, 440–450. doi:10.1002/em.20586.

Wallace, S. S. (2002). Biological consequences of free radical-damaged DNA bases1, 2 1Guest Editor: Miral Dizdaroglu 2This article is part of a series of reviews on “Oxidative DNA Damage and Repair.” The full list of papers may be found on the homepage of the journal. *Free Radical Biology and Medicine*. **33**, 1–14. doi:10.1016/S0891-5849(02)00827-4.

Weems, A. and McMurray, M. (2017). The step-wise pathway of septin hetero-octamer assembly in budding yeast. *eLife*. **6**. doi:10.7554/eLife.23689.

Welch, M. D., Iwamatsu, A. and Mitchison, T. J. (1997). Actin polymerization is induced by Arp 2/3 protein complex at the surface of Listeria monocytogenes. *Nature*. **385**, 265–269. doi:10.1038/385265a0.

Westermann, B. and Neupert, W. (2000). Mitochondria-targeted green fluorescent proteins: convenient tools for the study of organelle biogenesis in Saccharomyces cerevisiae. *Yeast (Chichester, England)*. **16**, 1421–1427. doi:10.1002/1097-0061(200011)16:15<1421::AID-YEA624>3.0.CO;2-U.

Westermann, B. (2008). Molecular machinery of mitochondrial fusion and fission. *The Journal of biological chemistry*. **283**, 13501–13505. doi:10.1074/jbc.R800011200.

Wloka, C. and Bi, E. (2012). Mechanisms of cytokinesis in budding yeast. *Cytoskeleton*. **69**, 710–726. doi:10.1002/cm.21046.

Wong, E. D., Wagner, J. A., Scott, S. V., Okreglak, V., Holewinske, T. J., Cassidy-Stone, A. and Nunnari, J. (2003). The intramitochondrial dynamin-related GTPase, Mgm1p, is a component of a

protein complex that mediates mitochondrial fusion. *The Journal of cell biology*. **160**, 303–311. doi:10.1083/jcb.200209015.

Wong, H.-S., Dighe, P. A., Mezera, V., Monternier, P.-A. and Brand, M. D. (2017). Production of superoxide and hydrogen peroxide from specific mitochondrial sites under different bioenergetic conditions. *The Journal of biological chemistry*. **292**, 16804–16809. doi:10.1074/jbc.R117.789271.

Wong, S. and Weisman, L. S. (2021). Roles and regulation of myosin V interaction with cargo. *Advances in biological regulation*. **79**, 100787. doi:10.1016/j.jbior.2021.100787.

Wurm, C. A. and Jakobs, S. (2006). Differential protein distributions define two sub-compartments of the mitochondrial inner membrane in yeast. *FEBS Letters*. **580**, 5628–5634. doi:10.1016/j.febslet.2006.09.012.

Xu, L. and Bretscher, A. (2014). Rapid glucose depletion immobilizes active myosin V on stabilized actin cables. *Current biology : CB*. **24**, 2471–2479. doi:10.1016/j.cub.2014.09.017.

Yang, H.-C., Palazzo, A., Swayne, T. C. and Pon, L. A. (1999). A retention mechanism for distribution of mitochondria during cell division in budding yeast. *Current biology : CB*. **9**, 1111-S2. doi:10.1016/S0960-9822(99)80480-1.

Zhou, C., Slaughter, B. D., Unruh, J. R., Eldakak, A., Rubinstein, B. and Li, R. (2011). Motility and segregation of Hsp104-associated protein aggregates in budding yeast. *Cell*. **147**, 1186–1196. doi:10.1016/j.cell.2011.11.002.

Zhou, C., Slaughter, B. D., Unruh, J. R., Guo, F., Yu, Z., Mickey, K., Narkar, A., Ross, R. T., McClain, M. and Li, R. (2014). Organelle-based aggregation and retention of damaged proteins in asymmetrically dividing cells. *Cell*. **159**, 530–542. doi:10.1016/j.cell.2014.09.026.

Zhuk, A. S., Stepchenkova, E. I., Pavlov, Y. I. and Inge-Vechtomov, S. G. (2017). Evaluation of methods of synchronization of cell division in yeast Saccharomyces cerevisiae. *Cell and Tissue Biology*. **11**, 111–122. doi:10.1134/S1990519X17020110.

Zimorski, V., Ku, C., Martin, W. F. and Gould, S. B. (2014). Endosymbiotic theory for organelle origins. *Current opinion in microbiology*. **22**, 38–48. doi:10.1016/j.mib.2014.09.008.

Danksagung

Mein Dank gilt zuerst Prof. Dr. Benedikt Westermann, der mich in meiner Dissertationsphase stets hervorragend fachlich und persönlich begleitet hat.

Des Weiteren gilt mein Dank meinen Mentoren Prof. Dr. Olaf Stemmann und Prof. Dr. Matthias Weiss für die konstruktive wissenschaftliche Begleitung meiner Arbeit.

Zusätzlich danke ich Herrn Dr. Till Klecker für die unzähligen wissenschaftlichen Diskussionen, die Möglichkeiten meine Arbeit zu schärfen und die tagtägliche wissenschaftliche Unterstützung.

Der Deutschen Forschungsgemeinschaft gilt mein Dank für die finanzielle Ermöglichung meiner Dissertation.

Frau Annette Suske, Frau Rita Grotjahn und Frau Petra Helies möchte ich für ihren Einsatz und ihre tagtägliche Unterstützung im Laboralltag danken.

Xenia Chelius danke ich für unzählige fachliche Gespräche, wissenschaftliche Diskussionen und die tolle Unterstützung im Alltag.

Verena Geiger und Valentin Huber möchte ich danken für die Unterstützung im Rahmen ihrer Abschlussarbeiten.

Mein Dank gilt dem gesamten Institut mit allen aktuellen und ehemaligen Mitgliedern.

Ich möchte meiner gesamten Familie, ganz besonders meiner Mutter Susanne Radmacher für die Ermöglichung meines Studiums und die emotionale Unterstützung in all den Jahren danken.

Vielen Dank an meine Schwiegereltern Christiane und Prof. Dr. Ulrich Bartosch für ihre akademische Wegbegleitung.

Ich möchte mich bei all meinen Freunden für die Begleitung und Unterstützung in der Phase meiner Dissertation bedanken, besonders Dr. Florian Weeber.

Zuletzt denke ich Leonard Bartosch, ohne den ich es nie bis hierher geschafft hätte.

Eidesstaatliche Versicherung und Erklärungen

(§ 9 Satz 2 Nr. 3 PromO BayNAT)

Hiermit versichere ich eidesstattlich, dass ich die Arbeit selbstständig verfasst und keine anderen als die von mir angegebenen Quellen und Hilfsmittel benutzt habe (vgl. Art. 97 Abs. 1 Satz 8 BayHIG).

(§ 9 Satz 2 Nr. 3 PromO BayNAT)

Hiermit erkläre ich, dass ich die Dissertation nicht bereits zur Erlangung eines akademischen Grades eingereicht habe und dass ich nicht bereits diese oder eine gleichartige Doktorprüfung endgültig nicht bestanden habe.

(§ 9 Satz 2 Nr. 4 PromO BayNAT)

Hiermit erkläre ich, dass ich Hilfe von gewerblichen Promotionsberatern bzw. -vermittlern oder ähnlichen Dienstleistern weder bisher in Anspruch genommen habe noch künftig in Anspruch nehmen werde.

(§ 9 Satz 2 Nr. 7 PromO BayNAT)

Hiermit erkläre ich mein Einverständnis, dass die elektronische Fassung meiner Dissertation unter Wahrung meiner Urheberrechte und des Datenschutzes einer gesonderten Überprüfung unterzogen werden kann.

(§ 9 Satz 2 Nr. 8 PromO BayNAT)

Hiermit erkläre ich mein Einverständnis, dass bei Verdacht wissenschaftlichen Fehlverhaltens Ermittlungen durch universitätsinterne Organe der wissenschaftlichen Selbstkontrolle stattfinden können.

…….

Ort, Datum, Unterschrift